Institute for
Communications
and Navigation

GNSS Receiver Front-end Modelling for Satellite and Pseudolite Signals

Mathieu Cattenoz

A Thesis submitted for the
Master Degree

Institute for Communications and Navigation

Prof. Dr. Christoph Günther

Supervised by Francis Soualle (EADS Astrium)
Kaspar Giger (TUM)

Munich, September 2011

Institute for Communications and Navigation

Technische Universität München
Theresienstrasse 90
80333 Munich

Abstract

For some applications such like guidance in airports, it might be necessary to combine ranging performance provided by GNSS like GPS or Galileo with those offered by ground emitters sharing many signal characteristics with the satellite signals, and called pseudolites. Hence, the emission frequency and signal structure are identical, but the received powers are much higher. Because of the near/far effect, performance for the tracking of either satellite or pseudolite signals may be highly degraded if no care is taken. To limit these effects, the most usual technical solution consists in transmitting the pseudolite signals in a pulsed way, authorizing some time interval for the tracking of the satellite signals only. A blanker implemented in the receiver front-end enables also to limit these high power pulsed interferences. In that way, it should be possible to track each signal in a wide area around the ground emitters. More particularly, the existing GNSS receivers should not be too degraded by the interfering pseudolite signals.

Therefore, it is central to be able to estimate the degradation for navigation signal tracking around pseudolites. It may also help for the dimensioning of some parameters like the pulsing scheme to limit the performance degradations. The current analytical models are not fully satisfying to cover specific effects like signal blanking or pulse overlapping. The proposed work gives analytical models for the signal-to-noise ratio (SNIR) with consideration of many parameters like front-end dynamics, blanking threshold, and pulse parameters. The models are established for three standard scenarios and should give a basis for the SNIR estimation at different distances to ground emitters. More particularly, detailed methods for the calculation of interference contribution to the SNIR are given. In a second part, the validity of the derived models is estimated in their conditions of application with Monte Carlo simulations. Finally, after a first analysis of some results, several concepts of improvement are proposed for the pulsing schemes.

Contents

Chapter 1

Technical Background

1.1 GNSS

A Gobal Navigation Satellite System (GNSS) gives the possibility to determine user's position, time and velocity anywhere on Earth. A known one is the NAVSTAR Global Positioning System (GPS), built by the United States and which has been fully operational since 1994. Signals are emitted continuously by the satellites of the constellation and can be tracked by receivers. The receivers determine the propagation time by using the information (satellite position, clock and also system time) embedded in the down-link message to deduce the pseudorange to each visible satellite. The computation of the position on the globe is then made by trilateration algorithm. Since three parameters of position and one parameter of time have to be determined, at least four satellite signals are needed. Moreover, the more visible the satellites, the higher the accuracy, going up to a position precision of some meters.

The isolation of signals from different sources is based on CDMA (Code Division Multiple Access). Each satellite emits a specific PRN (Pseudo Random Noise), a repeating known noise-like digital code [1]. Signals are emitted with a power of 20 W (order of magnitude) and travel over 20 000 km: the received power is very low in comparison with the noise (typically 20 or 30 dB less) and thus the S/N (signal-to-noise ratio) is negative. In order to extract the satellite signal from the noise, the receiver correlates the received signal with a copy of the spreading code (called replica), inducing a S/N gain. If the signal-to-noise plus interference ratio is large enough (at least 6 dB in [2]), the lock on a satellite signal is maintained.

Different signal modulations are implemented (e.g. BPSK, BOC, QPSK [3]), especially to enable the separation of different signals in the same frequency bands.

1.2 Ground Based Augmentation System

In order to preserve and augment availability (to counter the lack of GPS visibility for example) and continuity of accuracy and integrity, additional ranging sources are needed. One promising solution is the use of pseudo-satellites (called pseudolites, abbreviated PL) located on the ground. Pseudolites augment the

geometry provided by the satellite constellation. The availability of accuracy and integrity can be improved by one order of magnitude [4]. Typical applications are air traffic control in airports (for example ranging to improve vertical position accuracy or correction messages) and indoor navigation when the satellite visibility is too low [2].

1.3 Near/Far Problem

In the case of aircraft assistance for a landing approach, the pseudolite range should be 20 nautical miles (37 km) [2]. This requirement induces the emission of high-power pseudolite signals which might interfere with the satellite signals. For an aircraft close to a pseudolite, it might be impossible to acquire and track the satellite signals. Since the received power from a source is proportional to the inverse square of the distance to the pseudolite, the interference power decreases with distance. In a certain range, both satellites and pseudolites can be tracked. Far away, pseudolite signal is too weak to be tracked. These three zones are represented in figure 1.1.

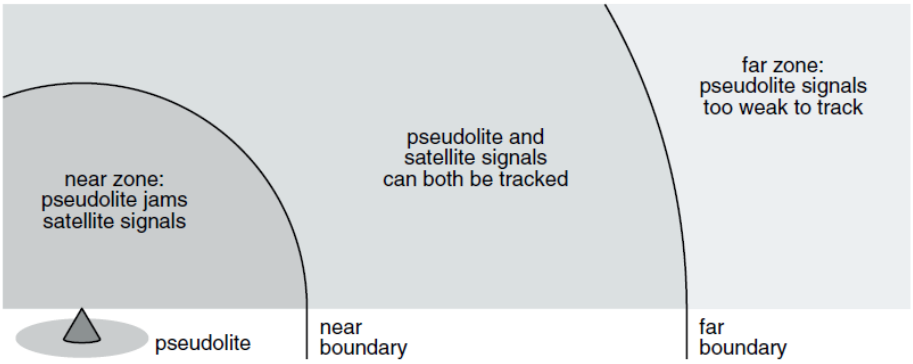

Figure 1.1: Zones of the near/far problem [2]

In order to mitigate these interferences, some solutions are proposed in [4]: frequency offset, new spreading codes and pulsed transmissions. This latter solution is described as the most effective one because GNSS receivers are robust against low-duty cycle pulsed interference. The pseudolite will interfere only during its activity. On the other hand, the pseudolite tracking will be less efficient than if it is continuously emitted. In [5], it is recommended to avoid pseudolite pulse overlapping because it reduces the ability of the receiver for signal tracking and increases the measurement noise. For this purpose, several pulsing schemes have been defined. Pseudolite pulses may be either synchronized or unsynchronized. A simple way for synchronization is the broadcasting of each pseudolite during a dedicated segment of the epoch. Some of the most well-known non-synchronized pulsing schemes are the RTCM (Radio Technical Commission for Maritime Use) and the RTCA (Radio Technical Commission for Aeronautics) standards. The first one defines a code emitted at 1.023 MHz in pulses: one segment of 1/11 code period (i.e. 93 chips) every code epoch of 1 ms and an extra segment every 10th epoch. This induces a mean pulse duty cycle of 10 % [6]. The second one defines a code emitted at 10.23 MHz in

pulses: 1997 segments of 140 code chips every 1 s. This induces a mean pulse duty cycle of 2.7 % [7]. For both standards, the time of emission is randomly generated by using a shift register. Therefore, pseudolites may interfere but two same pseudolites interfere seldom.

1.4 Front End

The main functional blocks of the analogue and digital front-end of the receiver are presented in the following. The principle objective of the front-end is to filter and condition the received signal for its later processing (determination of the pseudoranges). Here the correlation block is also considered as part of the digital front-end. The typical architecture of such a front-end is represented in figure 1.2.

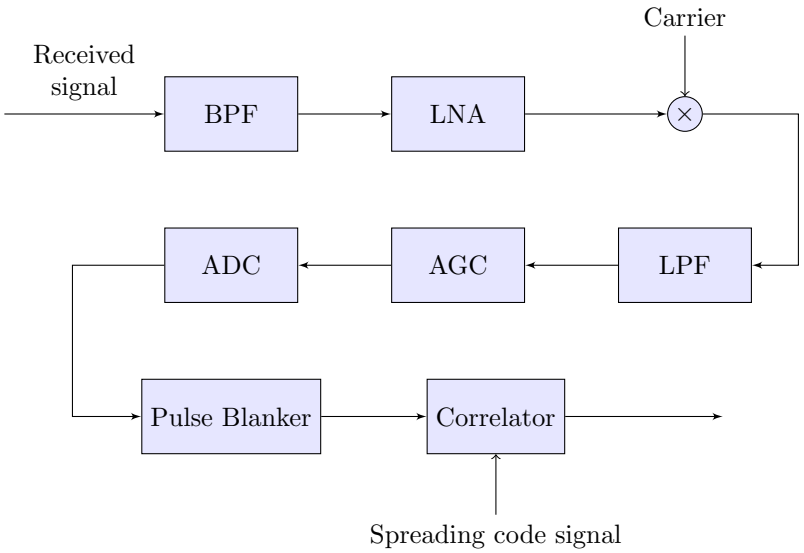

Figure 1.2: Typical architecture for GNSS front-end

Band-Pass Filter (BPF): It filters out all non-desirable signals (noise, interference) from the received signal and retains only the signal of interest (here the navigation signal for later processing).

Low-Noise Amplifier (LNA): This component amplifies very weak signals captured by the antenna.

Mixer: Its role is to down-convert the signal to baseband by a multiplication of the incoming signal with the output of a local oscillator with the same RF frequency.

Low-Pass Filter (LPF): Its aim is to reject frequencies beyond the desired band.

Automatic Gain Control (AGC): The role of the AGC is to regulate the signal power entering the Analogue-to-Digital Converter in order to adapt to variable antenna or front-end internal amplifier gains or changes of temperature. One usual technique is to use estimates of the noise-variance for the regulation [8].

Analogue-to-Digital Converter (ADC): The ADC converts the continuous signal to a discrete time digital representation. The quantization of signal amplitude is done on a number of levels equal to 2^N with N the number of bits. For one bit, for example, the digital signal will be equal to $+1$ when positive and -1 when negative. All samples above the maximal level are clipped. These processes induce so-called "quantization losses".

Blanker: This component blanks (i.e. puts to zero) all samples which are beyond the defined blanking threshold. The blanker is supposed to eliminate the high-power pulses which are likely to degrade the performance.

Correlator: This component multiplies the received signal with the spreading code replica and integrates the resulting product in order to "extract" the navigation signal originally drowned in the noise.

The output of the correlator is used later for signal acquisition, code and carrier phase estimation and demodulation.

Chapter 2

Objectives of the Thesis

In the frame of this study, pseudolites are typically operational in an area of few square kilometres and emit signals with high power in comparison to the power of signals transmitted by the satellites. On the one hand, this high level of power allows tracking the pseudolite signals over a wide range but on the other hand, this situation produces high interferences for the satellite signal acquisition, tracking and demodulation: the SNIR is susceptible to fall to such an extent that it is not possible to track a satellite navigation signal anymore. Therefore, the objective is to allow the tracking of pseudolites on a large range with limited impact on the satellite signal tracking.

In this work, the theoretical derivations which enable to determine the SNIR for satellite and pseudolite signal tracking will be developed. Then, a tool implemented in MATLAB will enable to validate the corresponding analytical models by providing quantitative results and estimate the precision of the established models. In a next part, some ideas to define an optimal pulsing scheme and an enhanced front-end receiver improving the performance will be proposed.

2.1 Operational Scenarios

The objective is to study the typical operational scenarios involving both satellite and pseudolite signals tracking, keeping in mind that all sources emit at the same or almost the same frequency:

- Tracking of the satellites without making use of pseudolite signals (standard scenario). In case of proximity with pseudolites, the receiver performance may be degraded (illustration on 2.1a).
- Tracking of satellites and one pseudolite (inter-operability in communication). This scenario is typical for the transmission of GNSS navigation information like satellite almanacs, clock or system time. Again, the transmitted pseudolite signal may disrupt the reception and processing of the satellite signals (illustration in 2.1b).
- Tracking of satellites and all pseudolites (inter-operability in navigation). The latter have typically the same role as satellites and therefore help to improve the localisation accuracy. A pseudolite emission is likely to

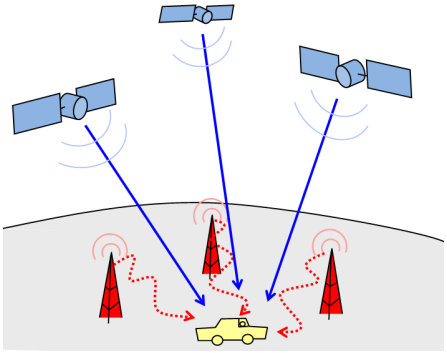

(a) Tracking of only satellites

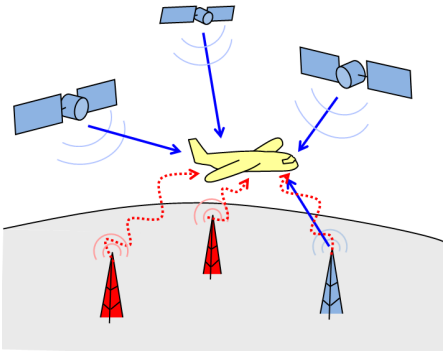

(b) Tracking of satellites and one pseudolite

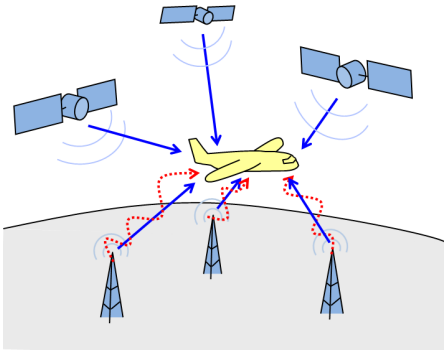

(c) Tracking of satellites and all pseudolites

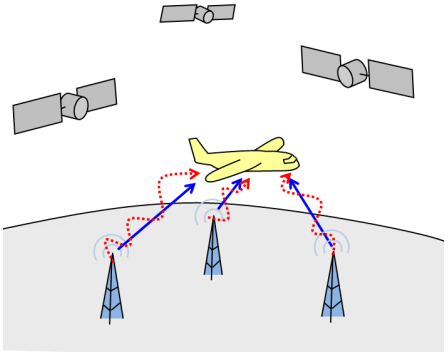

(d) Tracking of pseudolites only

Figure 2.1: Different operational scenarios involving pseudolite signals (tracked signals in blue, interfering signals in red)

interfere with the tracking of the satellite signal and also with the tracking of the signal from another pseudolite (illustration on 2.1c).

- Tracking of pseudolite signals only (inter-compatibility), typically in case of no satellite visibility (e.g. indoor navigation). Pseudolite mutual interference is possible (illustration in 2.1d).

2.2 Analytical Tools

It is essential to estimate the "quality" of the signal at the output of the front-end. The metric used is the SNIR. One solution is to simulate the behaviour of the front-end with Monte Carlo experiments on a software tool, but this process is very long, especially when many different parametres have to be studied. Moreover, it does not give as many insights as closed-form expressions, especially concerning the influence of parameters. The aim is therefore to exploit mathematical models giving directly the SNIR as a function of the parametres of the satellite and pseudolite signals as well as the front-end.

2.2.1 Existing Models

Model of Hegarty et Al.

This model established in [9] defines the ratio of S to $N_{0,\text{eff}}$ after correlation for satellite tracking when pulses are not blanked at all (pulse amplitude below the blanking threshold):

$$\frac{\mathcal{P}}{N_{0,\text{eff}}} = \frac{\mathcal{P}}{N_0 + I_{0,i} \cdot \text{DC}_i}$$

$$\text{with: } I_{0,i} = \int_{-\infty}^{\infty} S_C(f) S_{I_i}(f) df$$

$\mathcal{P}$	Power of the tracked signal
N_0	Noise power spectral density
DC_i	Duty cycle of the i-th low-level signal
$S_C(f)$	Normalized PSD of the reference spreading waveform
$S_{I_i}(f)$	Non-normalised PSD of the interfering signal of index i

Model of Cobb

The Cobb's model is the most encountered in literature dedicated to pseudolites. It is derived in [2] for the SNIR after correlation of the satellite signal tracking in the presence of a single pulse as:

$$\text{SNIR} = \frac{s \cdot (1 - \text{DC})}{p \cdot \text{DC} + (1 - \text{DC})}$$

This model has also been extended for pulse signal tracking in case of several non-overlapping pulses:

$$\text{SNIR} = \frac{s \cdot \text{DC}}{p \cdot (K_p - 1) \cdot \text{DC} + (1 - (K_p - 1) \cdot \text{DC})}$$

with:

$s = 10^{(S/N)_{\text{typ}}/10}$	Average signal-to-noise ratio without pseudolite interference
$p = 10^{(P/N)_{\text{typ}}/10}$	Ratio of pulse interference to noise
DC	Pseudolite pulse duty cycle
K_p	Number of non-overlapping pulses

The ratio P/N comes from the calculation of the worst-case cross-correlation expected between the tracked and the interfering C/A code signals, obtained by comparing each possible pair of C/A codes.

The advantages of this model are that the expression is straightforward and thus rather easy to calculate. Each contribution (tracked signal, noise, interference) can be clearly identified. Nevertheless, some limitations may be pointed out:

- The AGC (dynamic) and the blanking threshold amplitude are not considered.
- The contributions of noise and tracked signal are not taken into account during the pulse duty cycle.
- For calculation of interference contribution, the properties of partial cross-correlation should be considered during the pulse only (a section of epoch), instead of considering the cross-correlation over a complete code epoch. Moreover, the cross-correlations of this model are not evaluated for code delay expressed in fraction of chip, but only for an integer numbers of chips. The chip waveforms have an influence on the cross-correlation.
- This expression takes into account the maximal cross-correlation value which is the worst case that could occur only during a very small proportion of time, while most of the cross-correlation events between satellites and pseudolites will be much smaller.

2.2.2 Need for a New Analytical Model

Since the existing models appear either too conservative or inappropriate for a precise estimation of the SNIR for the presented scenarios, new analytical models will be derived for the general expression for the SNIR applied to the correlator output. The essential points of the mathematical derivations will be to consider the blanker and the AGC dynamic and also to establish a precise expression for the pulse interference contribution, depending on the signal type.

2.3 Pulsing Scheme

As exposed in section 1, the most efficient method to limit the impact of the pseudolites on satellite signal tracking is to make the pseudolite emits in pulses. As an illustration, let us consider a satellite signal received only during duty cycle of $(1 - \mathrm{DC})$ (i.e. a ratio equal to DC is blanked on the signal). The corresponding expression for the SNIR[1] is $\mathrm{SNIR} = \mathrm{SNIR}_0 \cdot (1 - \mathrm{DC})$ with SNIR_0 the SNIR without interference and DC the duty cycle of the interfering pulse. It can be noticed that the SNIR for satellite tracking is very sensitive to the value of DC.

As an example, for a SNIR_0 of 13 dB and a blanking duty cycle of 80 %, the SNIR becomes 6 dB which is the limit for signal tracking [2]. This may correspond to the presence of a pulse – completely blanked – with a duty cycle of 80 %. In case of the presence of interference during satellite signal blanking (e.g. the pulse is not blanked), the SNIR will degrad more. For the same case of $\mathrm{DC} = 80\%$ but now with interference power of 90 dBW, the SNIR is reduced from 6 to 0.3 dB (calculated with the mathematical model that will be derived later).

With these first considerations, it becomes clear that an efficient pulsing scheme has to be defined in order to track pseudolite signals in an area with limited impact on satellite signal tracking. Currently, the times of occurrence

[1] Since $\mathrm{SNIR}[x] = \frac{\mathcal{E}^2[x]}{\mathrm{var}[x]}$, this expression is justified by the fact that the expectation value and the variance are both proportional to $1 - \mathrm{DC}$.

of different pulses are not synchronized, as recommended in RTCA and RTCM standards. The current study may be a basis to show that, on contrary, by maximizing the overlapping between pulses, the degradation of performance in the tracking of satellite signal can be limited. Furthermore, if this "common" time of emission is known at the receiver side, it may give opportunities to enhance the receiver signal processing for a better performance.

Chapter 3

Baseline Mathematical Model

3.1 Introduction

The objective of this chapter is to establish a closed-form expression for the SNIR of the correlator output, applicable for each situation of figure 2.1. As mentioned in the previous section, the existing mathematical models are not fully satisfying to estimate the real behaviours of the receiver. The objective of this work is to consider some aspects which are not included in Cobb's model. This concerns especially:

- AGC dynamics
- Blanker (a pulse can be partially blanked)
- Consideration of tracked signal and noise also during pulse duty cycle
- Effective properties of the code (i.e. properties of the code restricted to its duty cycle activity instead of the code during the entire epoch)
- Consideration of any possible delay value between navigation signals (not necessarily expressed in number of chips, but also fraction of chip)

One main difficulty comes from the non-linearity of the blanker. Indeed, it is complex to express the impact of this component on a signal composed of deterministic signals (navigation signals) and a stochastic signal (noise).

The objective of this section is in a first part to introduce all definitions and approximations needed for the mathematical derivations, and in a second part, to establish a baseline model with the consideration of only linear functions in the front-end. It will be therefore considered that there is no blanker and no clipping (this could also correspond to the presence of blanker and clipping but with signals always below the respective thresholds), the regulation is constant and the rest of the chain is in linear regime. The aim is to deliver the methods and the baseline expressions useful for the establishment of the advanced models in the next section. In this purpose, a method for the calculation of interference contribution in the SNIR will be proposed.

A general front-end (after down-converting) will be considered with the modelling of the components described in figure 1.2 in page 6.

In section 4, the models will be extended with consideration of the blanker and with application of the definitions and approximations introduced in this section.

3.2 Definitions

The components of the front-end are modelled by mathematical functions (figure 3.1). These functions and the involved signals are defined in the following.

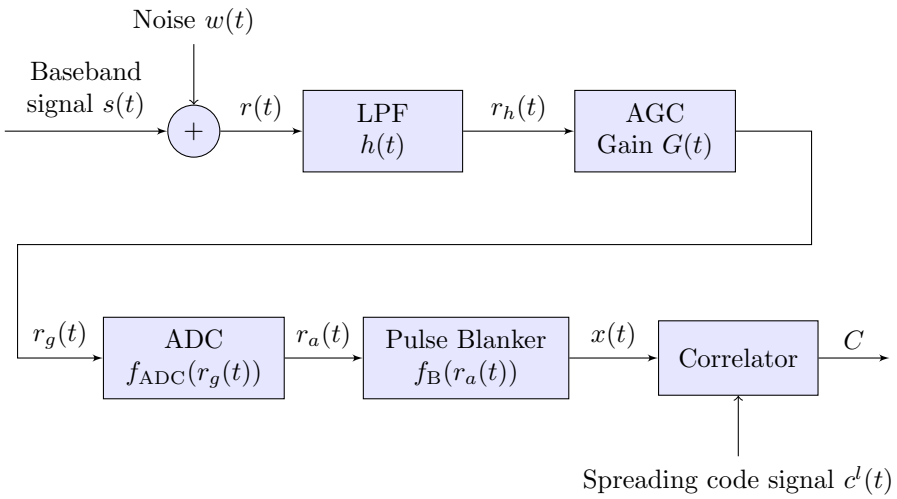

Figure 3.1: Front-end diagram

3.2.1 Spreading Code Signal

The spreading code signal is composed of the chips, each modulated with a waveform depending on the signal modulation (BPSK, BOC(1,1), etc.)

$$c^k(t) = \sum_{m=-\infty}^{\infty} c_m^k p^k(t - mT_c^k)$$

$c^k(t)$	Spreading code signal of emitter k (c^k has its values in $\{-1, 1\}$).
c_m^k	Chip bit (index m) of signal $c^k(t)$.
$p^k(t)$	Chip waveform of signal $c^k(t)$.
T_c^k	Chip duration of signal $c^k(t)$.

3.2.2 Navigation Signal at Receiver Antenna Output

The navigation signal is the received signal emitted by a GNSS source (satellite or pseudolite) down-converted. It corresponds to the delayed spreading code signal scaled with the received power at the receiver antenna output port.

For a source emitting continuously (a satellite typically):

$$\begin{aligned} s^k(t) &= \sqrt{\mathcal{P}^k}\; c^k\left(t-\tau^k\right) \\ &= \sqrt{\mathcal{P}^k}\sum_{m=-\infty}^{\infty} c_m^k p^k(t-mT_c^k-\tau^k) \end{aligned}$$

For a source emitting in pulses (a pseudolite typically):

$$\tilde{s}^k(t) = \begin{cases} s^k(t) & t \in \text{pulse intervals} \\ 0 & \text{otherwise} \end{cases}$$

A pulsed signal is assumed to have always the same pulse characteristics (duration and repetition frequency).

$s^k(t)$	Continuous (i.e. not pulsed) navigation signal received from source k (satellite or pseudolite).
$s^l(t)$	Tracked signal (continuous navigation signal from source l).
$\mathcal{P}^k$	Instantaneous power of signal $s^k(t)$ at the receiver input.
τ^k	Delay of the signal $s^k(t)$.
$\tilde{s}^k(t)$	Pulsed navigation signal received from source k.
T_p^k	Duration of one pulse of the signal from source k.
f_p^k	Pulse repetition frequency of signal from source k.
$\mathrm{PDC}^k = T_p^k f_p^k$	Pulse duty cycle of signal from source k.

Note: The origin of time t is defined such that the tracked navigation signal is not delayed: for the tracking of the signal from a source l, $\tau^l = 0$ and $s^l(t) = \sqrt{P^l}c^l(t)$.

3.2.3 Noise

The noise component encompasses the thermal noise and other similar wideband interferences. The noise $w(t)$ is assumed to have a Gaussian distribution called $p(w)$ and to be white, with a power spectral density N_0 (supposed on an infinite bandwidth before filtering).

3.2.4 Aggregated Received Signal

The signal received by the front-end is the sum of signals of all sources (satellites and pseudolites) and noise:

$$\begin{aligned} r(t) &= s(t) + w(t) \\ &= \sum_{k_s=1}^{K_\mathrm{s}} s^{k_s}(t) + \sum_{k_p=1}^{K_\mathrm{p}} \tilde{s}^{k_p}(t) + w(t) \end{aligned}$$

$r(t)$	Received signal
$s(t)$	Sum of all navigation signals received
$s^{k_s}(t)$	GNSS signal (continuous) received from **satellite** k_s

$\tilde{s}^{k_p}(t)$	GNSS signal (pulsed) received from **pseudolite** k_p
K_s	Number of satellites
K_p	Number of pseudolites

3.2.5 Signal After LPF

The low-pass filter $h(t)$ is assumed to be a brickwall filter of bandwidth $\beta/2$ (β is the equivalent passband bandwidth) in frequency domain.

$$r_h(t) = h(t) * r(t)$$

- Filtering of a received navigation signal:

$$\begin{aligned} h(t) * s^k(t) &= h(t) * \left(\sqrt{\mathcal{P}^k} \sum_{m=-\infty}^{\infty} c_m^k p^k(t - mT_c^k - \tau^k) \right) \\ &= \sqrt{\mathcal{P}^k} \sum_{m=-\infty}^{\infty} c_m^k \left(h(t) * p^k(t - mT_c^k - \tau^k) \right) \\ &= \sqrt{\mathcal{P}^k} \left(h * p^k \right)(t) * \sum_{m=-\infty}^{\infty} c_m^k \delta(t - mT_c^k - \tau^k) \end{aligned}$$

- Filtering of the noise: $n(t) = (h * w)(t)$
  The noise is white only on the preserved bandwidth and $n(t) \sim \mathcal{N}(0, \sigma^2)$ with $\sigma = \sqrt{N_0 \beta}$ the noise standard deviation after filtering.

3.2.6 Signal After AGC

The AGC applies a gain $G(t)$ on the input signal. The received power is estimated on a time interval RT (for Recovery Time). The gain value is set such that the output signal is normalized with respect to the estimated entry power. At the AGC output:

$$\begin{aligned} r_g(t) &= G(t) \cdot r_h(t) \\ G^2(t) &= \frac{1}{\frac{1}{\mathrm{RT}} \int_{t-\mathrm{RT}}^{t} {r_h}^2(t) dt} \end{aligned}$$

Remark: The effect of the AGC can be observed in figure 3.2a on page 17. One notices the regulation of the signal to the steady value of 1 (black dotted line).

3.2.7 Signal After ADC

The ADC has three effects on the input signal: sampling, quantization of signal, and clipping of parts of the signal above the clipping voltage L.

- Sampling: The continuous signal is sampled at frequency f_s. Since $\beta/2$ is the baseband bandwidth, the condition of Nyquist is fulfilled for $f_s = \beta$.
- Quantization: The samples of the signal take discrete values. The signal amplitude scale $[-L, L]$ is divided into quantization levels of equal distance to each other. This process implies quantization losses.

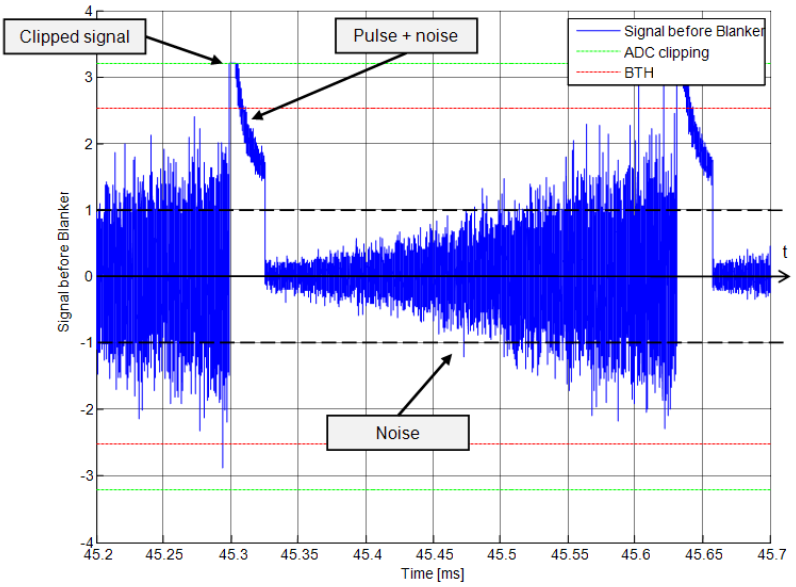

(a) Signal after ADC

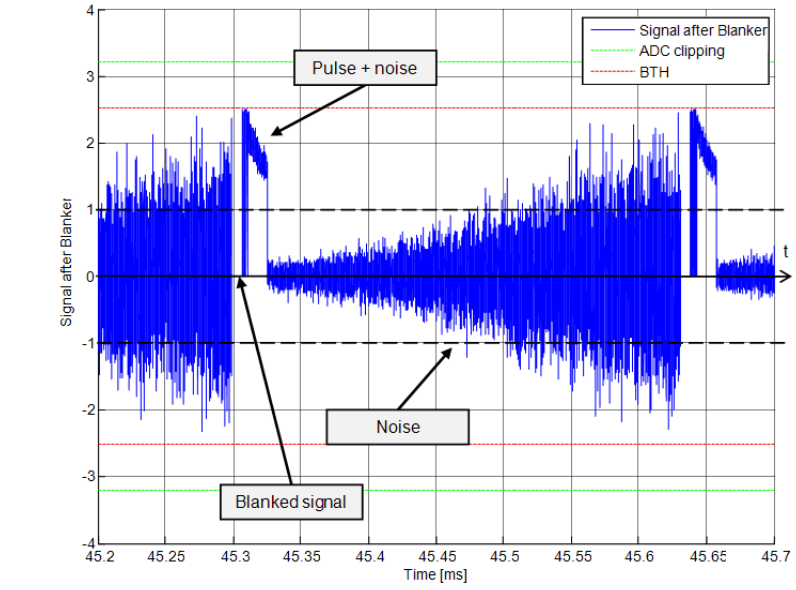

(b) Signal after blanker

Figure 3.2: Representations of a signal composed of noise, navigation signal (drown in the noise) and constant pulse (no modulation). The parameters are chosen arbitrary.

- Clipping: The signal is clipped when exceeding the threshold:

$$f_{\mathrm{ADC}}(r_g(t)) = \begin{cases} -L & \text{if } r_g(t) < -L \\ L & \text{if } r_g(t) > L \\ r_g(t) & \text{otherwise} \end{cases}$$

Remark: The effect of the ADC can be observed in figure 3.2a on page 17. One notices the clipping of the signal at 3.2 which is the clipping threshold (green dotted line).

3.2.8 Signal After Blanker

When the blanker is activated, the blanking threshold BTH is assumed to be defined between 0 and the ADC clipping voltage L. With this consideration, the clipping voltage has no longer to be taken into consideration. Signal at the blanker output:

$$x(t) = f_{\mathrm{B}}\left(r_a(t)\right) = \begin{cases} r_a(t) & \text{if } |r_a(t)| < \mathrm{BTH} \\ 0 & \text{otherwise} \end{cases}$$

Note: f_{B} is defined and odd on $\mathbb{R}$, and linear on $[-\mathrm{BTH}, \mathrm{BTH}]$. These properties will be useful for the mathematical derivations.

Remark: The effect of the blanker can be observed in figure 3.2b on page 17. One notices the blanking of the samples which were previously above the blanking threshold (red dotted line).

3.2.9 Signal After Correlation

For the tracking of the signal from source l, the correlator multiplies the input signal $x(t)$ with the spreading code signal $c^l(t)$ and integrates during a time period T. This value is normalized by the integration time.

$$C(i) = \frac{1}{T}\int_{(i-1)T}^{iT} x(t)c^l(t)dt$$

In the following, C will be written without index and it will correspond to $C(1)$ i.e. $\frac{1}{T}\int_0^T x(t)c^l(t)dt$.

Remark: It will be usually considered that the index l stands for the tracked navigation signal (no distinction between satellite and pseudolite) whereas the index k stands for an interfering signal.

3.2.10 Signal-to-Noise Plus Interference Ratio

The SNIR is the metrics reflecting the quality of the correlation signal. The developed expression will aim at modelling this function depending on the parameters.

$$\mathrm{SNIR}[C] = \frac{\left(\mathcal{E}[C]\right)^2}{\mathrm{var}[C]}$$

3.3 Approximations

In order to make the derivations easier, the following assumptions are assumed fulfilled.

Approx. 1 The chip waveforms $p^k(t)$ are assumed to be constant on intervals with values in $\{-1, 1\}$. This is the case for the common chip waveforms: BPSK, BOC, etc.

Approx. 2 Only noise and navigation signals are received. Other existing signals are not taken into account.

Approx. 3 The power of the satellite navigation signals is assumed to be much smaller than the noise power.

Approx. 4 A pulse is assumed to occur at a random time.
Since the spreading code is deterministic and the sum of the bits on the period is close to 0 (balancedness of the GNSS codes), the assumption induces that the spreading code during the pulse is a random portion of the original deterministic code. Thus, the spreading code during the pulse is considered random and balanced. The same property is deduced for a continuous signal out of the pulse. Consequently, it is considered that all spreading codes are a random and uniform succession of bits 1 and -1:

$$\mathcal{E}\left[c_m^k\right] = 0$$
$$\mathcal{E}\left[c_m^k c_{m'}^k\right] = \delta_{m,m'}$$

Approx. 5 It is considered that a pulse occurs and terminates always simultaneously with the front edge of a chip, i.e. at a time kT_c with k an integer. A consequence of this assumption and Approx. 4 will be that the signal $x(t)$ with t during a pulse is independent of $x(u)$ with u out of the pulse.

Approx. 6 It is assumed that the cumulative duration of the pulses during a time interval $[t, t+T], \forall\ t$ is always the same and equal to $\mathrm{DC} \cdot T$ (with DC the duty cycle of the considered pulse). This hypothesis can be considered valid when the pulse repetition frequency is high with respect to $\frac{1}{T}$.

Approx. 7 All signals are considered real. The down-conversion of received signal into baseband induces actually complex signals, but if the phase is perfectly known (thanks to a phase-locked loop), it may be possible to take only the real part.

Approx. 8 It is very complex to handle the function $h(t) * p^k(t)$ since the waveform has ripples. It is much easier to work on a waveform constant on intervals. Therefore, it will be considered that the filter $h(t)$ has only a small effect on the navigation signals, i.e. $h(t) * p^k(t) \approx p^k(t)$.
Condition of validity: For modulations with PSD concentrated around $1/T_c$ (e.g. BPSK, BOC(1,1)), the signal is preserved for $\beta/2 \gg 1/T_c$.
This simplification may appear conservative because the condition of validity is not necessary fulfilled in reality. Nevertheless, this condition will be assumed to be valid for most of the derivations. It will be nonetheless precised when the filter is considered (e.g. for the expression of interference contribution).

Approx. 9

- The ADC sampling fulfils the Nyquist condition ($f_s = \beta$). Aliasing is thus avoided.
- No quantization loss in the ADC: it is considered that the ADC is the identity function on $[-L, L]$. Quantization losses can be small for a large number of bits in the quantization (e.g. 8 bits).

A consequence is that the noise is white and:

$$\mathcal{E}[n(t)] = 0$$
$$\mathcal{E}[n^2(t)] = \sigma^2 = N_0\beta$$

Moreover, since $\mathrm{BTH} \leq L$, it is useless to consider the possible clipping. Finally, in these conditions, the ADC is the identity function on $\mathbb{R}$ and $r_a(t) = r_g(t)$.

Approx. 10 No transient effects of the AGC regulation: the regulation is either very fast or very slow with respect to the dynamics of the navigation signals. Typical signals after the AGC are represented in figure 3.3. Consequently, two cases are considered for constant signal power during a pulse of constant power and outside pulses:

- Fast AGC: instantaneous regulation of the signal when a pulse occurs or terminates. According to Approx. 3 (power of satellite signals negligible with respect to noise power):
  - Outside the pulses, $G(t)$ has a constant value: $G(t) = G_{\mathrm{POff}} = \frac{1}{\sigma}$
  - During a pulse, $G(t)$ has a constant value: $G(t) = G_{\mathrm{POn}} = \frac{1}{\sqrt{\sigma^2 + \sum_k \mathcal{P}^k}}$
- Slow AGC: no regulation dynamics, $G(t)$ is constant: $G(t) = \frac{1}{\sqrt{\sigma^2 + \sum_k \mathcal{P}^k \mathrm{PDC}^k}}$ In order to handle general parameters in the derivations, it can be equally written that $G(t) = G_{\mathrm{POff}}$ or $G(t) = G_{\mathrm{POn}}$.

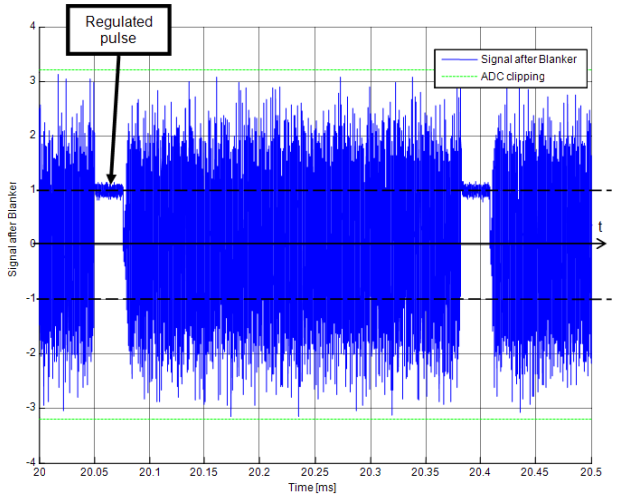

(a) Fast AGC

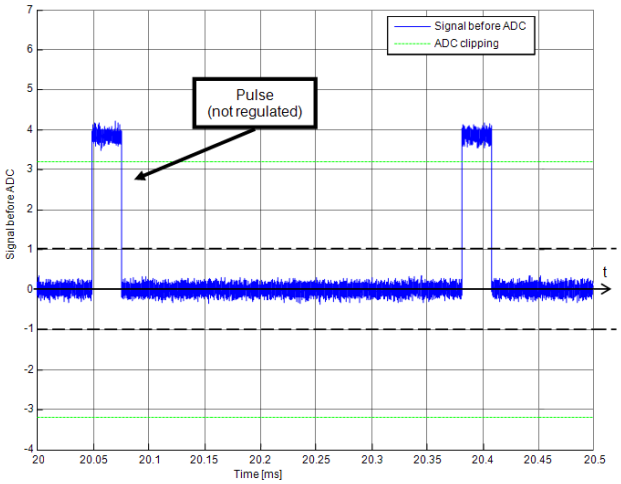

(b) Slow AGC

Figure 3.3: Signal representation (time domain) for noise and constant pulse (no modulation) for two ideal AGC behaviours

3.4 Expression for the Mean and Variance of the Correlator Output

As explained in section 3.1, no blanker and no clipping are considered in order to handle only linear functions. The regulation is assumed constant: $G(t) = G_0$. The signals are all emitted continuously (i.e. not pulsed). The objective here is to derive an expression for the SNIR at the correlator output for the tracking of a navigation signal, either emitted by a satellite or a pseudolite. The SNIR reflects the "quality" of the signal and is directly related to the performance of the processes located later in the chain like the phase and delay regulations of the tracked signal. Indeed, for too low SNIR, the tracking may be lost.

Since the SNIR is expressed as $\mathrm{SNIR}[C] = \frac{(\mathcal{E}[C])^2}{\mathrm{var}[C]}$, the mean and the variance of the correlator output C will be derived in this section.

3.4.1 Expressions for the Mean of the Correlator Output

$$\begin{aligned}
\mathcal{E}[C] &= \mathcal{E}\left[\frac{1}{T}\int_0^T \left(G_0 \cdot \left(\sum_k s^k(t) + n(t)\right)\right) \cdot c^l(t) dt\right] \\
&= \frac{G_0}{T}\int_0^T \mathcal{E}\left[\left(\sum_k s^k(t) + n(t)\right) \cdot c^l(t)\right] dt \\
&= \frac{G_0}{T}\int_0^T \left(\sum_{k,\ k\neq l} \mathcal{E}\left[s^k(t)\cdot c^l(t)\right] + \mathcal{E}\left[s^l(t)\cdot c^l(t)\right] + \mathcal{E}\left[n(t)\cdot c^l(t)\right]\right) dt
\end{aligned}$$

From the property of independence and balancedness of the spreading codes (Approx. 4), it is deduced that $\mathcal{E}\left[s^k(t)\cdot c^l(t)\right] = \mathcal{E}\left[s^k(t)\right]\cdot\mathcal{E}\left[c^l(t)\right] = 0$. Moreover, $\mathcal{E}\left[n(t)\cdot c^l(t)\right] = \mathcal{E}\left[n(t)\right]\cdot\mathcal{E}\left[c^l(t)\right] = 0$. Therefore:

$$\mathcal{E}[C] = \frac{G_0}{T}\int_0^T \mathcal{E}\left[s^l(t)\cdot c^l(t)\right] dt$$

By definition, $s^l(t) = \sqrt{\mathcal{P}^l}c^l(t)$, hence:

$$\begin{aligned}
\mathcal{E}[C] &= \frac{G_0}{T}\sqrt{\mathcal{P}^l}\int_0^T \mathcal{E}\left[\left(c^l(t)\right)^2\right] dt \\
&= G_0\sqrt{\mathcal{P}^l}
\end{aligned}$$

3.4.2 Expression for the Variance of the Correlator Output

$$\mathrm{var}[C] = \mathcal{E}\left[C^2\right] - \left(\mathcal{E}\left[C\right]\right)^2$$

$$\mathcal{E}\left[C^2\right] = \frac{{G_0}^2}{T^2}\int_0^T\int_0^T \mathcal{E}\left[\left(\sum_k s^k(t)+n(t)\right)\cdot c^l(t)\right.$$
$$\left.\cdot\left(\sum_{k'} s^{k'}(u)+n(u)\right)\cdot c^l(u)\right]dtdu$$
$$= \frac{{G_0}^2}{T^2}\int_0^T\int_0^T\left(\sum_k\sum_{k'\neq l}\mathcal{E}\left[s^k(t)c^l(t)s^{k'}(u)c^l(u)\right]\right.$$
$$+\sum_{k\neq l}\mathcal{E}\left[s^k(t)c^l(t)s^l(u)c^l(u)\right]+\mathcal{E}\left[s^l(t)c^l(t)s^l(u)c^l(u)\right]$$
$$+\mathcal{E}\left[n(t)c^l(t)n(u)c^l(u)\right]+\sum_k\mathcal{E}\left[s^k(t)c^l(t)n(u)c^l(u)\right]$$
$$\left.+\sum_{k'}\mathcal{E}\left[n(t)c^l(t)s^{k'}(u)c^l(u)\right]\right)dtdu$$

Each term of the double integral is derived in the following:

- For $k\neq k'$ and $k'\neq l$:
  $\mathcal{E}\left[s^k(t)c^l(t)s^{k'}(u)c^l(u)\right] = \mathcal{E}\left[s^{k'}(u)\right]\cdot\mathcal{E}\left[s^k(t)c^l(t)c^l(u)\right] = 0$
  Therefore:
  $\sum_k\sum_{k'\neq l,k'\neq k}\mathcal{E}\left[s^k(t)c^l(t)s^{k'}(u)c^l(u)\right]+\sum_{k\neq l}\mathcal{E}\left[s^k(t)c^l(t)s^l(u)c^l(u)\right]=0$
- $\mathcal{E}\left[s^l(t)c^l(t)s^l(u)c^l(u)\right] = \mathcal{P}^l\mathcal{E}\left[\left(c^l(t)\right)^2\left(c^l(u)\right)^2\right] = \mathcal{P}^l$
- Since $n(t)$ is white noise:
  $\mathcal{E}\left[n(t)c^l(t)n(u)c^l(u)\right] = \mathcal{E}\left[n(t)n(u)\right]\mathcal{E}\left[c^l(t)c^l(u)\right] = N_0\delta(t-u)\mathcal{E}\left[c^l(t)c^l(u)\right]$
- $\mathcal{E}\left[s^k(t)c^l(t)n(u)c^l(u)\right] = \mathcal{E}\left[n(u)\right]\cdot\mathcal{E}\left[s^k(t)c^l(t)c^l(u)\right] = 0$
  Therefore:
  $\sum_k\mathcal{E}\left[s^k(t)c^l(t)n(u)c^l(u)\right]+\sum_{k'}\mathcal{E}\left[n(t)c^l(t)s^{k'}(u)c^l(u)\right]=0$

Hence:

$$\mathcal{E}\left[C^2\right] = \frac{{G_0}^2}{T^2}\int_0^T\int_0^T\left(\sum_{k\neq l}\mathcal{E}\left[s^k(t)s^k(u)c^l(t)c^l(u)\right]\right.$$
$$\left.+N_0\delta(t-u)\mathcal{E}\left[c^l(t)c^l(u)\right]+\mathcal{P}^l\right)dtdu$$
$$= {G_0}^2\cdot\left(\sum_{k\neq l}\mathcal{E}\left[\left(\frac{1}{T}\int_0^T s^k(t)c^l(t)dt\right)^2\right]+\frac{N_0}{T}+\mathcal{P}^l\right)$$

Finally, one deduces the final expression for the variance:

$$\mathrm{var}\left[C\right] = {G_0}^2\cdot\left(\sum_{k\neq l}\mathrm{var}\left[\frac{1}{T}\int_0^T s^k(t)c^l(t)dt\right]+\frac{N_0}{T}\right)$$

The term $\mathrm{var}\left[\frac{1}{T}\int_0^T s^k(t)c^l(t)dt\right]$ is called the *interference contribution* from source k.

3.5 Expression for the Interference Contribution

In the previous section, the *interference contribution* to the SNIR has been expressed. The aim here is to derive explicit expressions for this term. In the first part, the relation with the SSC (Spectral Separation Coefficient) will be derived. This latter method has been often encountered in the literature about GNSS interference but may be too conservative in specific situations. In a second part, the relation with the waveforms convolution will be established in order to deliver a better expression for the *interference contribution*. And in the last part, the condition of application of each method will be discussed.

3.5.1 Spectral Separation Coefficient

This method is usually employed in the literature (e.g. [2], [9]). The *Spectral Separation Coefficient*, abbreviated in SSC, is a parameter defined for a navigation signal $s^k(t)$ (from source k) and a spreading code signal $c^l(t)$ (from source l) as:

$$\mathrm{SSC} = \int_{-\infty}^{\infty} |H_\beta(f)|^2 \cdot G_{s^k}(f) G_{c^l}(f) df = \int_{-\frac{\beta}{2}}^{\frac{\beta}{2}} G_{s^k}(f) G_{c^l}(f) df \tag{3.1}$$

As an illustration, the PSD of a BPSK signal is represented on 3.4 on page 25.

For a signal $s^k(t)$ with a power spectral density (PSD) S_{s^k}, G_{s^k} is the normalized power spectral density, defined as:

$$G_{s^k}(f) = \frac{S_{s^k}(f)}{\int_{-\infty}^{\infty} S_{s^k}(f) df} = \frac{S_{s^k}(f)}{\mathcal{P}^k}$$

Remark: $G_{s^k}(f) = S_{c^k}(f) = G_{c^k}(f)$, since $c^k(t)$ is normalized.

This method is used to express the interference contribution for an interfering navigation signal, but may be difficult to interpret because expressed in frequency domain without parameters such as the delay τ^k between the navigation signals. Therefore, it is legitimate to wonder if this expression is relevant to model the contribution of interference in the SNIR, or at least to give a worst case. For this purpose, the general expression of the interference contribution has been derived in appendix B in order to obtain the relation between the *interference contribution* and the SSC. The filter h_β has been taken into consideration. With the assumption that $T_c \ll T$, the following relation is deduced:

$$\left\langle \mathrm{var}\left[\frac{1}{T} \int_0^T \left(h_\beta * s^k\right)(t)\, c^l(t)\, dt \right] \right\rangle_{\tau^k} = \frac{\mathcal{P}^k}{T} \int_{-\frac{\beta}{2}}^{\frac{\beta}{2}} G_{c^l}(f) \cdot G_{s^k}(f) df = \frac{\mathcal{P}^k}{T} \mathrm{SSC} \tag{3.2}$$

It is reminded that τ^k is included in the explicit expression of the interfering signal: $s^k(t) = \sqrt{\mathcal{P}^k} c^k(t - \tau^k)$. It is noticed that the SSC gives the interference contribution averaged over the delay τ^k between the spreading code signals. Therefore, the SSC is relevant for navigation signals whose delay is rapidly

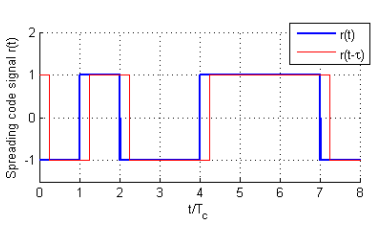

(a) Signal in time domain

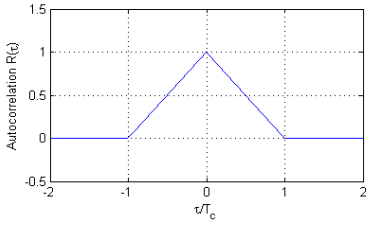

(b) Autocorrelation function

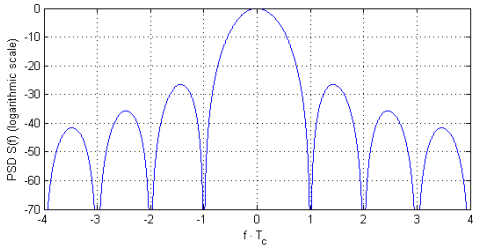

(c) Power spectrum density (Fourier transform of the autocorrelation function), logarithmic Y-axis

Figure 3.4: Representations for a BPSK signal

changing during the integration time. This is typically the case when considering at least one satellite signal (as tracked or interfering signal) because the delay evolves rapidly due to fast changing satellite position and Doppler effect.

A contrario, the delay τ between two navigation signals from pseudolites can be considered constant, and therefore the use of the SSC method seems not to be appropriate.

3.5.2 Waveform Convolution Coefficient

As explained previously, the use of the SSC is not appropriate for a fixed delay between two navigation signals, which is the case for pseudolites. The general expression for the *interference contribution* has been derived in appendix C in order to get an expression which is easier to understand and to handle. Contrary to the SSC, this expression should take into consideration a specific delay τ^k between the two considered spreading code signals. It is deduced from derivations of appendix C:

$$\operatorname{var}\left[\frac{1}{T}\int_0^T \left(h_\beta * s^k\right)(t)\, c^l(t)\, dt\right] = \mathcal{P}^k \frac{T_c}{T} \operatorname{WCC}\left(\tau^k\right)$$

with the *Waveform Convolution Coefficient* defined as:

$$\operatorname{WCC}\left(\tau^k\right) = \left(\frac{1}{T_c}\left(h_\beta * p^k * p^l\right)\left(\tau^k\right)\right)^2 * \sum_{m=-\infty}^{\infty} \delta\left(\tau^k - kT_c\right)$$

Discussion:

- Relation between SSC and WCC: $\text{SSC} = T_c \cdot \left\langle \text{WCC}\left(\tau^k\right) \right\rangle_{\tau^k}$
- The notation $\text{WCC}\left(\tau^k\right)$ comes from *Waveform Convolution Coefficient*. The term "coefficient" is used here because the function $\text{WCC}(\tau^k)$ has its values in $[0, 1]$, since the considered chip waveforms take values in $\{-1, 1\}$ (Approx. 1). To show this, the envelope of three succesive waveforms is plotted in figure 3.5 in red, blue and green, respectively. The envelope of WCC – which is the sum of each succesive waveforms – is represented with the dotted black line.
- Similarly to the noise contribution, the interference contribution is proportional to $\frac{1}{T}$.
- Since the chip waveforms are defined on $[0, T_c]$, the term $\frac{1}{T_c}\left(h_\beta * p^k * p^l\right)$ is interpreted as the normalized convolution of p^l with $\left(h_\beta * p^k\right)$.
- It is proved that the SSC does not give the worst case. For example in figure 3.6 on page 27, the worst case corresponds to WCC = 1, but the mean value of WCC (corresponding to $\frac{\text{SSC}}{T_c}$) is $\frac{2}{3}$.

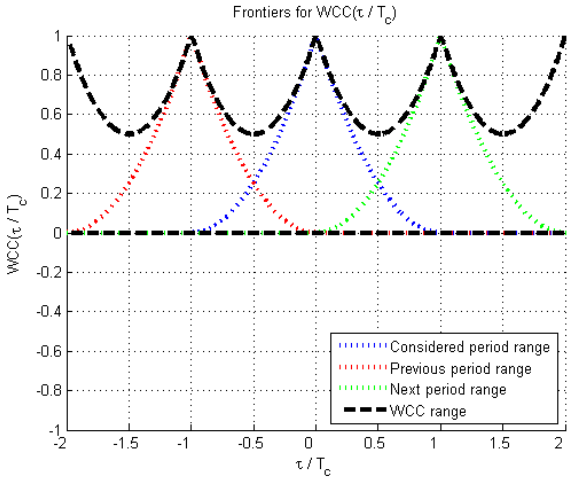

Figure 3.5: Frontiers for one pattern of the WCC

Some examples of calculation of WCC will be now given. First, the following steps are applied for the calculation of the *Waveform Convolution Coefficient*:

- Convolution of the (filtered) patterns of each navigation signal and normalization
- Squaring of the convolution
- Reproduction and adding of same patterns every T_c

The determination of WCC is illustrated for BPSK-BPSK, BPSK-BOC(1,1) and BOC(1,1)-BOC(1,1) in figures 3.6 (p. 27), 3.7 (p. 28) and 3.8 (p. 29), respectively. The mean value corresponds to $\frac{\text{SSC}}{T_c}$. For the sake of simplicity, no filter is considered.

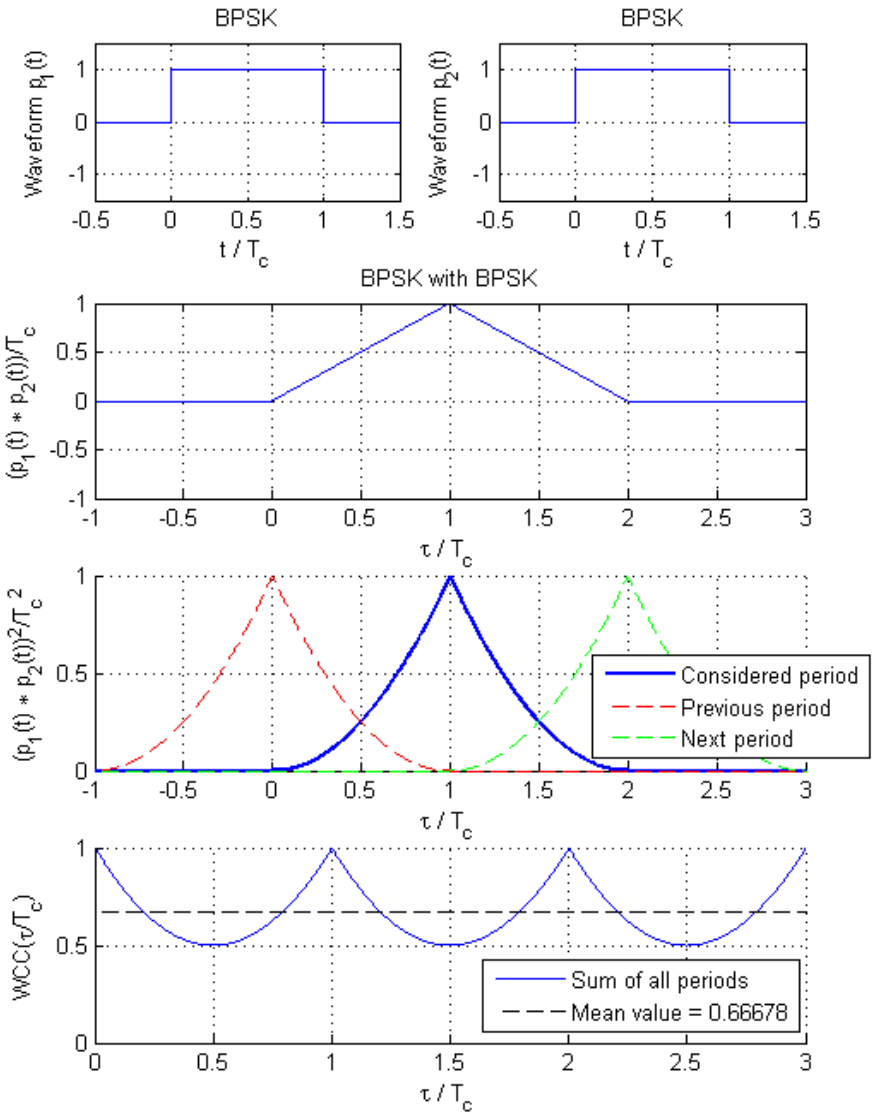

Figure 3.6: Chip waveform convolution method for BPSK-BPSK

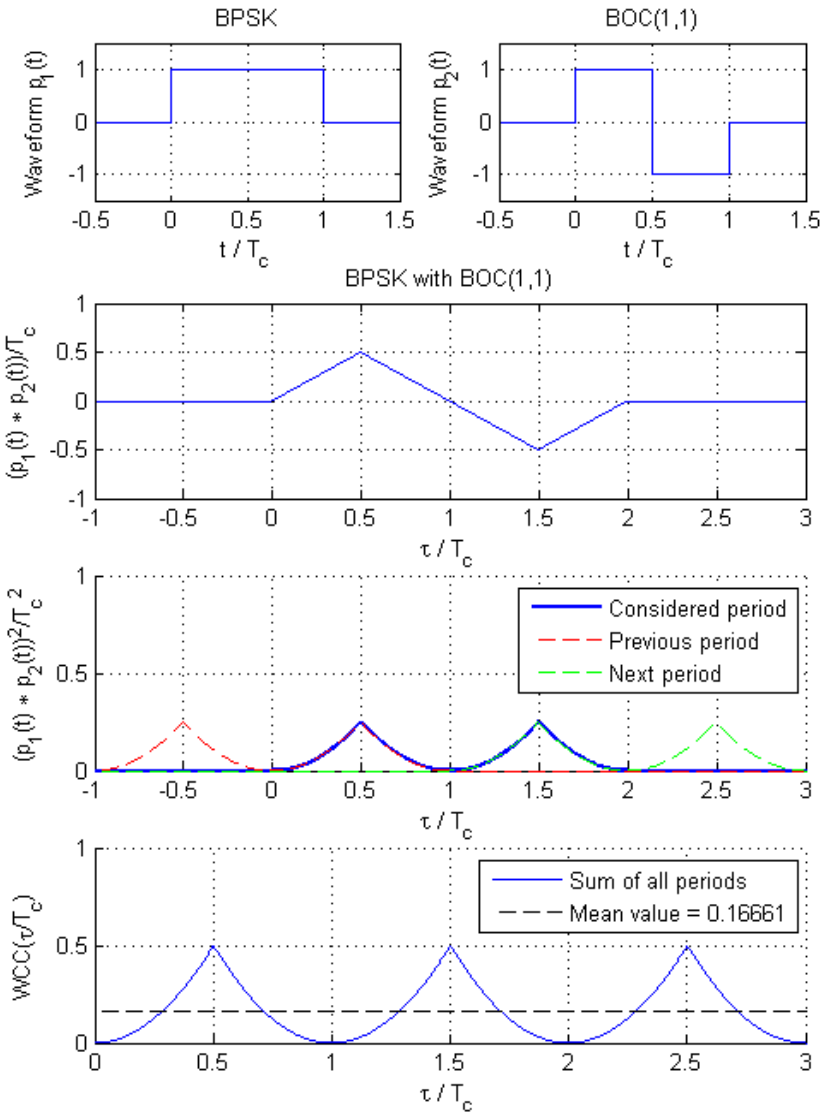

Figure 3.7: Chip waveform convolution method for BPSK-BOC(1,1)

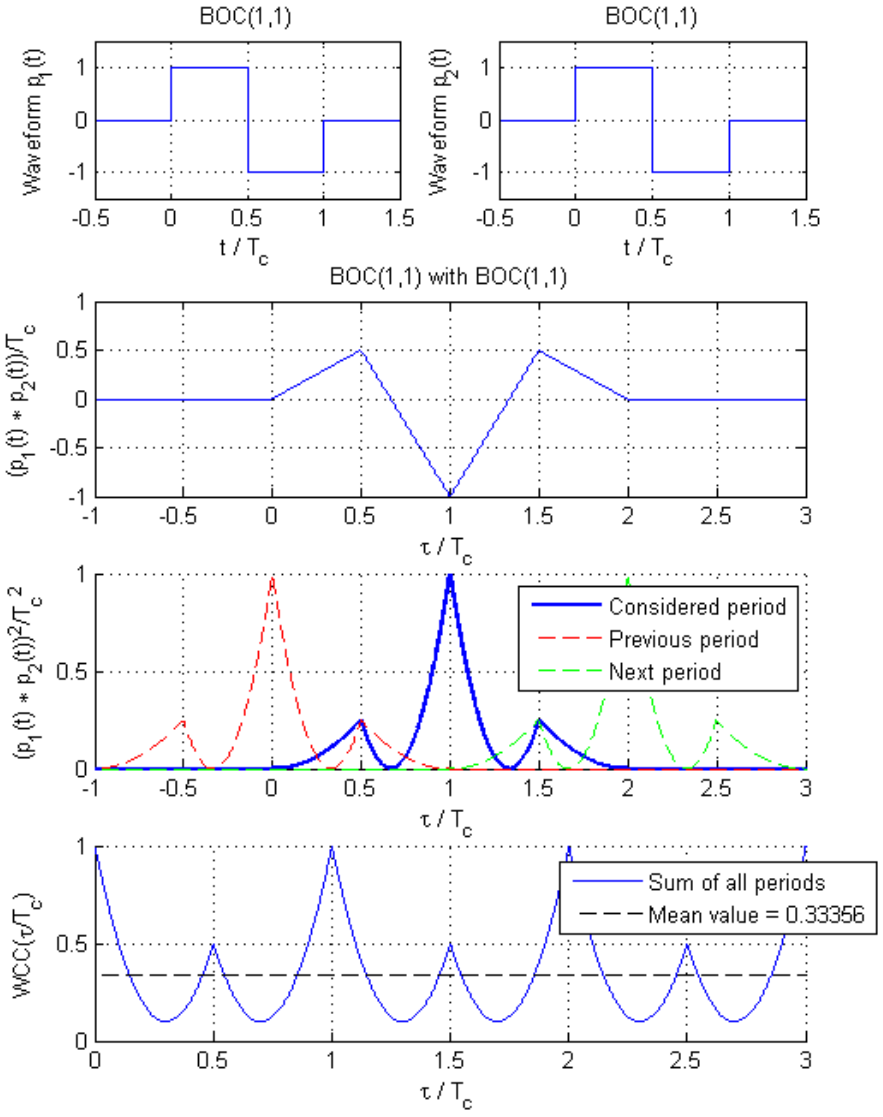

Figure 3.8: Chip waveform convolution method for BOC(1,1)-BOC(1,1)

3.5.3 Field of Application

With the considerations of this section, one comes to the following reasoning:

- The SSC is related to $\langle \mathrm{WCC}(\tau) \rangle$ which is the WCC averaged on the delay τ^k between the two considered spreading code signals. The use of SSC is therefore appropriate for a fast changing τ^k, typically when a satellite signal is involved, either tracked or interfering. The SSC may be calculated by the consideration of the SSC (as described in equation 3.1 on page 100) or by calculation of the averaged value of the signal obtained with the chip waveform convolution method.
- The *Waveform Convolution Coefficient* gives the interference contribution for a fixed τ^k. It is therefore appropriate for the calculation of interference contribution for two pseudolite signals because the delay is changing extremely slowly. Since this delay is usually unknown, it may be more appropriate to consider the worst case, i.e. the maximal value of $\mathrm{WCC}(\tau)$ on τ^k.

3.6 Expressions for the SNIR of the Correlator Output

The expressions previously established are carried forward here. They correspond to the absence of blanker and signals continuously emitted.

$$\mathcal{E}[C] = G_0 \sqrt{\mathcal{P}^l}$$

$$\mathrm{var}\,[C] = {G_0}^2 \cdot \left(\sum_{k \neq l} \mathrm{var} \left[\frac{1}{T} \int_0^T s^k(t) c^l(t) dt \right] + \frac{N_0}{T} \right)$$

$$\mathrm{var} \left[\frac{1}{T} \int_0^T s^k(t) c^l(t) dt \right] = \mathcal{P}^k \frac{T_c}{T} \mathrm{WCC}\left(\tau^k\right)$$

One comes to the final expression for the SNIR:

$$\mathrm{SNIR}[C] = \frac{\left(\mathcal{E}[C]\right)^2}{\mathrm{var}\,[C]} = \frac{\mathcal{P}^l}{\frac{1}{T}\left(N_0 + \sum_{k \neq l} \mathcal{P}^k T_c \mathrm{WCC}\left(\tau^k\right)\right)} \tag{3.3}$$

One notices from this expression that the contribution of each different signals to the SNIR can be separated. The following notations are introduced:

$$\mathrm{SNIR[C]} = \frac{S}{\frac{N}{T} + \sum_{k \neq l} \frac{I^k}{T}} \tag{3.4}$$

- Contribution of the tracked navigation signal: $S = \left(\mathcal{E}[C]\right)^2$
- Contribution of the noise: $N = T \cdot \mathrm{var}\left[\frac{1}{T}\int_0^T G(t) \cdot n(t) c^l(t) dt\right]$

- Contribution of the interfering navigation signal from source k: $I^k = T \cdot \mathrm{var}\left[\frac{1}{T}\int_0^T G(t) \cdot s^k(t)c^l(t)dt\right]$

In the present situation, $S = \mathcal{P}^l$, $N = N_0$ and $I^k = \mathcal{P}^k \cdot T_c \cdot \mathrm{WCC}\left(\tau^k\right)$.

3.7 Impact on Loop Performance

The SNIR has a direct influence on the noise jitters of the regulations after the correlator. As an example, the expression (from [10]) for the noise code tracking jitter for PLL (Phase Locked Loop) is given in the following (dynamic stress error neglected):

$$\sigma_{\mathrm{PLL}} = \frac{360}{2\pi}\sqrt{\frac{T \cdot B_L}{\mathrm{SNIR}[C]}\left(1 + \frac{1}{2\ \mathrm{SNIR}[C]}\right)} \quad \text{(degrees)}$$

with B_L the carrier loop noise bandwidth.

From [10], the rule of thumb for PLL tracking threshold is: $3\sigma_{\mathrm{PLL}} \leq 45\ ^\circ$. It comes that for a too low SNIR, the value of σ_{PLL} may exceed the previous threshold and the phase tracking could be lost.

Chapter 4

Advanced Mathematical Models

4.1 Introduction

The objective of this chapter is to establish models for the SNIR of the correlator output, now taking the blanker into consideration. The signal previously written $x(t)$ is now expressed as $f_{\mathrm{B}}(x(t))$ with f_{B} the mathematical representation of the blanker. As defined in section 3.2, this function is linear only for samples of amplitude between $-\mathrm{BTH}$ and BTH. Therefore, on the contrary to section 3, the signals are no longer independent of any other because the blanking of one signal at a time t may depend on the value of another signal at this time t. The mathematical derivations are therefore much more complex. But in some situations, they may become easier. Some examples are given in the following:

- Only noise: only one stochastic process with known parameters (Gaussian distribution).
- Noise and only one navigation signal: since the navigation signal is constant on intervals, the noise may be considered as the only stochastic process on these intervals.
- No noise and multiple navigation signals of same power $\mathcal{P}$: each signal takes randomly $-\sqrt{\mathcal{P}}$ or $\sqrt{\mathcal{P}}$ and eventually, the sum of all signals follows a binomial law.

The scenarios which approach these examples will be defined and a mathematical model will be established for each one. The definitions and approximation of section 3 are considered in this chapter. The blanker is the only non-linear function, the rest of the chain is assumed in linear regime.
Some terms are introduced:

Low-power signal encompasses all the navigation signals satisfying Approx. 3 (i.e. signals which have a much smaller power than the noise one)[1]. They are typically signals from satellites and pseudolites far away.

[1] To be more precise, when comparing the noise and interference contributions to the SNIR in expression 3.3, one comes to the condition $\sigma^2/\beta \gg \mathcal{P}^k \cdot T_c$ (with $\mathcal{P}^k$ the received power of a navigation signal)

High-power signals corresponds to all navigation signals with a much higher power contribution than the noise one, typically the signals from close pseudolites.

A *predominant signal* is a navigation signal with a power much larger than any other navigation signal. It includes typically the signal from a close single pseudolite or from a very close pseudolite emitting simultaneously with others.

A *similar-high-power signal* is a high-power navigation signal having a power close to those of other simultaneous signals (and all remaining signals have much lower power). This is the case typically for signals from a close pseudolite which emits simultaneously with other close pseudolites.

A description of the different operational scenarios for which analytical models will be derived is now proposed.

- **Low-power signals only** (dark-blue area in figure 4.1)
  - **Tracking of a low-power signal**
    It is a standard GNSS situation with constellation of visible satellites: satellite tracking without pulsed interference. But it may also be pseudolite tracking when far away from emitter.
- **One predominant signal** (light-blue areas in figure 4.1)
  - **Tracking of any signal except the predominant one**
    This corresponds typically to satellite tracking with interference from one single pseudolite or from one very close pseudolite in case of multi-pseudolites. For this latter case, the powers of other pseudolites are not necessarily low but should be much smaller than the predominant one.
  - **Tracking of the predominant signal**
    Typically when a single emitting pseudolite is tracked, or also when very close to one pseudolite in case of multi-pseudolites. For this latter case, the powers of other pseudolites are not necessarily low but should be much smaller than the predominant one.
- **Similar-high-power signals** (yellow areas in figure 4.1)
  - **Tracking of a low-power signal**
    This is the case when tracking one satellite signal at equal distance to each pseudolite (of same emission power) or when not to close from all pseudolites but not yet far away.
  - **Tracking of similar-high-power signal**
    This can correspond to pseudolite tracking at equal distance to each pseudolite, or when not too close from all pseudolites but not yet far away.
- **Other situations: presence of signals of different high powers** (red areas in figure 4.1)

– **Tracking of any signal**
It corresponds to intermediate situations: satellite or pseudolite tracking when localized between the area of "predominant power" (very close to one pseudolite) and the area of "similar-high powers" (at equal distance to each pseudolite), or between the latter area and the area of "low power signals" (far away from source).

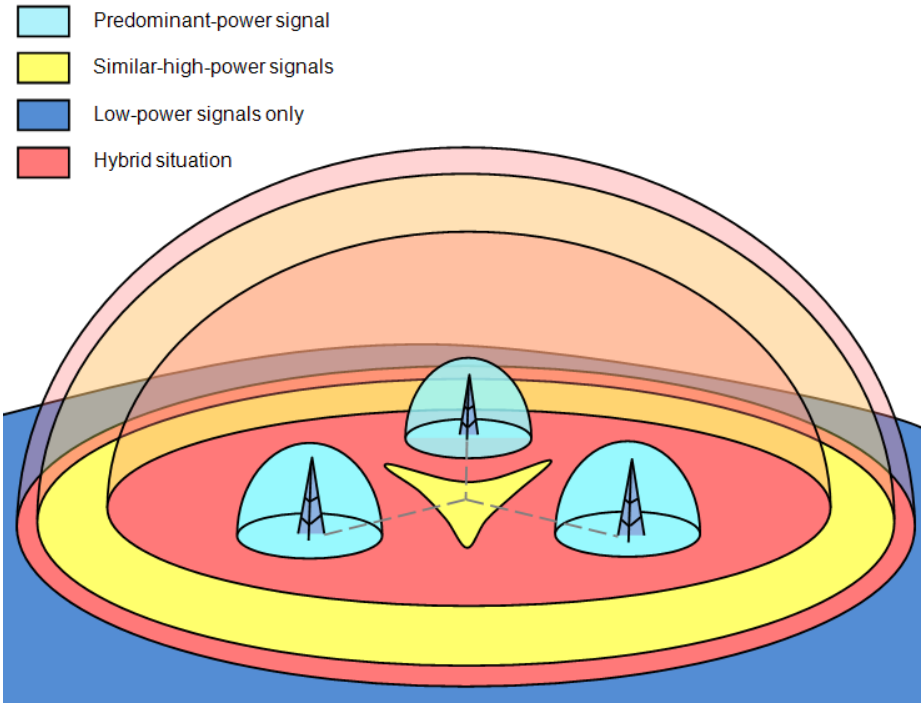

Figure 4.1: Separation of standard situations, here for multiple pseudolites emitting in same time

For the establishment of the associated models (standard models), all sources – satellites and pseudolites – are assumed to emit continuously (i.e. not in pulses). The extension for pulsed emissions will be introduced in a second part for the establishment of the final analytical models. A segmentation of the coherent integration intervals will be performed and the analytical SNIR models will be deduced by combining the applicable standard SNIR models for each interval.

4.2 Separation of Power Contributions to the Variance of the Correlator Output

Before deriving directly the standard models, some mathematical tools are already developed here. In this section, the general expression of $\mathrm{var}[C]$ in case of constant total received power is derived. It can apply to any situation as long as the received signal power can be considered constant. It can correspond

to the emission from one single pseudolite or from multiple pseudolites (signal overlapping) where one signal is predominant.

We try to get rid of f_{B} in order to handle only linear functions. Here the *blanking interval* I_B is the reunion of all intervals of $[0, T]$ where the signals is blanked because its amplitude is beyond the blanking threshold:

$$I_B = \left\{ t \in [0,T] \mid G(t) \cdot \left(\sum_k s^k(t) + n(t) \right) \notin [-\mathrm{BTH}, \mathrm{BTH}] \right\}$$

Because of constant total power signal, the AGC gain is constant: $G(t) = G_0$. Moreover, since the signal alternates around "symmetric values" (i.e. oscillates either around $\sqrt{\mathcal{P}}$ or $-\sqrt{\mathcal{P}}$ where $\mathcal{P}$ is the constant signal power) and therefore, for a defined signal power, the probability for a sample to be blanked depends only on the noise. In other words, the signal blanking at time t depends only on the value of $n(t)$.

$$\mathrm{var}[C] = \mathrm{var}\left[\frac{1}{T} \int\limits_{[0,T] \,\cap\, I_B} x(t) c^l(t) dt + \frac{1}{T} \int\limits_{[0,T] \setminus I_B} x(t) c^l(t) dt \right]$$

$x(t) = f_{\mathrm{B}}\left(G_0 \cdot \left(\sum_k s^k(t) + n(t) \right) \right)$, therefore $x(t) = 0$ in the blanking intervals:

$$\mathrm{var}[C] = \mathrm{var}\left[\frac{1}{T} \int\limits_{[0,T] \setminus I_B} G_0 \cdot \left(\sum_k s^k(t) + n(t) \right) c^l(t) dt \right]$$

Since the spreading codes are independent of each other:

$$\begin{aligned} \mathrm{var}[C] = \sum_k \mathrm{var}\left[\frac{1}{T} \int\limits_{[0,T] \setminus I_B} G_0 s^k(t) c^l(t) dt \right] \\ + \mathrm{var}\left[\frac{1}{T} \int\limits_{[0,T] \setminus I_B} G_0 n(t) c^l(t) dt \right] \end{aligned}$$

Concerning the tracked signal (source l), $s^l(t)c^l(t) = \sqrt{\mathcal{P}^l}$ and thus the associated term has no contribution to the variance, therefore it has to be removed from the sum:

$$\begin{aligned} \mathrm{var}[C] = \sum_{k,\ k \neq l} \mathrm{var}\left[\frac{1}{T} \int\limits_{[0,T] \setminus I_B} G_0 s^k(t) c^l(t) dt \right] \\ + \mathrm{var}\left[\frac{1}{T} \int\limits_{[0,T] \setminus I_B} G_0 n(t) c^l(t) dt \right] \end{aligned}$$

Interpretation:

- var $\left[\frac{1}{T}\int\limits_{[0,T]\setminus I_B} G_0 s^k(t)c^l(t)dt\right]$ is the contribution of the interfering signal from source k to the variance.
- var $\left[\frac{1}{T}\int\limits_{[0,T]\setminus I_B} G_0 n(t)c^l(t)dt\right]$ is the contribution of the noise to the variance.

4.3 Situation of Low-Power Signals

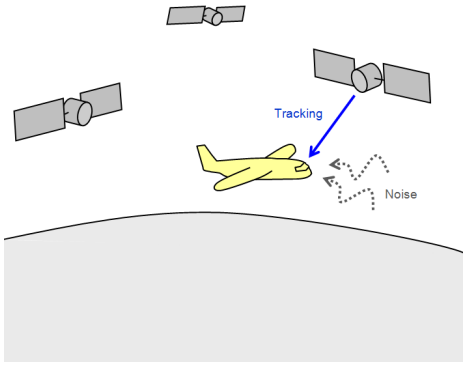

Figure 4.2: Example of application: reception of noise and satellite signals only

This situation corresponds typically to the tracking of a satellite signal or the tracking of a pseudolite signal with negligible pseudolite interference (cf. figure 4.2). According to Approx. 3, the power of the interfering satellite signals is much smaller than the noise power. Concerning the pseudolite signals, their power contribution should be much smaller than the noise one (more precisely, $\sigma^2/\beta \gg \mathcal{P}^k \cdot T_c$ for all k, with $\mathcal{P}^k$ the power of a navigation signal). Therefore, the contribution of the interfering navigation signals to var$[C]$ will be neglected. Nevertheless, the interfering signals may have an influence on the signal blanking.

For more simple derivations, it is considered that only one navigation signal is received. The influence of other signals will be analysed afterwards. The tracked navigation signal is assumed to be continuous and with a power $\mathcal{P}^l$ such that $G(t)\sqrt{\mathcal{P}^l} \ll$ BTH. Since $\mathcal{P}^l \ll \sigma^2$ from Approx. 3, the condition is valid for BTH $\geq G(t)\sigma$.
Since the signal power is constant because dominated by a constant noise power, $G(t)$ is constant: $G(t) = G_1$.

4.3.1 Expression for the Mean of the Correlator Output

$$\begin{aligned}\mathcal{E}[C] &= \mathcal{E}\left[\frac{1}{T}\int_0^T x(t)c^l(t)dt\right] \\ &= \frac{1}{T}\int_0^T \mathcal{E}\left[x(t)c^l(t)\right]dt\end{aligned}$$

$$\mathcal{E}\left[x(t)c^l(t)\right] = \mathcal{E}\left[f_{\mathrm{B}}\left(G_1\cdot\left(\left(h*\sqrt{\mathcal{P}^l}c^l\right)\left(t-\tau^l\right)+\left(h*w\right)(t)\right)\right)\cdot c^l(t)\right]$$

It has been established that $\left(h*c^l\right)(t) \approx c^l(t)$ (approximation) and $\tau^l = 0$ (definition). Thus:

$$\mathcal{E}\left[x(t)c^l(t)\right] \approx \mathcal{E}\left[f_{\mathrm{B}}\left(G_1\cdot\left(\sqrt{\mathcal{P}^l}c^l\left(t\right)+n(t)\right)\right)\cdot c^l(t)\right]$$

The relation between $\mathcal{E}\left[x(t)c^l(t)\mid c(t)=1\right]$ and $\mathcal{E}\left[x(t)c^l(t)\mid c(t)=-1\right]$ will be now established.

$$\mathcal{E}\left[x(t)c^l(t)\mid c(t)=-1\right] = \mathcal{E}\left[-f_{\mathrm{B}}\left(G_1\left(-\sqrt{\mathcal{P}^l}+n(t)\right)\right)\right]$$

Since f_{B} is odd:

$$\mathcal{E}\left[x(t)c^l(t)\mid c(t)=-1\right] = \mathcal{E}\left[f_{\mathrm{B}}\left(G_1\left(\sqrt{\mathcal{P}^l}-n(t)\right)\right)\right]$$

Since $n(t)$ has a symmetric distribution, it can be equivalently replaced by $-n(t)$:

$$\begin{aligned}\mathcal{E}\left[x(t)c^l(t)\mid c(t)=-1\right] &= \mathcal{E}\left[f_{\mathrm{B}}\left(G_1\left(\sqrt{\mathcal{P}^l}+n(t)\right)\right)\right] \\ &= \mathcal{E}\left[x(t)c^l(t)\mid c(t)=1\right]\end{aligned}$$

Since $\mathcal{E}\left[x(t)c^l(t)\mid c(t)=1\right] = \mathcal{E}\left[x(t)c^l(t)\mid c(t)=-1\right]$, it is possible to deduce:

$$\begin{aligned}\mathcal{E}[x(t)c^l(t)] &= \mathcal{E}\left[x(t)c^l(t)\mid c(t)=1\right] \\ &= \mathcal{E}\left[f_{\mathrm{B}}\left(G_1\left(\sqrt{\mathcal{P}^l}+n(t)\right)\right)\right] \qquad (4.1)\end{aligned}$$

$$\mathcal{E}[x(t)c^l(t)] = \int_{-\infty}^{\infty} f_{\mathrm{B}}\left(G_1\left(\sqrt{\mathcal{P}^l}+n\right)\right)\cdot p\left(n\right)dn$$

The signal probability density function of $G_1\left(\sqrt{\mathcal{P}^l}+n(t)\right)$ is represented on figure 4.3. Since f_{B} is linear on $[-\mathrm{BTH},\mathrm{BTH}]$ and equal to zero elsewhere:

$$\begin{aligned}\mathcal{E}[x(t)c^l(t)] &= \int_{G_1\left(\sqrt{\mathcal{P}^l}+n\right)\in[-\mathrm{BTH},\mathrm{BTH}]} G_1\left(\sqrt{\mathcal{P}^l}+n\right)\cdot\frac{1}{\sqrt{2\pi}\sigma}e^{-\frac{n^2}{2\sigma^2}}dn \\ &= G_1\int_{-\frac{\mathrm{BTH}}{G_1}-\sqrt{\mathcal{P}^l}}^{\frac{\mathrm{BTH}}{G_1}-\sqrt{\mathcal{P}^l}}\left(\sqrt{\mathcal{P}^l}+n\right)\cdot\frac{1}{\sqrt{2\pi}\sigma}e^{-\frac{n^2}{2\sigma^2}}dn \qquad (4.2)\end{aligned}$$

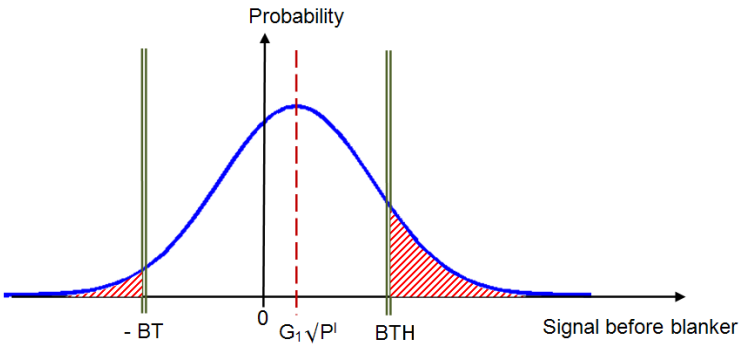

Figure 4.3: Illustration of the probability repartition of the signal before blanker. The red areas correspond to the parts which will be set to zero by the blanker

It is possible to express it with Q-functions which are defined in the appendix D.1. An additional approximation can be obtained with Taylor series with the assumption that $G_1\sqrt{\mathcal{P}^l} \ll \text{BTH}$. The detailed derivations are exposed in appendix A.1 and induce at second order:

$$\mathcal{E}[x(t)c^l(t)] \approx G_1\sqrt{\mathcal{P}^l}\left[1 - 2Q_0\left(\frac{\text{BTH}}{G_1\sigma}\right) - \frac{\text{BTH}}{G_1\sigma}\sqrt{\frac{2}{\pi}}e^{-\frac{\text{BTH}^2}{2(G_1\sigma)^2}}\right]$$

Since $\mathcal{E}[C] = \frac{1}{T}\int_0^T \mathcal{E}\left[x(t)c^l(t)\right]dt$ and $\mathcal{E}\left[x(t)c^l(t)\right]$ has been proved not to depend on the time t, it is finally deduced:

$$\mathcal{E}[C] = \mathcal{E}[x(t)c^l(t)] \approx G_1\sqrt{\mathcal{P}^l}\left[1 - 2Q_0\left(\frac{\text{BTH}}{G_1\sigma}\right) - \frac{\text{BTH}}{G_1\sigma}\sqrt{\frac{2}{\pi}}e^{-\frac{\text{BTH}^2}{2(G_1\sigma)^2}}\right] \quad (4.3)$$

Remark: This expression has been established for $\text{BTH} \gg G_1\sqrt{\mathcal{P}^l}$. Nevertheless, it can be noticed that the limit of the expression for BTH tending to 0 (i.e. whole signal blanked) is valid: for $\text{BTH} = 0$, $Q_0\left(\frac{\text{BTH}}{G_1\sigma}\right) = 1/2$ and therefore $\mathcal{E}[C] = 0$ as expected.

4.3.2 Expression for the Variance of the Correlator Output

By definition, $\text{var}[C] = \mathcal{E}[C^2] - (\mathcal{E}[C])^2$. The term $\mathcal{E}[C]$ has been derived previously. Let us now calculate $\mathcal{E}[C^2]$.

$$\mathcal{E}[C^2] = \mathcal{E}\left[\frac{1}{T^2}\int_0^T\int_0^T x(t)x(u)c^l(t)c^l(u)dtdu\right]$$

According to Approx. 5, $c(t)$ is independent of $c(u)$ when t and u are not on the same chip interval. We call $I_c(t)$ the chip interval containing t: $\exists\ m_1 \in \mathbb{Z}\ /\ t \in [m_1T_c, (m_1+1)T_c]$. In the following, in order to derive $\mathcal{E}[C^2]$, the integration interval is split into two complementary intervals:

- interval where t and u are **not** on the same chip interval , i.e. t fixed and $u \notin I_c(t)$ (i.e. $u \in [0,T] \setminus I_c(t)$)
- interval where t and u are on the same chip interval , i.e. t fixed and $u \in I_c(t)$

$$\mathcal{E}[C^2] = \underbrace{\frac{1}{T^2}\mathcal{E}\left[\int\limits_{t\in[0,T]}\int\limits_{u\notin I_c(t)} x(t)x(u)c^l(t)c^l(u)dudt\right]}_{\mathcal{E}_1} + \underbrace{\frac{1}{T^2}\mathcal{E}\left[\int\limits_{t\in[0,T]}\int\limits_{u\in I_c(t)} x(t)x(u)c^l(t)c^l(u)dudt\right]}_{\mathcal{E}_2}$$

1) Derivation of the term $\mathcal{E}_1$

$$\begin{aligned}\mathcal{E}_1 &= \frac{1}{T^2}\mathcal{E}\left[\int\limits_{t\in[0,T]}\int\limits_{u\notin I_c(t)} x(t)x(u)c^l(t)c^l(u)dudt\right] \\ &= \frac{1}{T^2}\int\limits_{t\in[0,T]}\int\limits_{u\notin I_c(t)} \mathcal{E}\left[x(t)x(u)c^l(t)c^l(u)\right]dudt\end{aligned}$$

Since t and u are not on the same chip interval, the signals (noise and navigation signal) at time t are independent of those at time u. Consequently:

$$\mathcal{E}\left[x(t)x(u)c^l(t)c^l(u)\,|u \notin I_c(t)\right] = \mathcal{E}\left[x(t)c^l(t)\right]\cdot\mathcal{E}\left[x(u)c^l(u)\right]$$

and therefore:

$$\mathcal{E}_1 = \frac{1}{T^2}\int\limits_{t\in[0,T]}\mathcal{E}\left[x(t)c^l(t)\right]dt\int\limits_{u\notin I_c(t)}\mathcal{E}\left[x(u)c^l(u)\right]du$$

Since $\mathcal{E}[C] = \frac{1}{T}\int_0^T \mathcal{E}\left[x(t)c^l(t)\right]dt = \frac{1}{T-T_c}\int\limits_{u\notin I_c(t)}\mathcal{E}\left[x(u)c^l(u)\right]du$, it comes:

$$\mathcal{E}_1 = \frac{T-T_c}{T}\left(\mathcal{E}[C]\right)$$

2) Derivation of the term $\mathcal{E}_2$

$$\mathcal{E}_2 = \frac{1}{T^2}\mathcal{E}\left[\int\limits_{t\in[0,T]}\int\limits_{u\in I_c(t)} x(t)x(u)c^l(t)c^l(u)dudt\right]$$
$$= \frac{1}{T^2}\int\limits_{t\in[0,T]}\int\limits_{u\in I_c(t)} \mathcal{E}\left[f_{\mathrm{B}}\left(G_1\left(\sqrt{\mathcal{P}^l}c^l(t)+n(t)\right)\right)c^l(t)\right.$$
$$\left.\cdot\, f_{\mathrm{B}}\left(G_1\left(\sqrt{\mathcal{P}^l}c^l(u)+n(u)\right)\right)c^l(u)\right]dudt$$

Since c^l has its values in $\{-1,1\}$, c^l is assimilated to $\mathrm{sign}(c^l)$, with:

$$\mathrm{sign}(x) = \begin{cases} 1 & \text{if } x>0 \\ -1 & \text{if } x<0 \\ 0 & \text{if } x=0 \end{cases}$$

Since f_{B} is odd and $(c(t))^2 = 1$:

$$f_{\mathrm{B}}\left(G_1\left(\sqrt{\mathcal{P}^l}c^l(t)+n(t)\right)\right)\cdot c^l(t) = f_{\mathrm{B}}\left(G_1\left(\sqrt{\mathcal{P}^l}c^l(t)+n(t)\right)\cdot c^l(t)\right)$$
$$= f_{\mathrm{B}}\left(G_1\left(\sqrt{\mathcal{P}^l}+n(t)\cdot c^l(t)\right)\right)$$

Therefore:

$$\mathcal{E}_2 = \frac{1}{T^2}\int\limits_{t\in[0,T]}\int\limits_{u\in I_c(t)} \mathcal{E}\left[f_{\mathrm{B}}\left(G_1\left(\sqrt{\mathcal{P}^l}+n(t)\cdot c^l(t)\right)\right)\right.$$
$$\left.\cdot\, f_{\mathrm{B}}\left(G_1\left(\sqrt{\mathcal{P}^l}+n(u)\cdot c^l(u)\right)\right)\right]dudt$$

By definition, $c^l(t) = \sum\limits_{m=-\infty}^{\infty} c_m^l p^l(t-mT_c)$ with $p^l(t)$ equal to zero outside $[0,T_c[$ (because the filter has no effect on the chip waveform, by hypothesis). Thus, it can be deduced that for t fixed, $\exists\ m\in\mathbb{Z}\ /\ c^l(t) = c_m^l p^l(t-mT_c)$. Moreover, since $u\in I_c(t)$, $c^l(u) = c_m^l p^l(u-mT_c)$. Similarly as before, it can be considered that $\mathrm{sign}\left(c_m^l\right) = c_m^l$ and $\mathrm{sign}\left(p^l(t-mT_c)\right) = \left(p^l(t-mT_c)\right)$.
Remark: In the previous expressions, m depends implicitly on t and is defined such that $0 < t-mT_c \leq T_c$, i.e. $m = \lfloor \frac{t}{T_c} \rfloor$ (floor of $\frac{t}{T_c}$).

Therefore:

$$\mathcal{E}_2 = \frac{1}{T^2}\int\limits_{t\in[0,T]}\int\limits_{u\in I_c(t)} \mathcal{E}\left[f_{\mathrm{B}}\left(G_1\left(\sqrt{\mathcal{P}^l}+n(t)\cdot c_m^l\cdot p^l(t-mT_c)\right)\right)\right.$$
$$\left.\cdot\, f_{\mathrm{B}}\left(G_1\left(\sqrt{\mathcal{P}^l}+n(u)\cdot c_m^l\cdot p^l(u-mT_c)\right)\right)\right]dudt$$

Since n has a symmetric distribution, n can be equivalently replaced by $n\cdot \mathrm{sign}\left(c_m^l\right)$ in the expression of $\mathcal{E}$. It is deduced:

$$\mathcal{E}_2 = \frac{1}{T^2}\int\limits_{t\in[0,T]}\int\limits_{u\in I_c(t)} \mathcal{E}\left[f_{\mathrm{B}}\left(G_1\left(\sqrt{\mathcal{P}^l}+n(t)\cdot p^l(t-mT_c)\right)\right)\right.$$
$$\left.\cdot f_{\mathrm{B}}\left(G_1\left(\sqrt{\mathcal{P}^l}+n(u)\cdot p^l(u-mT_c)\right)\right)\right]dudt$$

Since $\beta = f_s$ (Nyquist condition), the autocorrelation function of $n(t)$ is a sinc function with zeros every $\frac{k}{\beta} = \frac{k}{f_s}$, $k \in \mathbb{Z}^*$. Therefore, when considering sampled signals, any noise sample is uncorrelated with all neighbour samples: $\mathcal{E}\left[n\left(\frac{k_t}{f_s}\right) \cdot n\left(\frac{k_u}{f_s}\right)\right] = \sigma^2 \cdot \delta_{k_t,k_u}$. Consequently, the next step will be written by considering explicitly sampled signals, with the introduction of: $t = \frac{k_t}{f_s}$, $u = \frac{k_u}{f_s}$, $dt = \frac{1}{f_s}$ and $du = \frac{1}{f_s}$.

$$
\begin{aligned}
\mathcal{E}_2 = \frac{1}{T^2} \sum_{k_t=1}^{T \cdot f_s} \sum_{\frac{k_u}{f_s} \in I_c(t)} & \mathcal{E}\left[f_{\mathrm{B}}\left(G_1\left(\sqrt{\mathcal{P}^l} + n\left(\frac{k_t}{f_s}\right) \cdot p^l\left(\frac{k_t}{f_s} - mT_c\right)\right)\right)\right. \\
& \left. \cdot f_{\mathrm{B}}\left(G_1\left(\sqrt{\mathcal{P}^l} + n\left(\frac{k_u}{f_s}\right) \cdot p^l\left(\frac{k_u}{f_s} - mT_c\right)\right)\right)\right] \cdot \left(\frac{1}{f_s}\right)^2 \\
= \frac{1}{T^2} \sum_{k_t=1}^{T \cdot f_s} \sum_{\substack{\frac{k_u}{f_s} \in I_c(t) \\ k_u = k_t}} & \mathcal{E}\left[f_{\mathrm{B}}\left(G_1\left(\sqrt{\mathcal{P}^l} + n\left(\frac{k_t}{f_s}\right) \cdot p^l\left(\frac{k_t}{f_s} - mT_c\right)\right)\right)\right. \\
& \left. \cdot f_{\mathrm{B}}\left(G_1\left(\sqrt{\mathcal{P}^l} + n\left(\frac{k_u}{f_s}\right) \cdot p^l\left(\frac{k_u}{f_s} - mT_c\right)\right)\right)\right] \cdot \left(\frac{1}{f_s}\right)^2 \\
+ \frac{1}{T^2} \sum_{k_t=1}^{T \cdot f_s} \sum_{\substack{\frac{k_u}{f_s} \in I_c(t) \\ k_u \neq k_t}} & \mathcal{E}\left[f_{\mathrm{B}}\left(G_1\left(\sqrt{\mathcal{P}^l} + n\left(\frac{k_t}{f_s}\right) \cdot p^l\left(\frac{k_t}{f_s} - mT_c\right)\right)\right)\right. \\
& \left. \cdot f_{\mathrm{B}}\left(G_1\left(\sqrt{\mathcal{P}^l} + n\left(\frac{k_u}{f_s}\right) \cdot p^l\left(\frac{k_u}{f_s} - mT_c\right)\right)\right)\right] \cdot \left(\frac{1}{f_s}\right)^2
\end{aligned}
$$

$$
\begin{aligned}
\mathcal{E}_{2,1} = \frac{1}{T^2} \sum_{k_t=1}^{T \cdot f_s} \sum_{\substack{\frac{k_u}{f_s} \in I_c(t) \\ k_u = k_t}} & \mathcal{E}\left[f_{\mathrm{B}}\left(G_1\left(\sqrt{\mathcal{P}^l} + n\left(\frac{k_t}{f_s}\right) \cdot p^l\left(\frac{k_t}{f_s} - mT_c\right)\right)\right)\right. \\
& \left. \cdot f_{\mathrm{B}}\left(G_1\left(\sqrt{\mathcal{P}^l} + n\left(\frac{k_u}{f_s}\right) \cdot p^l\left(\frac{k_u}{f_s} - mT_c\right)\right)\right)\right] \cdot \left(\frac{1}{f_s}\right)^2 \\
= \frac{1}{f_s T^2} \sum_{k_t=1}^{T \cdot f_s} & \mathcal{E}\left[\left(f_{\mathrm{B}}\left(G_1\left(\sqrt{\mathcal{P}^l} + n\left(\frac{k_t}{f_s}\right) \cdot p^l\left(\frac{k_t}{f_s} - mT_c\right)\right)\right)\right)^2 \right] \frac{1}{f_s} \\
= \frac{1}{f_s T^2} \sum_{k_t=1}^{T \cdot f_s} & \mathcal{E}\left[\left(f_{\mathrm{B}}\left(G_1\left(\sqrt{\mathcal{P}^l} + n\left(\frac{k_t}{f_s}\right)\right)\right)\right)^2 \right] \frac{1}{f_s}
\end{aligned}
$$

And equivalently:

$$
\mathcal{E}_{2,1} = \frac{1}{f_s T^2} \int_0^T \mathcal{E}\left[\left(f_{\mathrm{B}}\left(G_1\left(\sqrt{\mathcal{P}^l} + n\left(t\right)\right)\right)\right)^2 \right] dt
$$

$$\mathcal{E}_{2,2} = \frac{1}{T^2} \sum_{k_t=1}^{T \cdot f_s} \sum_{\substack{\frac{k_u}{f_s} \in I_c(t) \\ k_u \neq k_t}} \mathcal{E}\left[f_{\mathrm{B}}\left(G_1\left(\sqrt{\mathcal{P}^l} + n\left(\frac{k_t}{f_s}\right) \cdot p^l\left(\frac{k_t}{f_s} - mT_c\right)\right)\right)\right.$$

$$\left. \cdot f_{\mathrm{B}}\left(G_1\left(\sqrt{\mathcal{P}^l} + n\left(\frac{k_u}{f_s}\right) \cdot p^l\left(\frac{k_u}{f_s} - mT_c\right)\right)\right)\right] \cdot \left(\frac{1}{f_s}\right)^2$$

The function $p^l\left(t - mT_c\right)$ takes $+1$ and -1. The different possible cases are now considered:

- For k_t and k_u such that $p^l\left(\frac{k_t}{f_s} - mT_c\right) = 1$ and $p^l\left(\frac{k_u}{f_s} - mT_c\right) = 1$ or $p^l\left(\frac{k_t}{f_s} - mT_c\right) = -1$ and $p^l\left(\frac{k_u}{f_s} - mT_c\right) = -1$:

$$\begin{aligned}
&\mathcal{E}\left[f_{\mathrm{B}}\left(G_1\left(\sqrt{\mathcal{P}^l} + n\left(\frac{k_t}{f_s}\right) \cdot p^l\left(\frac{k_t}{f_s} - mT_c\right)\right)\right)\right. \\
&\quad \left. \cdot\ f_{\mathrm{B}}\left(G_1\left(\sqrt{\mathcal{P}^l} + n\left(\frac{k_u}{f_s}\right) \cdot p^l\left(\frac{k_u}{f_s} - mT_c\right)\right)\right)\ \middle|\ k_t \neq k_u\right] \\
&\quad = \mathcal{E}\left[f_{\mathrm{B}}\left(G_1\left(\sqrt{\mathcal{P}^l} + n\left(\frac{k_t}{f_s}\right)\right)\right)\right. \\
&\qquad \left. \cdot\ f_{\mathrm{B}}\left(G_1\left(\sqrt{\mathcal{P}^l} + n\left(\frac{k_u}{f_s}\right)\right)\right)\ \middle|\ k_t \neq k_u\right] \\
&\quad = \mathcal{E}\left[f_{\mathrm{B}}\left(G_1\left(\sqrt{\mathcal{P}^l} + n\left(\frac{k_t}{f_s}\right)\right)\right)\right] \\
&\qquad \cdot \mathcal{E}\left[f_{\mathrm{B}}\left(G_1\left(\sqrt{\mathcal{P}^l} + n\left(\frac{k_u}{f_s}\right)\right)\right)\right]
\end{aligned}$$

- For k_t and k_u such that $p^l\left(\frac{k_t}{f_s} - mT_c\right) = 1$ and $p^l\left(\frac{k_u}{f_s} - mT_c\right) = -1$ or $p^l\left(\frac{k_t}{f_s} - mT_c\right) = 1$ and $p^l\left(\frac{k_u}{f_s} - mT_c\right) = -1$:

$$\begin{aligned}
&\mathcal{E}\left[f_{\mathrm{B}}\left(G_1\left(\sqrt{\mathcal{P}^l} + n\left(\frac{k_t}{f_s}\right) \cdot p^l\left(\frac{k_t}{f_s} - mT_c\right)\right)\right)\right. \\
&\quad \left. \cdot\ f_{\mathrm{B}}\left(G_1\left(\sqrt{\mathcal{P}^l} + n\left(\frac{k_u}{f_s}\right) \cdot p^l\left(\frac{k_u}{f_s} - mT_c\right)\right)\right)\ \middle|\ k_t \neq k_u\right] \\
&\quad = \mathcal{E}\left[f_{\mathrm{B}}\left(G_1\left(\sqrt{\mathcal{P}^l} + n\left(\frac{k_t}{f_s}\right)\right)\right)\right. \\
&\qquad \left. \cdot f_{\mathrm{B}}\left(G_1\left(\sqrt{\mathcal{P}^l} - n\left(\frac{k_u}{f_s}\right)\right)\right)\ \middle|\ k_t \neq k_u\right] \\
&\quad = \mathcal{E}\left[f_{\mathrm{B}}\left(G_1\left(\sqrt{\mathcal{P}^l} + n\left(\frac{k_t}{f_s}\right)\right)\right)\right] \\
&\qquad \cdot \mathcal{E}\left[f_{\mathrm{B}}\left(G_1\left(\sqrt{\mathcal{P}^l} - n\left(\frac{k_u}{f_s}\right)\right)\right)\right] \\
&\quad = \mathcal{E}\left[f_{\mathrm{B}}\left(G_1\left(\sqrt{\mathcal{P}^l} + n\left(\frac{k_t}{f_s}\right)\right)\right)\right] \\
&\qquad \cdot \mathcal{E}\left[f_{\mathrm{B}}\left(G_1\left(\sqrt{\mathcal{P}^l} + n\left(\frac{k_u}{f_s}\right)\right)\right)\right]
\end{aligned}$$

It is now proved that the result is the same for any values of $p^l(t - mT_c)$ and $p^l(u - mT_c)$. Therefore:

$$\mathcal{E}_{2,2} = \frac{1}{(f_s T)^2} \sum_{k_t=1}^{T \cdot f_s} \mathcal{E}\left[f_{\mathrm{B}}\left(G_1\left(\sqrt{\mathcal{P}^l} + n\left(\frac{k_t}{f_s}\right)\right)\right)\right] \cdot \sum_{\substack{\frac{k_u}{f_s} \in I_c(t) \\ k_u \neq k_t}} \mathcal{E}\left[f_{\mathrm{B}}\left(G_1\left(\sqrt{\mathcal{P}^l} + n\left(\frac{k_u}{f_s}\right)\right)\right)\right]$$

It has been already proved (equations 4.1 and 4.3 on page 37) that $\mathcal{E}\left[f_{\mathrm{B}}\left(G_1\left(\sqrt{\mathcal{P}^l} + n\left(t\right)\right)\right)\right] = \mathcal{E}\left[C\right]$. Hence:

$$\begin{aligned}\mathcal{E}_{2,2} &= \frac{1}{(f_s T)^2} \cdot f_s T \cdot (f_s T_c - 1) \cdot (\mathcal{E}[C])^2 \\ &= \left(\frac{T_c}{T} - \frac{1}{\beta T}\right) \cdot (\mathcal{E}\left[C\right])^2\end{aligned}$$

Since $\mathcal{E}_2 = \mathcal{E}_{2,1} + \mathcal{E}_{2,2}$, it is deduced:

$$\mathcal{E}_2 = \frac{1}{\beta T^2} \int_0^T \mathcal{E}\left[\left(f_{\mathrm{B}}\left(G_1\left(\sqrt{\mathcal{P}^l} + n(t)\right)\right)\right)^2\right] dt + \left(\frac{T_c}{T} - \frac{1}{\beta T}\right) (\mathcal{E}\left[C\right])^2$$

3) Summation of $\mathcal{E}_1$ and $\mathcal{E}_2$

$$\begin{aligned}\mathrm{var}[C] &= \mathcal{E}[C^2] - \mathcal{E}^2[C] \\ &= \mathcal{E}_1 + \mathcal{E}_2 - \mathcal{E}^2[C] \\ &= \frac{T - T_c}{T}\mathcal{E}^2\left[C\right] + \frac{1}{\beta T^2} \int_0^T \mathcal{E}\left[\left(f_{\mathrm{B}}\left(G_1\left(\sqrt{\mathcal{P}^l} + n(t)\right)\right)\right)^2\right] dt \qquad (4.4) \\ &\quad + \left(\frac{T_c}{T} - \frac{1}{\beta T}\right) \mathcal{E}^2\left[C\right] - \mathcal{E}^2[C] \\ &= \frac{1}{\beta T}\left(\frac{1}{T}\int_0^T \mathcal{E}\left[\left(f_{\mathrm{B}}\left(G_1\left(\sqrt{\mathcal{P}^l} + n(t)\right)\right)\right)^2\right] dt - \mathcal{E}^2[C]\right) \qquad (4.5)\end{aligned}$$

In the same way as for $\mathcal{E}[C]$ page 38, the term $\mathcal{E}\left[\left(f_{\mathrm{B}}\left(G_1\left(\sqrt{\mathcal{P}^l} + n(t)\right)\right)\right)^2\right]$ can be approximated with Taylor series. According to the derivations of section A.2, it is deduced (second order):

$$\begin{aligned}&\mathcal{E}\left[\left(f_{\mathrm{B}}\left(G_1\left(\sqrt{\mathcal{P}^l} + n(t)\right)\right)\right)^2\right] \\ &\quad \approx G_1^2\sigma^2\left(1 - 2Q_2\left(\frac{\mathrm{BTH}}{G_1\sigma}\right)\right) \\ &\qquad + G_1^2\mathcal{P}^l\left(1 - 2Q_0\left(\frac{\mathrm{BTH}}{G_1\sigma}\right) - \left(\frac{\mathrm{BTH}^2}{(G_1\sigma)^2} + 2\right)\frac{\mathrm{BTH}}{\sqrt{2\pi}G_1\sigma}e^{-\frac{\mathrm{BTH}^2}{2(G_1\sigma)^2}}\right)\end{aligned}$$

Remark: The Q-functions have been defined in the appendix D.1.

Since this term has been proved not to depend on the time t, it is deduced that $\frac{1}{T}\int_0^T \mathcal{E}\left[\left(f_{\mathrm{B}}\left(G_1\left(\sqrt{\mathcal{P}^l}+n(t)\right)\right)\right)^2\right]dt = \mathcal{E}\left[\left(f_{\mathrm{B}}\left(G_1\left(\sqrt{\mathcal{P}^l}+n(t)\right)\right)\right)^2\right]$ and finally:

$$\begin{aligned}\mathrm{var}[C] \approx \frac{1}{\beta T}\Bigg(&G_1^2\sigma^2\left(1-2Q_2\left(\frac{\mathrm{BTH}}{G_1\sigma}\right)\right)+G_1^2\mathcal{P}^l\Bigg(1-2Q_0\left(\frac{\mathrm{BTH}}{G_1\sigma}\right)\\&-\left(\frac{\mathrm{BTH}^2}{(G_1\sigma)^2}+2\right)\frac{\mathrm{BTH}}{\sqrt{2\pi}G_1\sigma}e^{-\frac{\mathrm{BTH}^2}{2(G_1\sigma)^2}}\\&-\left(1-2Q_0\left(\frac{\mathrm{BTH}}{G_1\sigma}\right)-\frac{\mathrm{BTH}}{G_1\sigma}\sqrt{\frac{2}{\pi}}e^{-\frac{\mathrm{BTH}^2}{2(G_1\sigma)^2}}\right)^2\Bigg)\end{aligned}$$

Remark: This expression has been established for $\mathrm{BTH} \gg G_1\sqrt{\mathcal{P}^l}$. Nevertheless, it can be noticed that the limit of the expression for BTH tending to 0 (i.e. whole signal blanked) is valid: for $\mathrm{BTH}=0$, $Q_0\left(\frac{\mathrm{BTH}}{G_1\sigma}\right)=1/2$, $Q_2\left(\frac{\mathrm{BTH}}{G_1\sigma}\right)=1/2$ and therefore $\mathrm{var}[C]=0$ as expected.

4.3.3 Simplification

The expressions at second order are complex to work with and to interpret. Let us now write these expressions at first order. It will be tested in section 5 if the first order allows a sufficient precision.

$$\mathrm{SNIR} = \frac{S}{N}$$

$$\sqrt{S} = \mathcal{E}[C] \approx G_1\sqrt{\mathcal{P}^l}\left(1-2Q_0\left(\frac{\mathrm{BTH}}{G_1\sigma}\right)-\frac{\mathrm{BTH}}{G_1\sigma}\sqrt{\frac{2}{\pi}}e^{-\frac{\mathrm{BTH}^2}{2(G_1\sigma)^2}}\right) \tag{4.6}$$

$$N = \mathrm{var}[C] \approx \frac{1}{\beta T}G_1^2\sigma^2\left(1-2Q_2\left(\frac{\mathrm{BTH}}{G_1\sigma}\right)\right) \tag{4.7}$$

$$\mathrm{SNIR} \approx \beta T\frac{\mathcal{P}^l\left(1-2Q_0\left(\frac{\mathrm{BTH}}{G_1\sigma}\right)-\frac{\mathrm{BTH}}{G_1\sigma}\sqrt{\frac{2}{\pi}}e^{-\frac{\mathrm{BTH}^2}{2(G_1\sigma)^2}}\right)^2}{\sigma^2\left(1-2Q_2\left(\frac{\mathrm{BTH}}{G_1\sigma}\right)\right)}$$

4.3.4 Interpretation

The aim here is to give physical meanings of the terms of the expression at first order.

Let us introduce first an indication which will help for the interpretation: the general expression $Q_0(\frac{-K-\mu}{\sigma}) - Q_0(\frac{K-\mu}{\sigma})$, equal to $\int_{\frac{-K-\mu}{\sigma}}^{\frac{K-\mu}{\sigma}} \frac{1}{\sqrt{2\pi}} e^{-\frac{n^2}{2}} dn$ (or $\int_{-K}^{K} \frac{1}{\sqrt{2\pi}\sigma} e^{-\frac{(n-\mu)^2}{2\sigma^2}} dn$) by definition, is the probability that a sample of the Gaussian noise ($\mathcal{N}(\mu, \sigma^2)$) belongs to $[-K, K]$. This is the same reasoning for Q_2 with the difference that the distribution is weighted by the corresponding power (i.e. $n^2 p(n)$ instead of $p(n)$).

- When considering BTH tending to infinity (equivalent to no blanker at all), the following well-known expression is deduced: SNIR $= \beta T \frac{\mathcal{P}^l}{\sigma^2} = \frac{\mathcal{P}^l}{\frac{1}{T} N_0}$
- The factor $G_1\sigma$ is the standard deviation of $x(t)$.
- The term $1 - 2Q_0\left(\frac{\text{BTH}}{G_1\sigma}\right) = Q_0\left(-\frac{\text{BTH}}{G_1\sigma}\right) - Q_0\left(\frac{\text{BTH}}{G_1\sigma}\right)$ corresponds to the proportion of navigation signal not blanked, in this case, the proportion of noise below the blanking threshold.
- The term $\frac{\text{BTH}}{G_1\sigma}\sqrt{\frac{2}{\pi}} e^{-\frac{\text{BTH}^2}{2(G_1\sigma)^2}}$ corresponds to the bias in the balancedness of the noise repartition because of the offset due to navigation signal: for blanking threshold close to the signal, one side of the noise is more blanked than the other and its repartition is thus no longer centred.
- The term $1 - 2Q_2\left(\frac{\text{BTH}}{G_1\sigma}\right) = Q_2\left(-\frac{\text{BTH}}{G_1\sigma}\right) - Q_2\left(\frac{\text{BTH}}{G_1\sigma}\right)$ corresponds to the proportion of navigation signal not blanked in the entire signal, weighted by its own power. This weighting corresponds to noise shaping: the blanking affects mainly large values of the noise (located in the sides of the distribution) and thus, the variance of its repartition is reduced.

4.3.5 Consideration of Low-Power Interfering Navigation Signals

It has been already written that the interference contribution to the variance of C is neglected with respect to the one of the noise. Nevertheless, the interfering signals may have an influence on the blanking, as studied in the following.

- At first order, the equation 4.7 shows that the navigation signal has no influence in the expression of the noise contribution. Therefore, it is the same for any interfering signal.
- At first order, the equation 4.6 shows that the tracked navigation signal has an influence (by the presence of $\mathcal{P}^l$). The last term of the expression reflects that the tracked navigation signal induces a bias in the balancedness of the noise repartition. The other navigation signals obviously also have a contribution to this bias, but since these signals are multiplied by $c^l(t)$, their contribution vanishes with the integration. To prove this, one should rewrite the derivations for the mean of C with consideration of $s^l(t) + \sum_{k \neq l} s^k(t)$ instead of only $s^l(t)$.

Since this reasoning is not a mathematical proof, it will be only assumed that the interfering navigation signals have no impact in the SNIR.

Consequently, it is deduced that the derived expressions for the reception of noise and only one low-power navigation signal are also valid for the reception of noise and multiple low-power navigation signals.

4.4 Situation of One Predominant Signal

4.4.1 Tracking of Signal in Presence of One Predominant Signal

This situation corresponds typically to the tracking of a signal during the emission of a signal from one single pseudolite or from one close pseudolite among multiple pseudolites (Cf. figure 4.4). The tracked signal is not the predominant one. In this section, it will be established that the sum of the noise and the

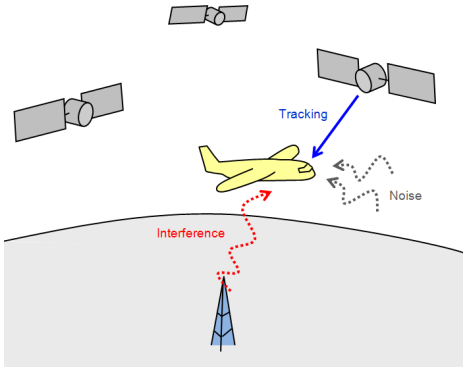

Figure 4.4: Example of application: tracking of satellite signal with strong interference from pseudolite

tracked navigation signal is alternating around a constant value (i.e. oscillates either around $\sqrt{\mathcal{P}_2}$ or $-\sqrt{\mathcal{P}_2}$ where $\mathcal{P}_2$ is the constant signal power). Then, we will introduce the condition of application of the model for "low-power signals" of section 4.3 in order to adapt this model to the present situation.

It is reminded that the predominant signal is assumed to be emitted continuously (not yet considered pulsed). Because of Approx. 1, the power of the predominant signal is constant. Since all other navigation signals have much smaller power, it can be considered that the total power is approximately equal to the predominant signal power and is also constant. One of the consequences is that $G(t)$ is constant: $G(t) = G_2$. The term $\mathcal{P}_2$ is the total received power from all the sources and is approximately equal to the power of the predominant signal. One can consider here that $\mathcal{P}_2 = \sum_k \mathcal{P}^k$. We are tracking the navigation signal from source l and this signal has a much smaller power than the total power of other navigation signals: $\mathcal{P}^l \ll \mathcal{P}_2$. Since $\mathcal{P}^l$ is small with respect to the total power of other signals, it can be considered that $\mathcal{P}_2 \approx \sum_{k,\ k \neq l} \mathcal{P}^k$ with

$\mathcal{P}_2$ constant.

One can write:

$$x(t) = f_{\mathrm{B}}\left(G_2\left(\sum_{k,\ k\neq l}\sqrt{\mathcal{P}^k}c^k(t) + \sqrt{\mathcal{P}^l}c^l(t) + n(t)\right)\right)$$

It is now introduced that:

$$\begin{aligned} r(t) &= \sum_{k,\ k\neq l}\sqrt{\mathcal{P}^k}c^k(t) + \sqrt{\mathcal{P}^l}c^l(t) + n(t) = r_1(t) + r_2(t) \\ r_1(t) &= \sqrt{\mathcal{P}^l}c^l(t) + n(t) \\ r_2(t) &= \sum_{k,\ k\neq l}\sqrt{\mathcal{P}^k}c^k(t) \end{aligned}$$

As deduced before, $(r_2(t))^2$ is constant (and approximately equal to the predominant signal power), thus it can be considered that:

$$r_2(t) \in \left\{-\sqrt{\mathcal{P}_2}, \sqrt{\mathcal{P}_2}\right\}$$

It can be now noticed that $r(t)$ is alternatively equivalent to $r_1(t) - \sqrt{\mathcal{P}_2}$ and $r_1(t) + \sqrt{\mathcal{P}_2}$ (equivalent situation on figure 4.3 when replacing $\mathcal{P}^l$ by $\mathcal{P}^l + \mathcal{P}_2$). Since the blanking interval is $[-\mathrm{BTH}, \mathrm{BTH}]$, this situation is equivalent to $r(t) = r_1(t)$ with a blanking interval alternatively of:

$$[-\mathrm{BTH} + G_2\sqrt{\mathcal{P}_2},\ \mathrm{BTH} + G_2\sqrt{\mathcal{P}_2}] \ \text{ and } \ [-\mathrm{BTH} - G_2\sqrt{\mathcal{P}_2},\ \mathrm{BTH} - G_2\sqrt{\mathcal{P}_2}]$$

This is actually the condition of the establishment of the expressions of $\mathcal{E}[C]$ and $\mathrm{var}[C]$ for the baseline model in section 4.3 with the only difference that the intervals of no-blanking is now alternatively the previous ones instead of $[-\mathrm{BTH},\ \mathrm{BTH}]$. And the condition of validity is:

$$\left|\mathrm{BTH} - G_2\sqrt{\mathcal{P}_2}\right| \ll G_2\sqrt{\mathcal{P}^l}$$

With these considerations, we can now deduce directly the expressions for the contributions of tracked signal and noise from the expressions established for the baseline model. In the derivations, it is equivalent to consider $\sqrt{\mathcal{P}_2}$ or $-\sqrt{\mathcal{P}_2}$ for the blanking interval, thus, one can consider one case only for the no-blanking interval in replacement of $[-\mathrm{BTH},\ \mathrm{BTH}]$, e.g.

$$[-\mathrm{BTH} - G_2\sqrt{\mathcal{P}_2},\ \mathrm{BTH} - G_2\sqrt{\mathcal{P}_2}]$$

Remark: It is reminded that $Q_0(\frac{-K-\mu}{\sigma}) - Q_0(\frac{K-\mu}{\sigma})$ is the probability that a Gaussian noise ($\mathcal{N}(\mu, \sigma^2)$) is in $[-K, K]$.

- Standard deviation of $x(t)$: the former term $G_2\sigma$ stays unchanged.
- Proportion of navigation signal not blanked: the former term $1-2Q_0\left(\frac{\mathrm{BTH}}{G_2\sigma}\right)$ coming from $Q_0\left(\frac{-\mathrm{BTH}}{G_2\sigma}\right) - Q_0\left(\frac{\mathrm{BTH}}{G_2\sigma}\right)$ becomes $Q_0\left(\frac{-\mathrm{BTH}-G_2\sqrt{\mathcal{P}_2}}{G_2\sigma}\right) - Q_0\left(\frac{\mathrm{BTH}-G_2\sqrt{\mathcal{P}_2}}{G_2\sigma}\right)$.

- Bias in the balancedness of noise repartition: the former term $-\frac{\mathrm{BTH}}{G_2\sigma}\sqrt{\frac{2}{\pi}}e^{-\frac{\mathrm{BTH}^2}{2(G_2\sigma)^2}}$ coming from $-\frac{\mathrm{BTH}}{G_2\sigma}\frac{1}{\sqrt{2\pi}}e^{-\frac{\mathrm{BTH}^2}{2(G_2\sigma)^2}}$ $-\frac{\mathrm{BTH}}{G_2\sigma}\frac{1}{\sqrt{2\pi}}e^{-\frac{\mathrm{BTH}^2}{2(G_2\sigma)^2}}$ becomes $-\frac{\mathrm{BTH}}{G_2\sigma}\frac{1}{\sqrt{2\pi}}e^{-\frac{\left(\mathrm{BTH}-G_2\sqrt{\mathcal{P}_2}\right)^2}{2(G_2\sigma)^2}}$ $-\frac{\mathrm{BTH}}{G_2\sigma}\frac{1}{\sqrt{2\pi}}e^{-\frac{\left(\mathrm{BTH}+G_2\sqrt{\mathcal{P}_2}\right)^2}{2(G_2\sigma)^2}}$
- Noise shaping: the former term $1-2Q_2\left(\frac{\mathrm{BTH}}{G_2\sigma}\right)$ coming from $Q_2\left(\frac{-\mathrm{BTH}}{G_2\sigma}\right)-Q_2\left(\frac{\mathrm{BTH}}{G_2\sigma}\right)$ becomes $Q_2\left(\frac{-\mathrm{BTH}-G_2\sqrt{\mathcal{P}_2}}{G_2\sigma}\right)-Q_2\left(\frac{\mathrm{BTH}-G_{\mathrm{POn}}\sqrt{\mathcal{P}_2}}{G_{\mathrm{POn}}\sigma}\right)$

Because of constant power, the contribution of the interfering signals in the variance can be established from derivations of section 4.2.

Finally:

$$\sqrt{S}=\mathcal{E}[C]=G_2\sqrt{\mathcal{P}^l}\left[Q_0\left(\frac{-\mathrm{BTH}-G_2\sqrt{\mathcal{P}_2}}{G_2\sigma}\right)-Q_0\left(\frac{\mathrm{BTH}-G_2\sqrt{\mathcal{P}_2}}{G_2\sigma}\right)-\frac{\mathrm{BTH}}{G_2\sigma}\frac{1}{\sqrt{2\pi}}\left(e^{-\frac{\left(\mathrm{BTH}-G_2\sqrt{\mathcal{P}_2}\right)^2}{2(G_2\sigma)^2}}+e^{-\frac{\left(\mathrm{BTH}+G_2\sqrt{\mathcal{P}_2}\right)^2}{2(G_2\sigma)^2}}\right)\right]$$

$$N=\frac{1}{\beta T}G_2^2\sigma^2\left(Q_2\left(\frac{-\mathrm{BTH}-G_2\sqrt{\mathcal{P}_2}}{G_2\sigma}\right)-Q_2\left(\frac{\mathrm{BTH}-G_2\sqrt{\mathcal{P}_2}}{G_2\sigma}\right)\right)$$

Concerning the interference contribution, it has been established in section 4.2:

$$I^k=G_2^2\cdot\mathrm{var}\left[\frac{1}{T}\int\limits_{[0,T]\setminus I_B}s^k(t)c^l(t)dt\right]$$

The expression of the noise contribution without blanker has been already established in section 3.5. The aim is now to establish the link between this expression and the one with blanker.

It has been established in section 3.5 that:

$$\mathrm{var}\left[\frac{1}{T}\int_0^T s^k(t)c^l(t)dt\right]\propto 1/T$$

And from the appendix D.2, one finally deduces that:

$$\mathrm{var}\left[\frac{1}{T}\int\limits_{[0,T]\setminus I_B}s^k(t)c^l(t)dt\right]=\frac{T_B}{T}\mathrm{var}\left[\frac{1}{T}\int_0^T s^k(t)c^l(t)dt\right]$$

with T_B the length of the no-blanking interval in $[0,T]$. Actually, $\frac{T_B}{T}$ is the ratio of navigation signal not blanked, which has been established in this section as:

$$\frac{T_B}{T}=Q_0\left(\frac{-\mathrm{BTH}-G_2\sqrt{\mathcal{P}_2}}{G_2\sigma}\right)-Q_0\left(\frac{\mathrm{BTH}-G_2\sqrt{\mathcal{P}_2}}{G_2\sigma}\right)$$

Therefore, it is deduced:

$$I^k = G_2^2 \cdot \mathcal{P}^k \cdot \frac{T_c}{T} \cdot \mathrm{WCC}\left(\tau^k\right) \cdot \left(Q_0\left(\frac{-\mathrm{BTH} - G_2\sqrt{\mathcal{P}_2}}{G_2\sigma}\right) - Q_0\left(\frac{\mathrm{BTH} - G_2\sqrt{\mathcal{P}_2}}{G_2\sigma}\right)\right)$$

4.4.2 Tracking of the Predominant Signal

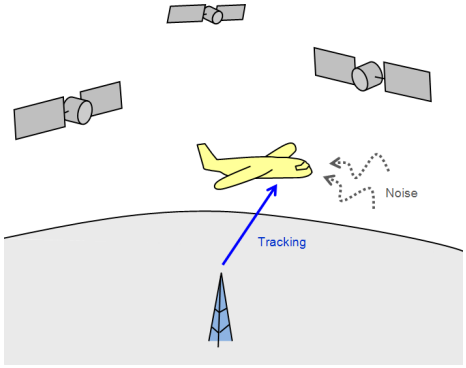

Figure 4.5: Example of application: tracking of pseudolite signal in case of no other pseudolite present

This situation corresponds typically to pseudolite tracking in the case of a single emitting pseudolite (no overlapping) or in case of multiple pseudolites (overlapping) where one has predominant power (Cf. figure 4.5).
In this section, we will establish that the sum of all navigation signals when subtracting the tracked one (pseudolite) can be neglected. It will be therefore the equivalent conditions of application of the baseline model, but without the condition $G_2\sqrt{\mathcal{P}^l} \ll \mathrm{BTH}$. We will thus derive a model but without all simplifications.

Since there is one predominant signal, it is considered that the power of the received signal is constant, thus it is introduced that $G(t) = G_2$.

We consider that we are tracking the navigation signal from source l (with power $\mathcal{P}_2$) and this signal has a much larger power than the total power of other navigation signals: $\mathcal{P}^l = \mathcal{P}^2 \gg \sum_{k \neq l} \sqrt{\mathcal{P}^k}$

One can write:

$$x(t) = f_{\mathrm{B}}\left(G_2\left(\sum_{k \neq l} \sqrt{\mathcal{P}^k} c^k(t) + \sqrt{\mathcal{P}_2} c^l(t) + n(t)\right)\right)$$

$$x(t) \approx f_{\mathrm{B}}\left(G_2\left(\sqrt{\mathcal{P}_2} c^l(t) + n(t)\right)\right)$$

With this consideration, we can now deduce directly the expressions for the contributions of tracked signal and noise from the intermediate expressions established for the baseline model. The "only" difference is that the condition $G_2\sqrt{\mathcal{P}_2} \ll \mathrm{BTH}$ is not valid here, thus no approximation can be done.

Expression for the Mean of the Correlator Output

From equation 4.2 on page 37:

$$\mathcal{E}[C] = G_2 \int_{-\frac{\mathrm{BTH}}{G_2}-\sqrt{\mathcal{P}_2}}^{\frac{\mathrm{BTH}}{G_2}-\sqrt{\mathcal{P}_2}} \left(\sqrt{\mathcal{P}_2}c^l(t) + n(t)\right) p(n)dn$$

It is now introduced: $b_1 = \frac{-\mathrm{BTH}-G_2\sqrt{\mathcal{P}_2}}{G_2\sigma}$ and $b_2 = \frac{\mathrm{BTH}-G_2\sqrt{\mathcal{P}_2}}{G_2\sigma}$.

$$\begin{aligned}\sqrt{S} = \mathcal{E}[C] &= G_2\sqrt{\mathcal{P}_2}\int_{b_1}^{b_2}\frac{1}{\sqrt{2\pi}}e^{-\frac{n^2}{2}}dn + G_2\sigma\int_{b_1}^{b_2}\frac{n}{\sqrt{2\pi}}e^{-\frac{n^2}{2}}dn \\ &= G_2\sqrt{\mathcal{P}_2}\left[Q_0(b_1) - Q_0(b_2)\right] + G_2\sigma\left[Q_1(b_1) - Q_1(b_2)\right]\end{aligned}$$

Expression for the Variance of the Correlator Output

From equation 4.5 on page 43:

$$\mathrm{var}[C] = \frac{1}{\beta T}\left(\mathcal{E}\left[{f_\mathrm{B}}^2\left(G_2\left(\sqrt{\mathcal{P}_2} + n(t)\right)\right)\right] - \left(\mathcal{E}[C]\right)^2\right)$$

And:

$$\begin{aligned}&\mathcal{E}\left[{f_\mathrm{B}}^2\left(G_2\left(\sqrt{\mathcal{P}_2} + n(t)\right)\right)\right] \\ &\quad= G_2^2\mathcal{P}_2\int_{b_1}^{b_2}\frac{1}{\sqrt{2\pi}}e^{-\frac{n^2}{2}}dn + G_2^2 2\sqrt{\mathcal{P}_2}\sigma\int_{b_1}^{b_2}\frac{n}{\sqrt{2\pi}}e^{-\frac{n^2}{2}}dn \\ &\qquad+ G_2^2\sigma^2\int_{b_1}^{b_2}\frac{n^2}{\sqrt{2\pi}}e^{-\frac{n^2}{2}}dn \\ &\quad= G_2^2\Big(\mathcal{P}_2\left[Q_0(b_1) - Q_0(b_2)\right] + 2\sqrt{\mathcal{P}_2}\sigma\left[Q_1(b_1) - Q_1(b_2)\right] \\ &\qquad+\sigma^2\left[Q_2(b_1) - Q_2(b_2)\right]\Big)\end{aligned}$$

Finally, with the relation $N + I = \mathrm{var}[C]$, one deduces:

$$\begin{aligned}N + I = \frac{G_2^2}{\beta T}\Big(&\mathcal{P}_2\left[Q_0(b_1) - Q_0(b_2)\right] + 2\sqrt{\mathcal{P}_2}\sigma\left[Q_1(b_1) - Q_1(b_2)\right] \\ &+ \sigma^2\left[Q_2(b_1) - Q_2(b_2)\right] \\ &- \left(\sqrt{\mathcal{P}_2}\left[Q_0(b_1) - Q_0(b_2)\right] + \sigma\left[Q_1(b_1) - Q_1(b_2)\right]\right)^2\Big)\end{aligned}$$

4.5 Situation of Similar-High-Power Signals

4.5.1 Tracking of Low-Power Signal in Presence of Similar-High-Power Signals

This situation corresponds typically to satellite tracking in the case that several pseudolites emit in same time (pulse overlapping) with same received power (Cf.

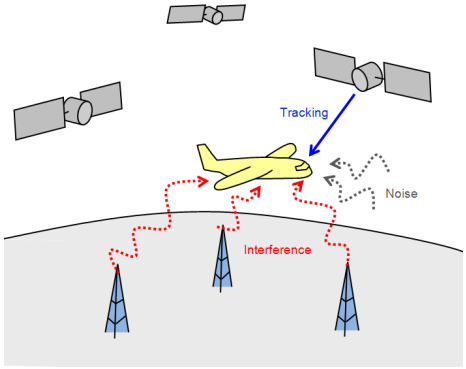

Figure 4.6: Example of application: tracking of satellite signal in case of proximity with pseudolites emitting in same time (with similar power)

figure 4.5). The analysis corresponds to the worst case that all signals have the exact same frequency and phase.

This situation is specific: the addition of signals of similar power produces constructive and destructive "interferences", therefore the total power cannot be considered as constant during a pulse. Approx. 10 is not valid here and we will have to define a value for $G(t)$. For the sake of simplification, it is considered that since it is a sum of signals of high power, the noise can be neglected. We consider that K_p high power signals are received, all with same power $\mathcal{P}_3$. We consider a time t randomly chosen on $[0, T]$. We call p_+, and p_- the probabilities that one navigation signal has the value $\sqrt{\mathcal{P}_3}$, and $-\sqrt{\mathcal{P}_3}$, respectively. Because of the randomness of the spreading codes, $p_+ = p_- = \frac{1}{2}$. We call $s(t)$ the sum of the high-power signals.

For K_p high-power signals, $s(t)$ can take the following values:

$$\begin{aligned} &-K_p\sqrt{\mathcal{P}_3},\ -(K_p+2)\sqrt{\mathcal{P}_3},\ \cdots, K_p\sqrt{\mathcal{P}_3} \\ \text{i.e. } &-K_p\sqrt{\mathcal{P}_3} + 2N_s\sqrt{\mathcal{P}_3} \qquad \text{for } N_s = 0, \cdots, K_p \end{aligned}$$

N_s is the random variable corresponding to the number of signals of amplitude $\sqrt{\mathcal{P}_3}$.

Using the binomial distribution:

$$P\left(s(t) = -K_p\sqrt{\mathcal{P}_3} + 2N_s\sqrt{\mathcal{P}_3}\right) = \binom{K_\mathrm{p}}{N_s} {p_+}^{N_s} {p_-}^{K_\mathrm{p}-N_s} = \binom{K_\mathrm{p}}{N_s} \frac{1}{2^{K_\mathrm{p}}}$$

for $N_s = 0, \cdots, K_p$

It is now deduced:

- Since the mean of N_s is $\frac{K_\mathrm{p}}{2}$, the mean of $s(t)$ is 0.
- Since the variance of N_s is $K_\mathrm{p} p_+ p_- = \frac{K_\mathrm{p}}{4}$, it is calculated that the variance of $s(t)$ is $K_\mathrm{p}\mathcal{P}_3$.

It is considered that the AGC recovery time is longer than a few T_c, thus the signal power is constant from the point of view of the AGC and therefore, $G(t)$ is considered constant. In this specific situation, Approx. 10 is not valid because of a non-constant pulse, but after calculation, it is established that here again the value of G_3 is $\frac{1}{\sqrt{K_\mathrm{p}\mathcal{P}_3}}$ (since the variance of $s(t)$ is $K_\mathrm{p}\mathcal{P}_3$).

Expression for the Mean of the Correlator Output

Let us now establish the proportion of signal which is not blanked:

$$\begin{aligned} P\left(G_3 s(t) \in [-\mathrm{BTH}, \mathrm{BTH}]\right) &= 1 - P\left(G_3 s(t) > \mathrm{BTH}\right) - P\left(G_3 s(t) < -\mathrm{BTH}\right) \\ &= 1 - 2P\left(s(t) > \frac{\mathrm{BTH}}{G_3}\right) \\ &= 1 - 2P\left((-K_p + 2N_s) \cdot \sqrt{\mathcal{P}_3} > \frac{\mathrm{BTH}}{G_3}\right) \\ &= 1 - 2P\left(N_s > \frac{\mathrm{BTH}}{2G_3\sqrt{\mathcal{P}_3}} + \frac{K_\mathrm{p}}{2}\right) \end{aligned}$$

Let us define: $k_0 = \left\lceil \frac{\mathrm{BTH}}{2G_3\sqrt{\mathcal{P}_3}} + \frac{K_\mathrm{p}}{2} \right\rceil$

$$\begin{aligned} P\left(G_3 s(t) \in [-\mathrm{BTH}, \mathrm{BTH}]\right) &= 1 - 2\sum_{k=k_0}^{K_\mathrm{p}} \binom{K_\mathrm{p}}{k} \frac{1}{2^{K_\mathrm{p}}} \\ &= 1 - \frac{1}{2^{K_\mathrm{p}-1}} \sum_{k=k_0}^{K_\mathrm{p}} \binom{K_\mathrm{p}}{k} \end{aligned}$$

As a consequence:

$$\sqrt{S} = \mathcal{E}[C] = G_3\sqrt{\mathcal{P}^l}\left(1 - \frac{1}{2^{K_\mathrm{p}-1}} \sum_{k=k_0}^{K_\mathrm{p}} \binom{K_\mathrm{p}}{k}\right)$$

$$\text{with: } k_0 = \left\lceil \frac{\mathrm{BTH}}{2G_3\sqrt{\mathcal{P}_3}} + \frac{K_\mathrm{p}}{2} \right\rceil$$

Expression for the Variance of the Correlator Output

We will now establish the variance of the signal after blanking and correlation (not yet integration). Since $K_p - 2N_s$ is the random variable corresponding to $s(t)$, the variance of the signal before blanking is:

$$\mathrm{var}\left[2N_s - K_\mathrm{p}\right] = \sum_{k=0}^{K_\mathrm{p}} (2k - K_\mathrm{p})^2 \mathcal{P}_3 \cdot P(N_s = k) = K_\mathrm{p}\mathcal{P}_3$$

For the tracking of $s^l(t)$, since its power is negligible, $c^l(t)$ is independent of $s(t)$ and $\mathrm{var}\left[f_\mathrm{B}\left(s(t)\right) \cdot c^l(t)\right] = \mathrm{var}\left[f_\mathrm{B}\left(s(t)\right)\right]$. The multiplicative term $c^l(t)$ has been removed because $s^l(t)$ is neglected in $s(t)$ (low power signal) and thus, because

of the symmetry of the distribution, $s(t)c^l(t)$ can be equivalently replaced by $s(t)$. Therefore, the variance of the signal after blanking and correlation is:

$$\begin{aligned}\mathrm{var}\left[f_{\mathrm{B}}(2N_s - K_{\mathrm{p}})\right] &= \sum_{k=0}^{K_{\mathrm{p}}} (2k - K_{\mathrm{p}})^2 \mathcal{P}_3 \cdot P(N_s = k) \\ &\quad - 2 \sum_{k=\lceil k_0 \rceil}^{K_{\mathrm{p}}} (2k - K_{\mathrm{p}})^2 \mathcal{P}_3 \cdot P(N_s = k) \\ &= K_{\mathrm{p}} \mathcal{P}_3 \left(1 - \frac{1}{2^{K_{\mathrm{p}}-1} K_{\mathrm{p}}} \sum_{k=k_0}^{K_{\mathrm{p}}} (2k - K_{\mathrm{p}})^2 \binom{K_{\mathrm{p}}}{k}\right)\end{aligned}$$

The strong signals are independent of each other, also after blanking. We will consider that the strong signals keep their properties after blanking but with a power scaled by:

$$\left(1 - \frac{1}{2^{K_{\mathrm{p}}-1} K_{\mathrm{p}}} \sum_{k=k_0}^{K_{\mathrm{p}}} (2k - K_{\mathrm{p}})^2 \binom{K_{\mathrm{p}}}{k}\right)$$

Since the blanking has already been considered, $\mathrm{var}[C]$ can be split (with k_p the index for the high-power signals):

$$\begin{aligned}\mathrm{var}[C] = {G_3}^2 \sum_{k_p=1}^{K_{\mathrm{p}}} \mathrm{var}\left[\frac{1}{T} \int_0^T s^{k_p}(t) c^l(t) dt\right] \\ \cdot \left(1 - \frac{1}{2^{K_{\mathrm{p}}-1} K_{\mathrm{p}}} \sum_{k=k_0}^{K_{\mathrm{p}}} (2k - K_{\mathrm{p}})^2 \binom{K_{\mathrm{p}}}{k}\right)\end{aligned}$$

Therefore (k_p is the index for the high-power signals):

$$\begin{aligned}I^{k_p} = \mathrm{var}[C] &= {G_3}^2 \mathcal{P}_3 \cdot \frac{T_c}{T} \cdot \mathrm{WCC}\left(\tau^{k_p}\right) \\ &\quad \cdot \left(1 - \frac{1}{2^{K_{\mathrm{p}}-1} K_{\mathrm{p}}} \sum_{k=k_0}^{K_{\mathrm{p}}} (2k - K_{\mathrm{p}})^2 \binom{K_{\mathrm{p}}}{k}\right) \\ \text{with: } k_0 &= \left\lceil \frac{\mathrm{BTH}}{2G_3\sqrt{\mathcal{P}_3}} + \frac{K_{\mathrm{p}}}{2} \right\rceil\end{aligned}$$

Since the noise contribution to the variance is neglected, $\mathrm{var}[C] \approx \sum_{k_p} I^{k_p}$.

Discussion:

- In case of an infinite blanking threshold:

$$\begin{aligned}\sqrt{S} &= G_3\sqrt{\mathcal{P}^l} \\ I^{k_p} &= {G_3}^2 \cdot \mathcal{P}_3 \cdot \frac{T_c}{T} \cdot \mathrm{WCC}\left(\tau^{k_p}\right)\end{aligned}$$

- The mean power has been considered to establish the interference contribution. This is relevant because the integration averages the signal.

4.5.2 Tracking of High-Power Signal in Presence of Similar-High-Power Signals

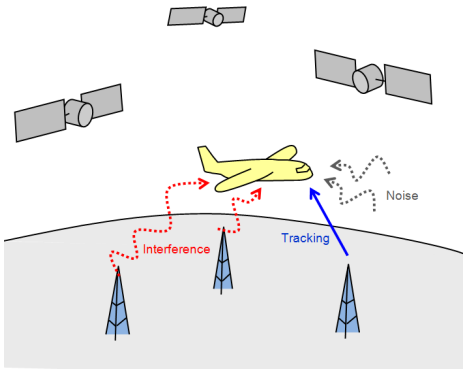

Figure 4.7: Example of application: tracking of pseudolite signal in case of proximity with pseudolites emitting in same time (with similar power)

It can correspond typically to pseudolite signal tracking when at equal distance to other pseudolites (Cf. figure 4.7). This situation is similar to the previous one, with the only difference that since the tracked signal $s^l(t)$ has now a power which is not negligible anymore, $c^l(t)$ has to be taken into consideration in the variance:

$$\text{var}\left[f_{\text{B}}\left(\sum_k \sqrt{\mathcal{P}_3}c^k(t)\right)\cdot c^l(t)\right] = \text{var}\left[f_{\text{B}}\left(\sum_{k,\ k\neq l} \sqrt{\mathcal{P}_3}c^k(t)\cdot c^l(t) + \sqrt{\mathcal{P}_3}\right)\right]$$

The mean is the same as previously because since the received signal is the same, the proportion of blanked signal is also the same. Therefore:

$$N \approx 0$$

$$\sqrt{S} = G_3\sqrt{\mathcal{P}_3}\left(1 - \frac{1}{2^{K_{\text{p}}-1}}\sum_{k=k_0}^{K_{\text{p}}}\binom{K_{\text{p}}}{k}\right)$$
$$\text{with: } k_0 = \left\lceil \frac{\text{BTH}}{2G_3\sqrt{\mathcal{P}_3}} + \frac{K_{\text{p}}}{2}\right\rceil$$

Finally, this situation is equivalent to the previous one with some new parameters for the expression of the variance:

- The blanking interval is now $[-\text{BTH} - G_3\sqrt{\mathcal{P}_3},\ \text{BTH} - G_3\sqrt{\mathcal{P}_3}]$ instead of $[-\text{BTH},\ \text{BTH}]$, with G_3 defined the same way as before (because same signal power).
- The index k is running from 0 to $(K_{\text{p}} - 1)$ instead of K_{p}.

Let us introduce $\begin{cases} k_- = \left\lceil \frac{\mathrm{BTH}}{2G_3\sqrt{\mathcal{P}_3}} + \frac{K_\mathrm{p}-1}{2} \right\rceil \\ k_+ = \left\lceil \frac{\mathrm{BTH}}{2G_3\sqrt{\mathcal{P}_3}} + \frac{K_\mathrm{p}+1}{2} \right\rceil \end{cases}$

$$
\begin{aligned}
&\mathrm{var}\left[f_\mathrm{B}(2N_s - K_\mathrm{p} + \sqrt{\mathcal{P}_3})\right] \\
&\quad = \sum_{k=0}^{K_\mathrm{p}-1} (2k - K_\mathrm{p})^2 \mathcal{P}_3 \cdot P(N_s = k) - \sum_{k=k_-}^{K_\mathrm{p}-1} (2k - K_\mathrm{p})^2 \mathcal{P}_3 \cdot P(N_s = k) \\
&\qquad - \sum_{k=k_+}^{K_\mathrm{p}-1} (2k - K_\mathrm{p})^2 \mathcal{P}_3 \cdot P(N_s = k) \\
&\quad = \mathcal{P}_3 \left(K_\mathrm{p} - 1 - \frac{1}{2^{K_\mathrm{p}-1}} \left(\sum_{k=k_-}^{K_\mathrm{p}-1} (2k - K_\mathrm{p})^2 \binom{K_\mathrm{p}-1}{k} \right.\right. \\
&\qquad \left.\left. + \sum_{k=k_+}^{K_\mathrm{p}-1} (2k - K_\mathrm{p})^2 \binom{K_\mathrm{p}-1}{k} \right) \right)
\end{aligned}
$$

Finally (k_p is the index for the high-power signals):

$$
\begin{aligned}
I^{k_p} &= {G_3}^2 \mathcal{P}_3 \cdot \frac{T_c}{T} \cdot \mathrm{WCC}\left(\tau^{k_p}\right) \\
&\quad \cdot \left(1 - \frac{1}{2^{K_\mathrm{p}-1}\left(K_\mathrm{p}-1\right)} \left(\sum_{k=k_-}^{K_\mathrm{p}-1} (2k - K_\mathrm{p})^2 \binom{K_\mathrm{p}-1}{k} \right.\right. \\
&\qquad \left.\left. + \sum_{k=k_+}^{K_\mathrm{p}-1} (2k - K_\mathrm{p})^2 \binom{K_\mathrm{p}-1}{k} \right) \right) \\
\text{with: } &\begin{cases} k_- = \left\lceil \frac{\mathrm{BTH}}{2G_3\sqrt{\mathcal{P}_3}} + \frac{K_\mathrm{p}-1}{2} \right\rceil \\ k_+ = \left\lceil \frac{\mathrm{BTH}}{2G_3\sqrt{\mathcal{P}_3}} + \frac{K_\mathrm{p}+1}{2} \right\rceil \end{cases}
\end{aligned}
$$

Discussion: In case of infinite blanking threshold, it becomes:

$$
\begin{aligned}
\sqrt{S} &= G_3\sqrt{\mathcal{P}_3} \\
I^{k_p} &= {G_3}^2 \cdot \mathcal{P}_3 \cdot \frac{T_c}{T} \cdot \mathrm{WCC}\left(\tau^{k_p}\right)
\end{aligned}
$$

Note: The tracked signal, although being a high-power signal, has no contribution to var$[C]$, as exposed in section 4.2. Therefore, when making the sum of the I^{k_p} for the calculation of the variance, the term I^l has to be considered equal to zero (l is the index of the tracked signal).

This is coherent : for example, if there are two strong navigation signals, when tracking a low power signal, there will have the interference coming from the two strong signals. But when tracking one of the strong navigation signals, the interference will come from the other strong signal only.

4.6 Other Situations: Tracking in Presence of Signals of Different High Powers

This situation corresponds to the presence of signals with high powers which can be different to each other. In this case, it is not possible to give explicit expressions for the contributions to the SNIR because $s(t)$ at a time t is the sum of random variables.

For example for 3 pseudolites of respective power $\mathcal{P}$, $9\mathcal{P}$ and $16\mathcal{P}$, there will be $2^3 = 8$ possible combinations: 8 $\sqrt{\mathcal{P}}$, 6 $\sqrt{\mathcal{P}}$, 2 $\sqrt{\mathcal{P}}$, -2 $\sqrt{\mathcal{P}}$, -6 $\sqrt{\mathcal{P}}$, -8 $\sqrt{\mathcal{P}}$, each with a probability of $\frac{1}{8}$, and 0 with a probability of $\frac{1}{4}$. Therefore, in this kind of situation, all the possible values for $s(t)$ and the associated probabilities have to be calculated on a case by case basis.

4.7 Final Analytical Models

In the former sections, the expressions of the contributions to SNIR for satellite and pseudolite tracking have been established for the three standard situations:

- *Situation 1*: Only low-power signals
- *Situation 2*: One predominant signal
- *Situation 3*: Low-power signals and K_{p} similar-high-power signals

The aim is here to "merge" these situations applicable to the continuous reception of satellite or pseudolite signals. For this purpose, a segmentation of the coherent integration intervals will be performed (typically intervals when the pulse is present and predominant, and intervals when pulse is absent) and the analytical SNIR models are deduced by combining the applicable elementary SNIR for each interval. Fr example *scenario 1* from $t = 0$ till $t = T - T_p$ and *scenario 2* from $t = T - T_p$ up to $t = T$, etc.

In order to established the expressions, it is considered that the signals are no longer continuous. For instance, the previous example will correspond to the addition of:

- A sum of only low power signals, restricted to $[0,\ T - T_p]$ (i.e. equal to 0 on $[T - T_p,\ T]$).
- A sum of low power signals and only one high power signal, restricted to $[T - T_p,\ T]$.

Of course, a signal can be present on the whole interval $[0,\ T]$, but not always in the same situation. Many small restrictions may be imbricated. What is actually considered is the mean duty cycle of each situation because from Approx. 6, the cumulative duration of the pulses during a time interval $[t, t + T], \forall\ t$ is always the same.

4.7.1 Segmentation of Coherent Integration Interval

Let us first establish the general expressions for $\mathcal{E}[C]$ and $\mathrm{var}[C]$ for a situation restricted to intervals of cumulative duration T_p within $[0,\ T]$. We call I_p this interval (thus, the signal is 0 on $[0,\ T] \setminus I_p$).

General Expression for $\mathcal{E}[C]$ for a Restricted Signal

$$\begin{aligned}\mathcal{E}[C] &= \mathcal{E}\left[\frac{1}{T}\int_0^T \tilde{x}(t)c^l(t)dt\right] \\ &= \mathcal{E}\left[\frac{1}{T}\int\limits_{[0,T]\,\cap\,I_p} \tilde{x}(t)c^l(t)dt + \frac{1}{T}\int\limits_{[0,T]\,\setminus\,I_p} \tilde{x}(t)c^l(t)dt\right] \\ &= \mathcal{E}\left[\frac{1}{T}\int\limits_{[0,T]\,\cap\,I_p} \tilde{x}(t)c^l(t)dt\right]\end{aligned}$$

And since $\mathcal{E}\left[\frac{1}{T}\int_0^T x(t)c^l(t)dt\right]$ does not depend on the time of integration T, it is deduced that:

$$\mathcal{E}\left[\frac{1}{T}\int_0^T x(t)c^l(t)dt\right] = \mathcal{E}\left[\frac{1}{T_p}\int\limits_{[0,T]\,\cap\,I_p} \tilde{x}(t)c^l(t)dt\right]$$

And consequently:

$$\mathcal{E}[C] = \frac{T_p}{T}\cdot\mathcal{E}\left[\frac{1}{T}\int_0^T x(t)c^l(t)dt\right]$$

The coefficient $\frac{T_p}{T}$ is actually the duty cycle of the signal and $\mathcal{E}\left[\frac{1}{T}\int_0^T x(t)c^l(t)dt\right]$ corresponds to $\mathcal{E}[C]$ as expressed in previous sections, depending on the situation.

General Expression for var$[C]$ for a Restricted Signal

$$\begin{aligned}\mathrm{var}[C] &= \mathrm{var}\left[\frac{1}{T}\int_0^T \tilde{x}(t)c^l(t)dt\right] \\ &= \mathrm{var}\left[\frac{1}{T}\int\limits_{[0,T]\,\cap\,I_p} \tilde{x}(t)c^l(t)dt\right]\end{aligned}$$

All expressions of var$[C]$ established for any situation are inversely proportional to the (effective) time of integration. Therefore, from the appendix D.2, one deduces directly:

$$\mathrm{var}[C] = \frac{T_p}{T}\cdot\mathrm{var}\left[\frac{1}{T}\int_0^T x(t)c^l(t)dt\right]$$

Here again, the coefficient $\frac{T_p}{T}$ is the duty cycle of the signal and the term $\mathrm{var}\left[\frac{1}{T}\int_0^T x(t)c^l(t)dt\right]$ corresponds to var$[C]$ as expressed in previous sections, depending on the situation.

4.7.2 Final Models

In this section is given the method to determine the final models with "concatenation" of standard models previously established. The models allow to define the following parameters:

- Global parameters: T, T_c, β
- AGC behaviour (slow or fast)
- Blanking threshold BTH
- Duty cycles of situation 1 (DC_1), situation 2 (DC_2), situation 3 (DC_3)
- Noise standard deviation σ
- Power $\mathcal{P}_2$ of the predominant signal of situation 2
- Number K_p and power $\mathcal{P}_3$ of strong signals of situation 3
- Delay τ_2 of the tracked signal with respect to the predominant signal of situation 2
- Delay τ^{k_p} of the tracked signal with one strong signal (index k_p) of situation 3
- Power of tracked signal $\mathcal{P}^l$

To each situation is associated a specific duty cycle and a gain value:

- ***Situation 1*: Only low-power signals**, with a duty cycle of DC_1 and a gain of:
$$G_1 = \begin{cases} \frac{1}{\sigma} & \text{for fast AGC} \\ \frac{1}{\sqrt{\sigma^2+\mathrm{DC}_2\cdot\mathcal{P}_2+\mathrm{DC}_3\cdot\frac{1}{2}K_\mathrm{p}\mathcal{P}_3}} & \text{for slow AGC} \end{cases}$$
- ***Situation 2*: One predominant signal** of power $\mathcal{P}_2$, with a duty cycle of DC_2 and a gain of:
$$G_2 = \begin{cases} \frac{1}{\sqrt{\sigma^2+\mathcal{P}_2}} & \text{for fast AGC} \\ \frac{1}{\sqrt{\sigma^2+\mathrm{DC}_2\cdot\mathcal{P}_2+\mathrm{DC}_3\cdot\frac{1}{2}K_\mathrm{p}\mathcal{P}_3}} & \text{for slow AGC} \end{cases}$$
- ***Situation 3*: Low-power signals and K_p similar-high-power signals** of equal power $\mathcal{P}_3$, with a duty cycle of DC_3 and a gain of:
$$G_3 = \begin{cases} \frac{1}{\sqrt{\frac{1}{2}K_\mathrm{p}\mathcal{P}_3}} & \text{for fast AGC} \\ \frac{1}{\sqrt{\sigma^2+\mathrm{DC}_2\cdot\mathcal{P}_2+\mathrm{DC}_3\cdot\frac{1}{2}K_\mathrm{p}\mathcal{P}_3}} & \text{for slow AGC} \end{cases}$$

By using the segmentation principle, one can define: $\mathrm{DC}_1 + \mathrm{DC}_2 + \mathrm{DC}_3 = 1$.

$$\mathcal{E}[C] = \mathrm{DC}_1\cdot\mathcal{E}[C]\Big|_{\text{sit. 1}} + \mathrm{DC}_2\cdot\mathcal{E}[C]\Big|_{\text{sit. 2}} + \mathrm{DC}_3\cdot\mathcal{E}[C]\Big|_{\text{sit. 3}}$$
$$\mathrm{var}[C] = \mathrm{DC}_1\cdot\mathrm{var}[C]\Big|_{\text{sit. 1}} + \mathrm{DC}_2\cdot\mathrm{var}[C]\Big|_{\text{sit. 2}} + \mathrm{DC}_3\cdot\mathrm{var}[C]\Big|_{\text{sit. 3}}$$

This general expression applies for the presence of one single-pseudolite pulse during DC_2 and one multi-pseudolites pulse during DC_3. It is also possible to define an even more general expression which takes into consideration the presence of N_1 situations of "only satellite signal" (not necessarily with same parameters), the presence of N_2 situation of "predominant pulse" and N_3 situations of "similar-high-power pulses", with of course $\sum_{i=1}^{N_1} \mathrm{DC}_{1,i} + \sum_{i=1}^{N_2} \mathrm{DC}_{2,i} + \sum_{i=1}^{N_3} \mathrm{DC}_{3,i} = 1$.

$$\mathcal{E}[C] = \sum_{i=1}^{N_1} \mathrm{DC}_{1,i} \cdot \mathcal{E}[C]\Big|_{\text{sit. } 1,i} + \sum_{i=1}^{N_2} \mathrm{DC}_{2,i} \cdot \mathcal{E}[C]\Big|_{\text{sit. } 2,i} + \sum_{i=1}^{N_3} \mathrm{DC}_{3,j} \cdot \mathcal{E}[C]\Big|_{\text{sit. } 3,i}$$

$$\begin{aligned}\mathrm{var}[C] = &\sum_{i=1}^{N_1} \mathrm{DC}_{1,i} \cdot \mathrm{var}[C]\Big|_{\text{sit. } 1,i} + \sum_{i=1}^{N_2} \mathrm{DC}_{2,i} \cdot \mathrm{var}[C]\Big|_{\text{sit. } 2,i} \\ &+ \sum_{i=1}^{N_3} \mathrm{DC}_{3,i} \cdot \mathrm{var}[C]\Big|_{\text{sit. } 3,i}\end{aligned}$$

Fi gure 4.8 illustrates a situation where $N_1 = 1$, $N_2 = 2$ (presence of two single pulses) and $N_3 = 1$. If for example one pulse in situation 2 (predominant pulse) has its power getting much smaller than the noise one, then the situation of the pulse becomes situation 1: for pseudolite tracking, the model of "low powers" has to be applied.

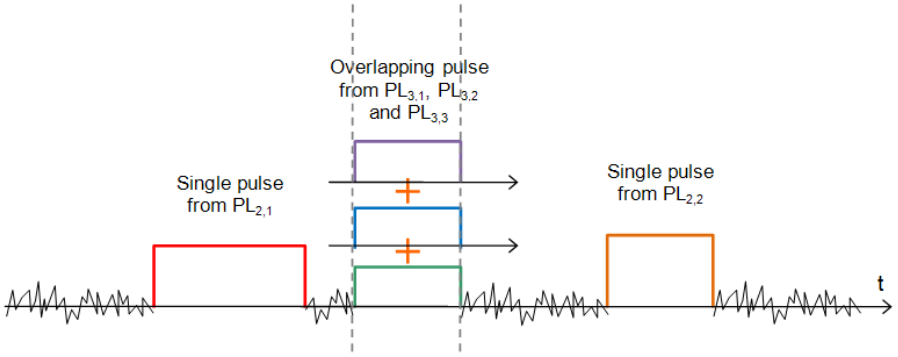

Figure 4.8: Representation of a situation of two single pulses and one overlapping pulse

Notes:

- Tracking a signal during a situation where this signal is not present (e.g. pulse tracking when pulse is off) corresponds to the model of "low-power signal" with a tracked signal power $\mathcal{P}^l$ equal to zero. Indeed, during this situation, the traked signal has no contribution to the mean of C but the other signals may have a contribution to the variance of C.
- As explained in section 3.5, in case of satellite tracking, one should consider the SSC (i.e. $\langle \mathrm{WCC}(\tau) \rangle$) in the expression of the interference contribution. In the other cases, since it involves only pseudolites (fixed delay

between navigation signals), τ is fixed and one could consider the maximal value of WCC(τ) on τ (worst case) in the expression of the interference contribution.

4.8 Application

4.8.1 Situation Classification

When considering a real configuration with the presence of pseudolites, one should be able to know which model to apply at each position. Since the pseudolite received power varies considerably with increasing distance, a situation of "predominant pulse" close to the emitter may become a situation of "low-power only" when further away. For the attribution of a model at a certain location, it is therefore essential to consider and compare all received signals in order to determine which standard situations to attribute to this location. The principle is illustrated in figure 4.9 on page 61.

In order to give a first representation of the method, a situation classification[2] is proceeded for the following example (airport configuration): two pseudolites with an emission power of -15 dBW are located at the extremities of a zone of dimensions 2 km $\times$ 6 km. The signal power is considered proportional to the inverse square of the distance to the source (free-space isotropic propagation). The resulting classification of situations is represented in figure 4.10.

The main information to take from figure 4.10b is the existence of an area corresponding to the "hybrid situation" (red area in the figure) which shows that a standard model does not necessarily apply to each position of the area. This is the main limitation of the established models.

4.8.2 Model Application

Once the classification of situations has been established from the comparison of received powers at each position, the analytical expressions can be directly applied in order to compute the SNIR in each area associated to a standard model. As explained previously, the standard models do not authorize to define the SNIR everywhere since no model has been established for the hybrid situations. Therefore, for these areas, one solution could be to choose the worst case (i.e. the smallest SNIR) between the direct neighbour models of the involved area.
This principle has been applied to the configuration previously described and the resulting SNIR is represented in figure 4.11. It can be noticed that sudden transitions in the SNIR occur. They are caused by a transition between a hybrid area where a "worst case" model applies and an area where a standard model directly applies. In the hybrid situations, the SNIR is underestimated and it may lead to conservative results.

[2]The conditions are arbitrary chosen in order to give a qualitative representation of the situation classification: 1) Situation "predominant pseudolite power": one pseudolite signal has a power at least two times higher than the sum of other navigation signal powers. 2) Situation "similar-high powers": each pseudolite has a power equal at least to 70 % of the highest one and the total sum of pseudolite powers is higher than the noise power. 3) Situation "low-power signals": noise power is two times higher than the sum of other signals.

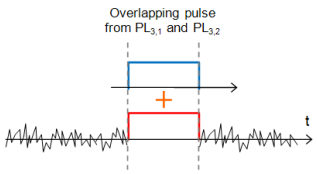

(a) Pulses of similar power: classification in situation *similar-high-power pulses*. Both pulses are considered as similar-high-power signals.

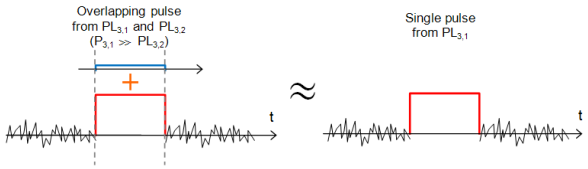

(b) One pulse power much larger than the other one: classification in situation *one predominant pulse*. The red pulse is considered as the predominant signal whereas the blue one is considered as a low-power signal.

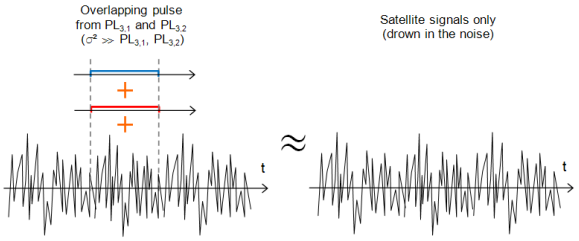

(c) Pulse powers much smaller than the noise one: classification in situation *low-power signals*. Both pulses are considered as low-power signals (i.e. like satellite signals).

Figure 4.9: Illustration for the classification of the same pulses at three different locations

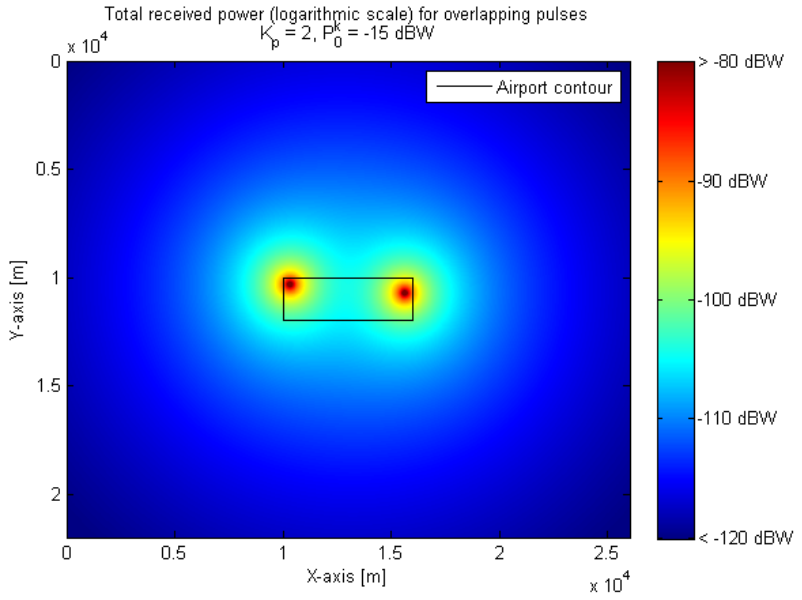

(a) Total received power.

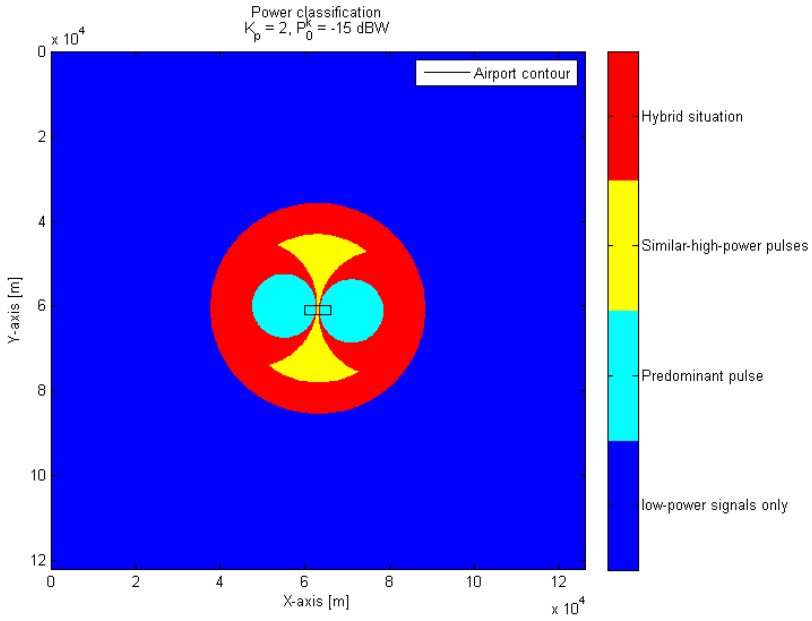

(b) Situation classification (zoom-out)

Figure 4.10: Situation classification for two simultaneous pseudolites

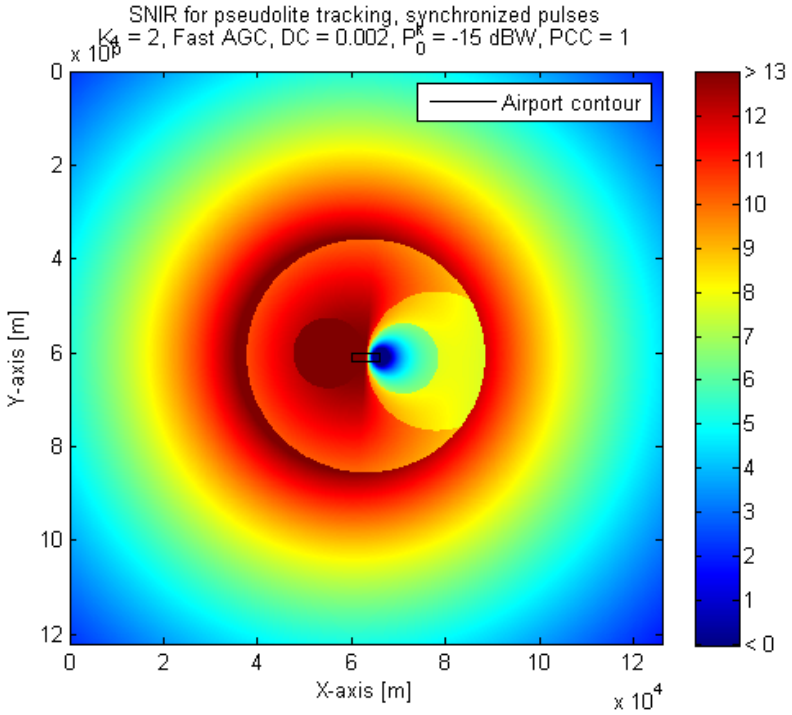

Figure 4.11: SNIR mapping for two simultaneous pseudolites (same configuration as for figures 4.10 in the case of tracking of the left pseudolite)

Chapter 5

Validation of the Model

We now have a mathematical model for the expression of SNIR depending on many parameters. But many aspects cannot be integrated in the equations. Moreover, many approximations and simplifications have been done. Therefore, it is important to estimate the relevance of this model. For this purpose, a Monte Carlo method based on an existing software tool is proposed.

5.1 Description of the Software Tool

5.1.1 Principle

Our simulations are based on a MATLAB programme which simulates a standard GNSS receiver front-end as described in figure 3.1. Each element of the front-end (LPF, AGC, etc) is emulated. The given input signal is transmitted in the chain, through each component successively. We have to introduce adapted operations which are supposed to be equivalent to the theory. Let us describe the different steps for the acquisition of a new value of the correlator output C (for one Monte Carlo realisation):

- Generation and summation of navigation signals (continuous or pulsed) randomly or from a specific pattern
- Conversion of the signal in frequency domain and filtering with a rectangular window. Down-conversion in time domain
- Generation and addition of a Gaussian noise (no need for filtering because the noise satisfies the Nyquist condition)
- Regulation of the AGC. The gain is the inverse of the square root of the power estimated on the latest time interval.
- Blanking: all samples with energy beyond the blanking threshold are put to zero.
- Correlation of the signal with the spreading code signal which corresponds to the tracked emitter. Integration on the replica code period (1 ms).

In a second time, $\mathcal{E}[C]$ and var$[C]$ are calculated over all the estimated values of C. The estimation of SNIR can then be directly deduced.

It is possible to generate different signals to inject in the front-end input: Gaussian noise and navigation signals, based on different parameters to determine.

5.1.2 Parameters

The parameters used in the software tools are described in this section. Since the tool has been developed by EADS Astrium, most of these parameters have been inherited from former studies focused on pulsed signals and performed by Astrium (typical values). Nevertheless, these parameters can be considered as representative of typical GNSS receiver front-ends.

Front-end Parameters

- Filter bandwidth (passband): $\beta = 40.92$ MHz.
  This value is chosen high enough, in order to limit the impact on spreading code signals spectrum.
- AGC recovery time: RT $= 1$ µs $\cdots$ 1 s
  The range of the recovery time values is large in order to simulate different AGC behaviours (fast/slow).
- ADC quantization resolution: 8 bits i.e. 256 levels.
  A large number of bits is chosen in order to limit the quantization losses.
- ADC sampling frequency: $f_s = 40.92$ MHz
  This value is chosen equal to β, to avoid aliasing.
- ADC maximal level: $L = \sqrt{10}$
  This value is actually not the optimal one for minimal quantization losses as shown in figure 5.1 for $N = 8$. One should normally choose the value of 2 for the ratio of clipping threshold to noise power standard deviation. This value has been actually chosen in order to enable to fix the blanking threshold up to 10 dB above noise level. Hence, this enables to have a larger dynamics of pulse signal amplitude which will not be "clipped" before entering the blanker. Indeed, the objective is to observe impact of the blanking threshold. Nevertheless, despite a non optimal L/σ ratio, the induced quantization losses are still limited (around 0.3 dB).
- Blanking threshold: BTH $= 0 \cdots$ 10 dB above noise variance.
  The effect of the blanker can be therefore precisely studied.
- Integration duration: $T = 1$ ms
  This is the typical value.

Signal Parameters

For the application, it is proposed to consider the Galileo E6 signals for the signal structure (chip waveform, code length, carrier frequency).

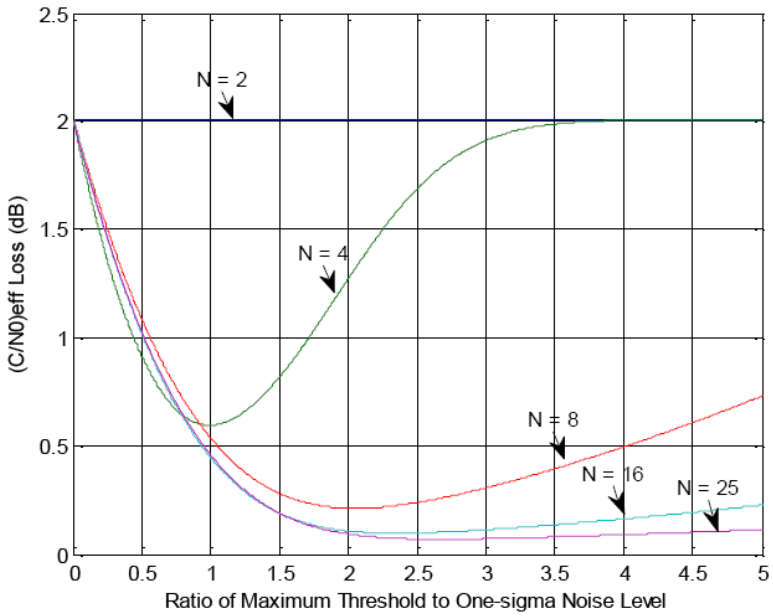

Figure 5.1: SNR losses - Rectangular symbols, noise only, two-sided receiver bandwidth equal to ten times the chipping rate, Nyquist sample rate [11]

- Noise power density: N_0 = -201.5 dBW/Hz
- Satellite signal
  - Code modulation: BPSK
  - Received power: -158.5 dBW
  - Modulation Frequency: f_e = 1278.75 MHz
  - Epoch duration: 1 ms
  - Number of chips in one epoch: $\frac{T}{T_c} = 5115$
- Pseudolite signal
  - Code modulation: BPSK
  - Emission power: -30 $\cdots$ 15 dBW
  - Modulation Frequency: f_e = 1278.75 MHz
  - Epoch duration: 1 ms
  - Number of chips in one epoch: $\frac{T}{T_c} = 5115$
  - Pulse duration: 27 µs
  - pulse repetition frequency: PRF = 1000 $\cdots$ 4000 Hz

5.1.3 Generated Signals

The figures 5.2a and 5.2b show representations of signal $r_g(t)$ (i.e. signal after regulation and before blanking) that it is possible to generate with the software

tool. Their behaviour is very close to the reality, as it may be noticed for these two examples when making the comparison with data obtained from a study on a real front-end receiver (figures 5.3a and 5.3b).

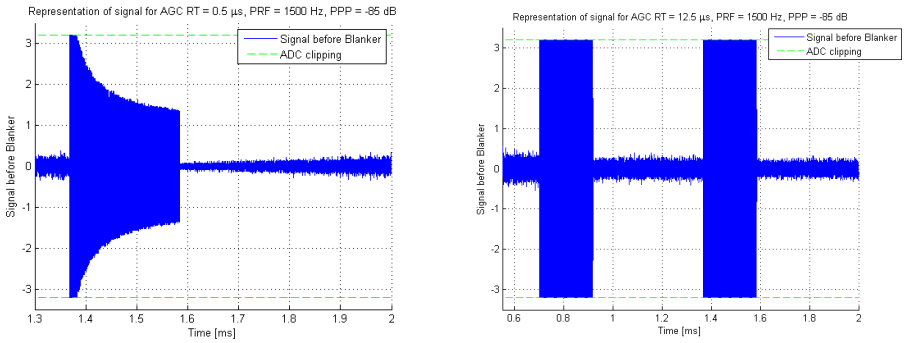

(a) AGC recovery time close to pulse duration (b) AGC recovery time much smaller than pulse duration

Figure 5.2: Examples of signal $r_g(t)$ (signal after regulation) generated with the MATLAB tool

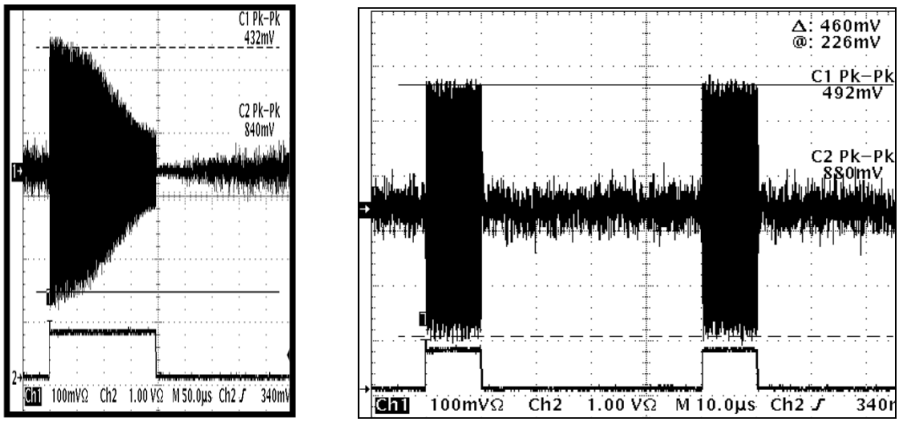

(a) AGC recovery time close to pulse duration

(b) AGC recovery time much smaller than pulse duration

Figure 5.3: Examples of signal $r_g(t)$ (signal after regulation) from measurements on a real front-end receiver [12]

5.2 Description of the Monte Carlo Simulation

The Monte Carlo method is usually used to determine the behaviour of a system which is not completely deterministic and too complex to be directly expressed. This method consists of generating many successive realisations with the same parameters, such that the results approach the real value. What we call "realisation" is one value of C, i.e. the value obtained after the correlation and integration on 1 ms.

In our case, the stochastic aspect concerns:

- the noise, considered here Gaussian. A new random value is generated for each sample.
- the code of the spreading code signal, random by hypothesis. A new navigation code is randomly generated at each realisation

Others parts of the system are considered deterministic. Many parameters of the system (front-end and input signal) can be modified, depending on which aspect we would like to focus on. A specific and fixed set of parameters on which is based a Monte Carlo experiment is called a configuration.

5.3 Comparison Between Model and Monte-Carlo Simulations

5.3.1 Validation of Spectral Separation and Waveform Convolution Coefficients

Here, since these methods apply for var $\left[\frac{1}{T}\int_0^T s^k(t)c^l(t)dt\right]$, the Monte Carlo experiments are not based on the software tool but on a new MATLAB tool which generates many random codes (succession of 1 and -1) with a defined pattern waveform. The important parameter here is the delay τ between the two navigation signals:

$$\begin{cases} s^k(t) = \sqrt{\mathcal{P}^k} \sum_{m=-\infty}^{\infty} c_m^k p^k(t - mT_c - \tau) \\ c^l(t) = \sum_{n=-\infty}^{\infty} c_n^l p^l(t - nT_c) \end{cases}$$

This delay τ can be visualized in figure 5.4.

Monte Carlo experiments have been launched for different values for the delay τ between the two spreading code signals. The results for two BPSK modulations are plotted in figure 5.5. One can observe that the points coming from the Monte Carlo experiments are on the red solid line corresponding the curves obtained from the mathematical expression. Moreover, the dotted red line of SSC/T (calculated from the analytic expression) matches with the dotted blue line of the average value of Monte Carlo experiments.

The SSC has also been estimated with Monte Carlo experiments for different values of β. The results and the comparison with the analytic model are

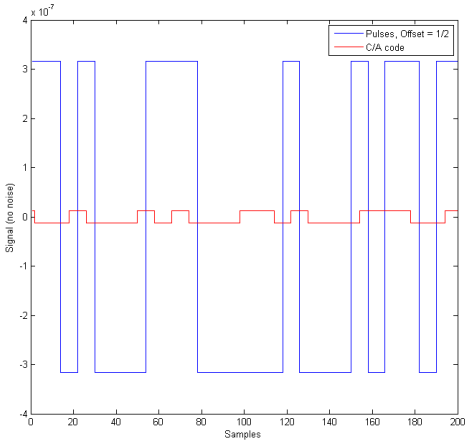

Figure 5.4: Representation of two navigation signals with a delay $\tau = \frac{1}{2}T_c$

represented in figure 5.6 for BPSK codes. Here again, the theory matches very well with the experiment. When comparing the results obtained from Monte Carlo simulations with ones derived from the analytical expressions, a really good match can be observed.

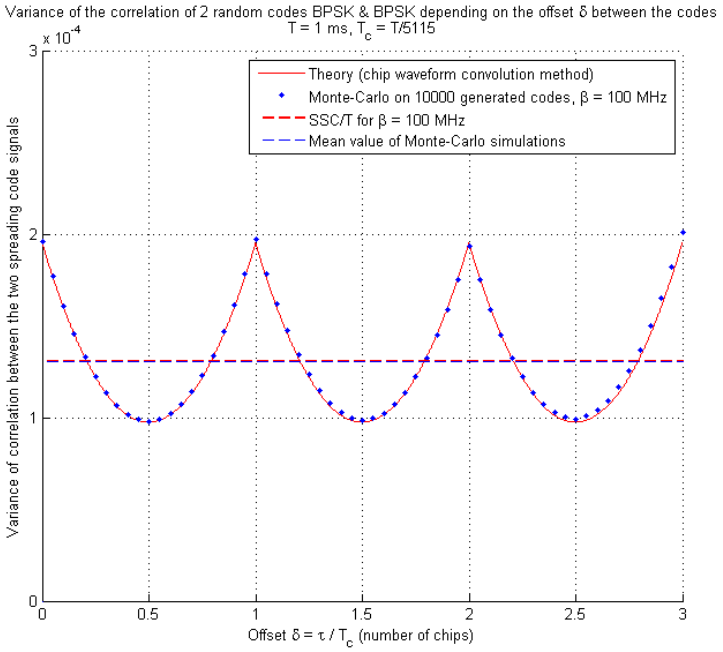

Figure 5.5: Interference contribution depending on the delay τ between two random navigation signals, both BPSK, for $\beta = 100$ MHz

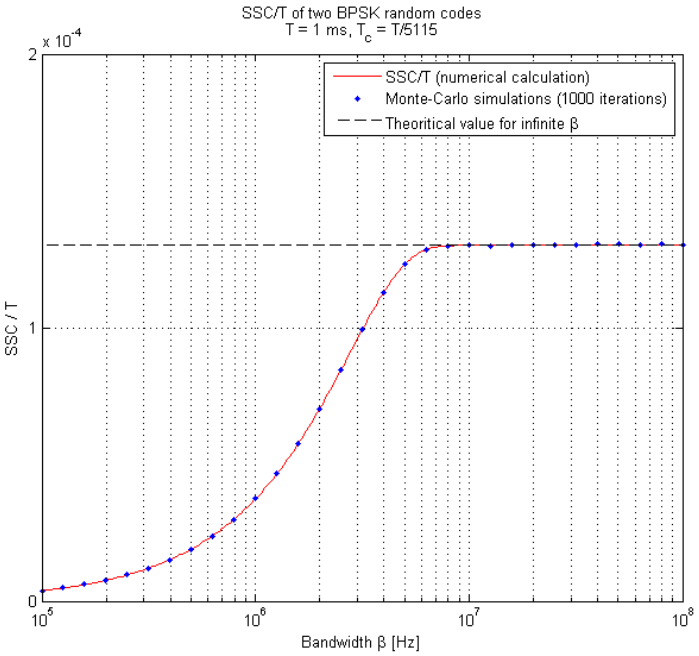

Figure 5.6: Mean on τ of interference contribution depending on the bandwidth β. Both navigation signals are random BPSK

5.3.2 Validation of the Model for Low-Power Signals

The expressions for $\mathcal{E}[C]$ and for var$[C]$ for "low-power signals only" have been expressed in section 4.3. In order to estimate the validity of these expressions at first order, Monte Carlo experiments are proceeded with the MATLAB tool for the tracking of satellite signal in presence of noise for different values of the blanking threshold BTH. The chosen parameters are those defined previously (except N_0 which was arbitrary). The obtained results are plotted with blue points in figure 5.7. For the comparison with the mathematical model, the curves obtained with the aforementioned expressions are plotted with the red solid line.
The curves matche very well. It can be deduced that for this configuration, the approximations and simplifications are acceptable for the precision of the mathematical model.

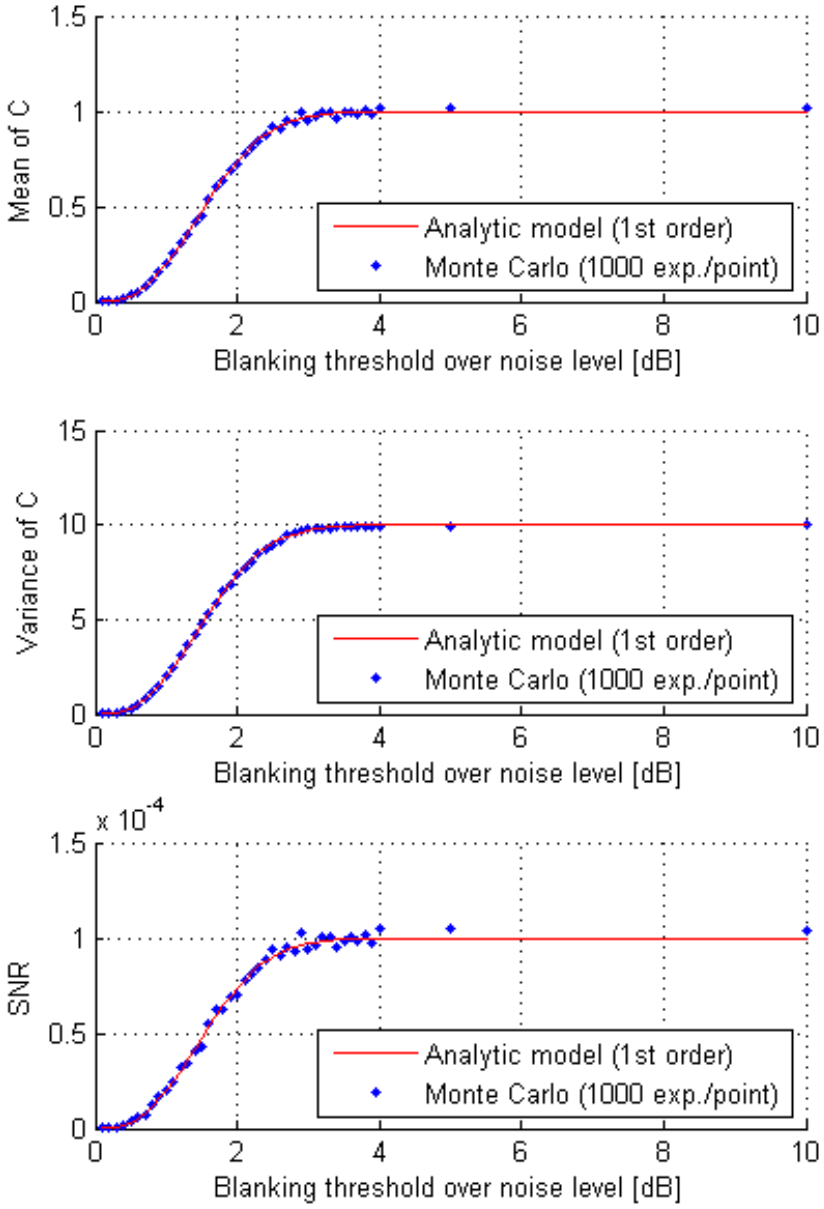

Figure 5.7: Mean, variance and SNIR of C, plotted from the mathematical model and Monte Carlo simulations

5.3.3 Validation of the Model for One Predominant Signal

For the validation of this model, one specific situation is considered: satellite tracking in presence of one interfering predominant pulse. The pulse of 27 µs is repeated with constant frequency. The involved speading codes are random and redefined at each new epoch. Eight configurations are considered, all those which are possible to define with the combination of the following parameters:

- AGC behaviour: slow (RT = 1 s) or fast (RT = 1 µs)
- Pulse repetition frequency PRF: 1010 Hz or 4010 Hz (corresponding to a pulse duty dycle of 2.7 % or 10.8 %, respectively)
- Pulse received power $\mathcal{P}_2$: -90 dBW or -110 dBW

The blanker is considered off or on. For the latter case, the blanking threshold varies between 0 and 10 dB over noise level.

The results are plotted in figures 5.8, 5.9, 5.10 and 5.11. A good matching between the curves obtained by the theory and the points from Monte Carlo experiments can be observed.
Nevertheless, some small discrepencies may be observed, for example in figure 5.10 for slow AGC and for a blanking threshold between 4 and 10 dB over noise level: the theoretical SNIR degradation is some decibels above the degradation established with Monte Carlo simulations. For the moment, it is difficult to say if the problem comes from the MATLAB tool or from the model. It may be an effect of the AGC (steady value not completely reached) but further investigations should be proceeded. It is the same issue concerning the fast AGC for a blanking threshold around 0 dB.

The step observed for fast AGC around "BTH = 0 dB" (obvious on figures 5.9 and 5.11) can be explained. Indeed, the interfering pulse is regulated by the AGC and oscillates around 0 dB because of the noise. Moreover, the higher the power of the pulse, the smaller the oscillations due to the noise in the regulated pulse. When the blanking threshold is decreased and becomes smaller than 0 dB, of course more noise outside the pulse is lost but in the same time, it removes the interfering contribution of the pulse. This gain in the SNIR may compensate the lost during this interval of BTH. As an illustration, one can refer to figure 3.3a.

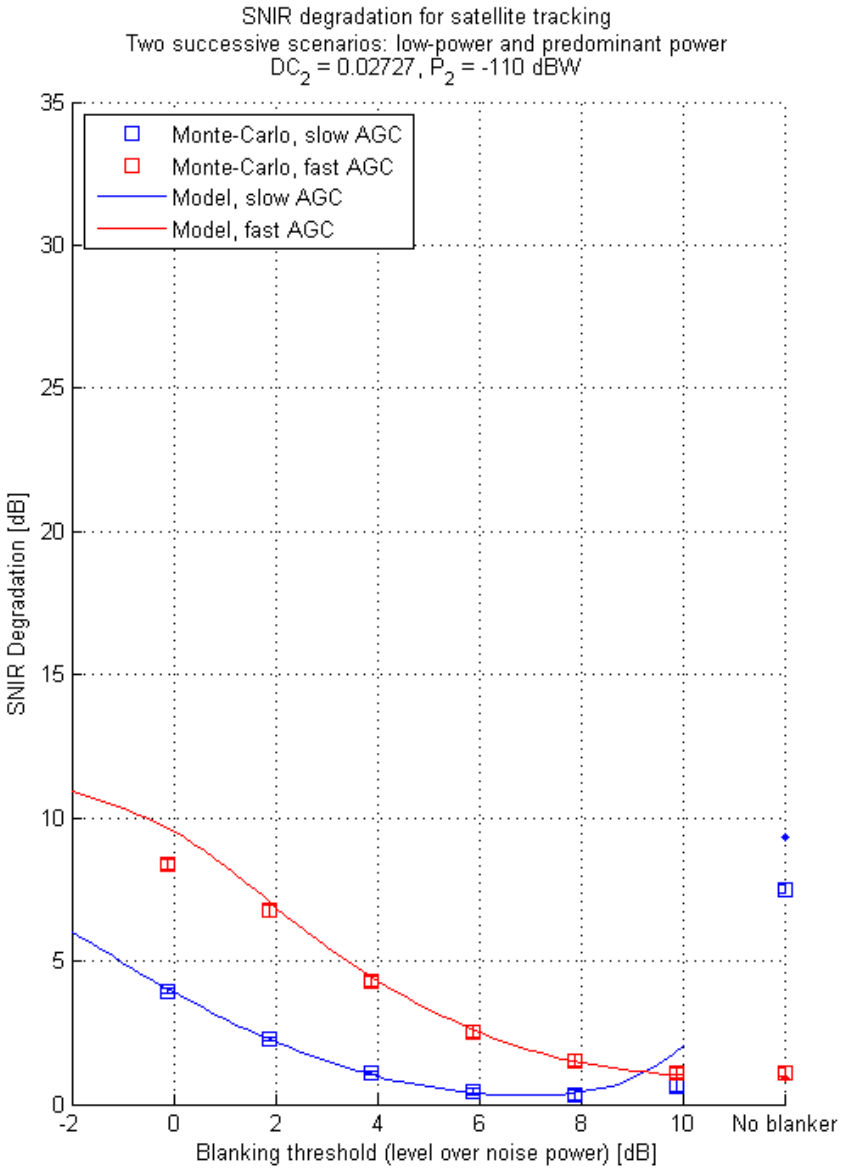

Figure 5.8: SNIR degradation for satellite tracking in presence of one predominant interfering pulse

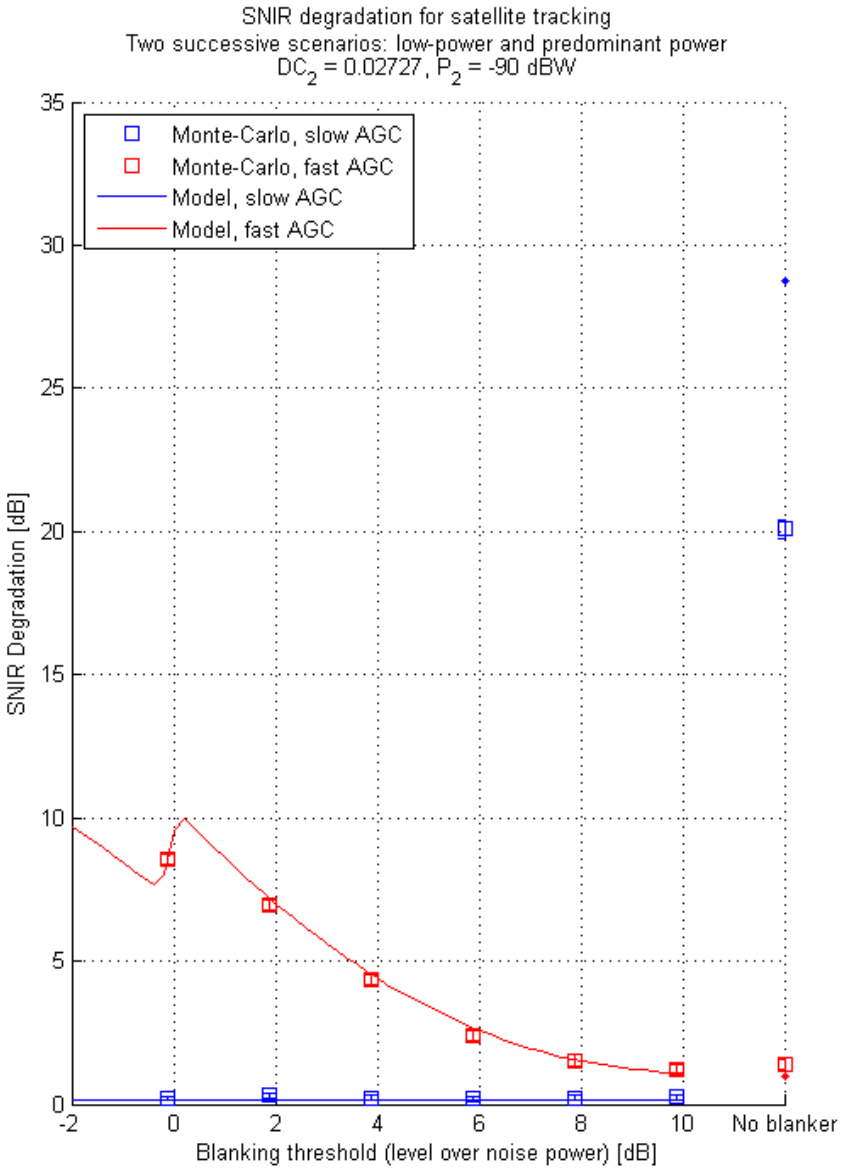

Figure 5.9: SNIR degradation for satellite tracking in presence of one predominant interfering pulse

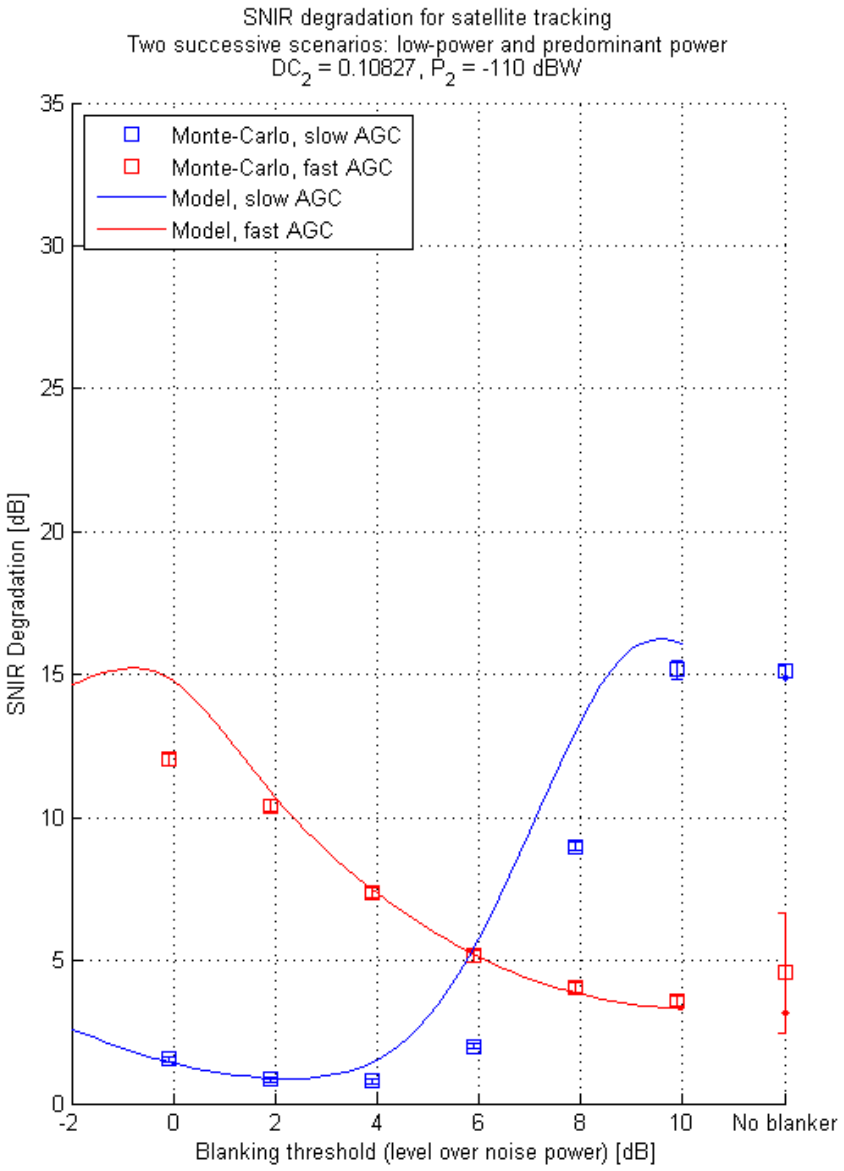

Figure 5.10: SNIR degradation for satellite tracking in presence of one predominant interfering pulse

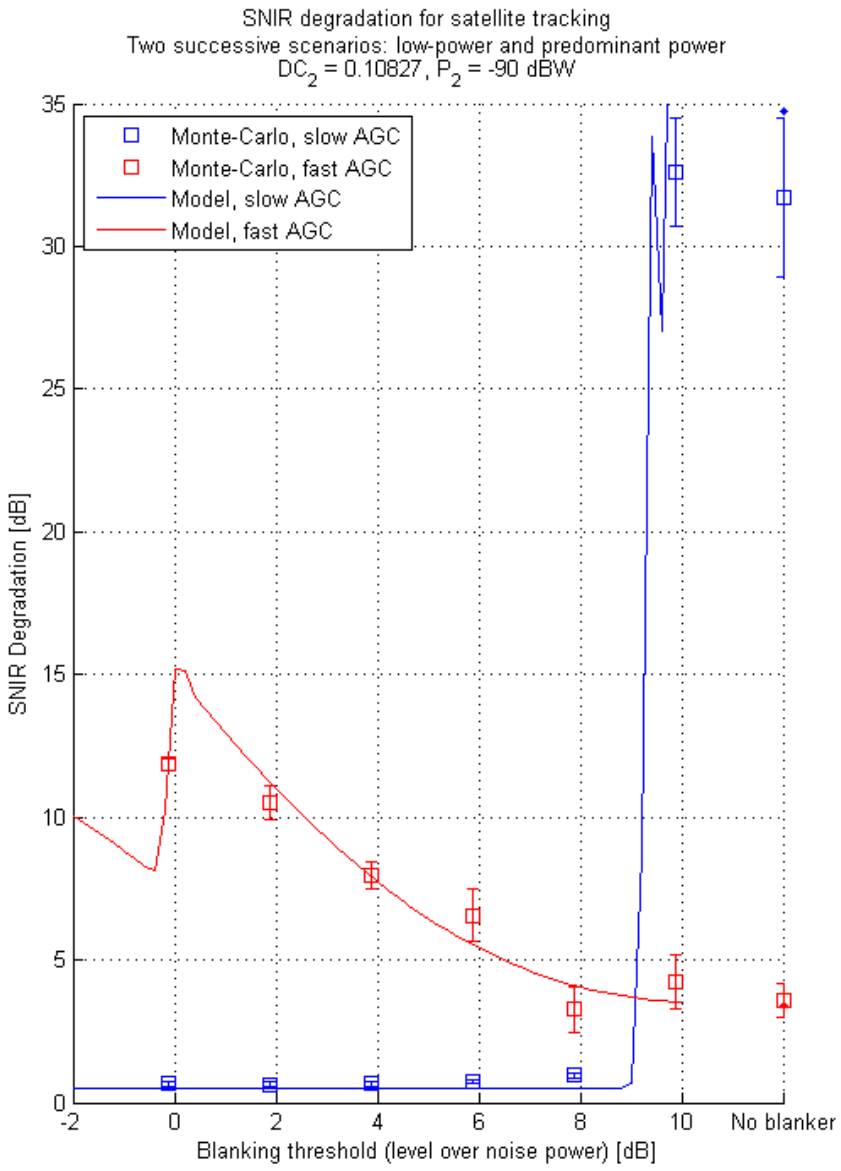

Figure 5.11: SNIR degradation for satellite tracking in presence of one predominant interfering pulse

5.3.4 Validation of the Separation Between Slow and Fast AGC Behaviours

It has been considered for the derivations of the model that the AGC gain G is constant on intervals. This would correspond to a very slow AGC (constant regulation of signal) or a very fast AGC (with a gain changing very rapidly between the situations "pulse on" and "pulse off", and constant during these situations). It is known that for a fixed pulse length, the situation "pulse on" or "pulse off" depends on the rapidity of the regulation, in other words, on the value of the recovery time RT. Let us determine the range of validity of this hypothesis by analysing the influence of RT on the SNIR degradation.

For this purpose, a campaign of Monte Carlo simulations has been launched for a specific configuration, for a range of BTH values and for different values of RT. The values of RT are chosen between 1 µs and 1 s with a step of 0.33 dB between two successive curves. The results are shown in figure 5.12. The curves will be interpreted in a next section, and with the observation of the figure, two sets of curves clearly appear. It is possible to distinguish three types of AGC behaviour:

- cluster of blue curves: configurations such that $\mathrm{RT} \leq \mathrm{PD}/2$, considered as **fast AGC**
- cluster of red curves: configurations such that $\mathrm{RT} \geq 4 \cdot \mathrm{PD}$, considered as **slow AGC**
- black curves between the two clusters: configurations such that $\mathrm{PD}/2 < \mathrm{RT} < 4 \cdot \mathrm{PD}$, considered as **intermediate AGC**

The range of the intermediate situation is 10 dB large around the value of the pulse duration PD. This range is relatively restricted. Beyond this range, two specific AGC behaviours are observed: when verifying the condition of fast or slow AGC, any value of RT will give approximately the same behaviour. In these cases, it is effectively not necessary to consider the exact value of RT because it is enough to know if RT verifies the condition of fast AGC or slow AGC. In these situations, the gain G can be effectively considered constant on intervals as defined in Approx. 10. Therefore, this hypothesis is valid as long as $\mathrm{RT} \notin [\mathrm{PD}/2,\ 5\dot{\mathrm{P}}\mathrm{D}]$.

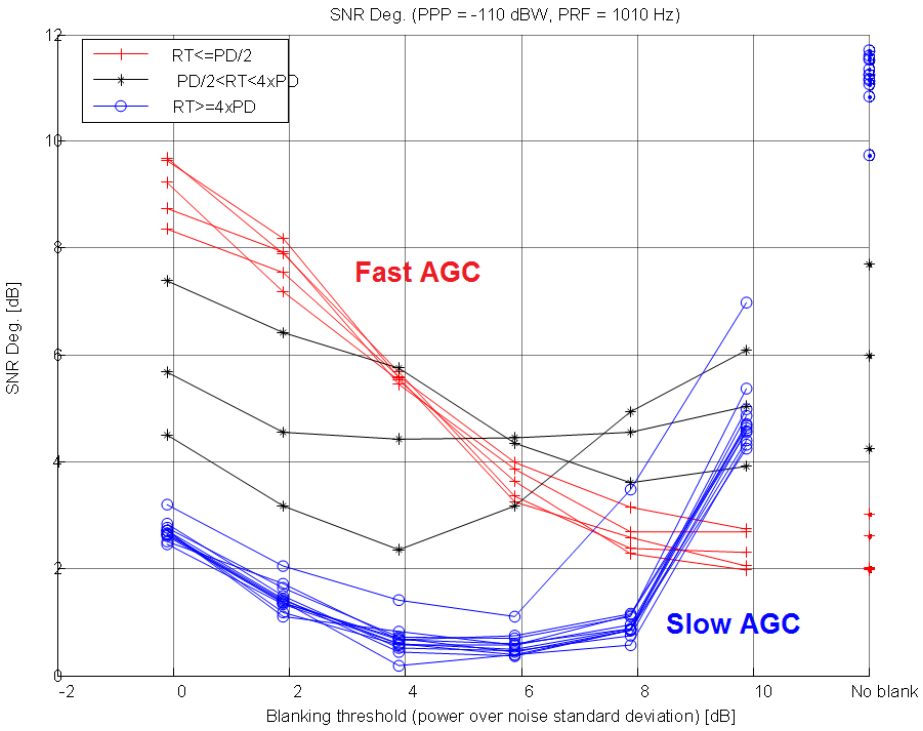

Figure 5.12: SNIR degradation with respect to blanking threshold for increasing AGC recovery time (Incremented of RT by 0.33 dB for each successive curve)

Chapter 6

Pulsing Scheme Considerations

In this section, it is proposed to determine optimal parameters such as pulse duration and duty cycle, and a pulsing scheme for the pseudolite emission, in order to limit the performance degradation for the existing GNSS receivers and optimise the performance for either satellite and pseudolite signals tracking. Since the aim is not to modify all mass-market GNSS receivers, the constraints regarding such a receiver category will be considered with highest priority.

6.1 Consideration of Existing Parameters

Some information about existing parameters and recommendations are given in the following:

- Concerning the AGC dynamics, according to [13] and receivers manufacturers contacted during the project, mass-market GNSS receivers have an AGC recovery time either around 1 µs or around 1 s. Moreover, this kind of receiver does not usually have a blanker.
- For a dedicated receiver, it is possible to define a specific value for the AGC recovery time and to use a blanker.
- It is considered at EADS Astrium that the pseudolite emission power is usually comprised between 0 and 45 dBmW (typical 30 dBmW i.e. 0 dBW) and that between 4 and 10 pseudolites are typically implemented in an airport (ranging purposes).
- According to [2], for aircraft assistance for a landing approach, the tracking of pseudolite signal should be possible at a distance up to 20 nautical miles (37 km).

6.2 Dimensioning

6.2.1 Pulse Duration

We have to define the duration of the time intervals allocated for the pseudolites. With the considered approximations, the absolute pulse duration does not have a direct influence on the equations. What is important is its relative value in comparison with the recovery time of the AGC:

- Pulse duration much larger than AGC recovery time: fast AGC
- Pulse duration much smaller than AGC recovery time: slow AGC
- Pulse duration close to AGC recovery time: "hybrid" AGC

This last behaviour induces bad performance and has to be avoided. This can be observed on figure 5.12 (black curves) where the SNIR degradation is large for any value for the blanking threshold. The intermediate behaviour $\mathrm{RT} \in [\mathrm{PD}/2, 5\mathrm{PD}]$ is very harmful for the SNIR. Thus, the recovery time has to be chosen such that the condition of fast or slow AGC is satisfied.

It has been mentioned that he typical values for the AGC recovery time are around 1 µs or around 1 s. Some technical considerations may be taken into account:

- The pulse duration can be hardly defined less than 1 µs (1 µs is the duration of one chips for GPS C/A).
- The pulse duration cannot be around 1 ms or more, because if the pulse covers entire spreading code periods, some processes (e.g. tracking loops) coming next in the processing chain may be disturbed. Indeed, the receiver may lose the track of the signal.

With these considerations, it seems to be appropriate to fix the pulse duration rather between 10 and 100 µs. Consequently, the GNSS receiver with an AGC recovery time around 1 µs will be considered as fast AGC, whereas those around 1 s will be considered as slow AGC, and the hybrid behaviour will be avoided.

6.2.2 Pulse Duty Cycle

There are two opposite effects when increasing the pulse duty cycle for a defined number of pseudolites: the performance increases for pseudolite tracking but decreases for satellite tracking. Thus a trade-off on the value of the pulse duty cycle has to be defined. Moreover, on the one hand, it is possible to adapt the chain of a dedicated receiver for common pseudolite and satellite tracking in order to improve the performance for pseudolite and satellite tracking. On the other hand, already existing mass market receivers cannot be all adapted. Therefore this latter constraint is critical for the dimensioning of the pulse duty cycle.

We consider now a satellite signal tracking (of received power $\mathcal{P}^l$) by a "mass-market" receiver in the following context:

- No blanker (cheap receivers do not have any blanker)

- Single interfering signal with received power $\mathcal{P}_2$ and duty cycle DC_2. Both navigation signals have same chip duration T_c
- Worst case for the interference contribution in case of BPSK (i.e. WCC = 1)

The expression of SNIR can be deduced:

$$\mathrm{SNIR} = \frac{\mathcal{P}^l \left(G_1 \cdot (1 - \mathrm{DC}_2) + G_2 \cdot \mathrm{DC}_2\right)^2}{\frac{N_0}{T}\left(G_1^2 \cdot (1 - \mathrm{DC}_2) + G_2^2 \cdot \mathrm{DC}_2\right) + G_2^2 \cdot \mathrm{DC}_2 \frac{T_c}{T} \mathcal{P}_2}$$

$$G_1 = \begin{cases} \frac{1}{\sigma} & \text{for fast AGC} \\ \frac{1}{\sqrt{\sigma^2 + \mathrm{DC}_2 \cdot \mathcal{P}_2}} & \text{for slow AGC} \end{cases}$$

$$G_2 = \begin{cases} \frac{1}{\sqrt{\sigma^2 + \mathcal{P}_2}} & \text{for fast AGC} \\ \frac{1}{\sqrt{\sigma^2 + \mathrm{DC}_2 \cdot \mathcal{P}_2}} & \text{for slow AGC} \end{cases}$$

For a value of SNIR equal to 6 dB[1], one can derive directly the relation between DC_2 and $\mathcal{P}^k$. As an interpretation, the deduced DC_2 for a defined $\mathcal{P}^k$ is the maximal possible pulse duty cycle such that it is possible to track the satellite. The corresponding curves are plotted with the defined parameters in figure 6.1.

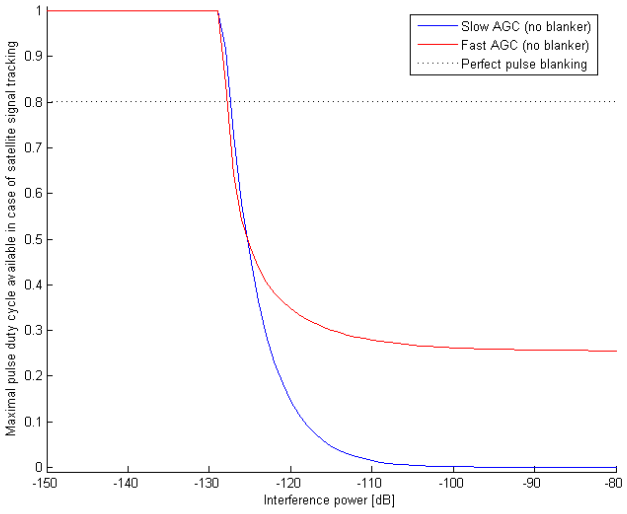

Figure 6.1: Maximal pulse duty cycle available such that satellite tracking is possible, depending on the total received interference power

- Slow AGC (without blanker): the regulation is the same during and outside the pulse. Therefore, the more interference power, the more impacting contribution in the SNIR and the more the duty cycle of the pulse has to

[1] This is the limit for signal tracking given in [2]. Actually, this value depends on parameters like the integration time and the bandwidth of the loops (e.g. PLL)

be limited to make the satellite tracking possible. This explains why the blue curve tends to 0. In case of small interference power, the interfering signal is drown in the noise, thus its impact is null for any pulse duration and the satellite can be tracked during the whole period. This explains why the blue curve is equal to 1 for small interference power.

- Fast AGC (without blanker): the interference power is regulated. Therefore, for any interference power, the signal is regulated to the steady value. The SNIR is impacted during a pulse because of the compression of the tracked navigation signal during pulse and interference contribution, although it is limited. For very high interference power, it is not possible to track the satellite signal during the pulse but the pulse contribution stays the same. That is why the red curve reaches a steady value ($\mathrm{DC}_2 = 0.25$ in our case) for high interference power. In case of small interference power, here again, it is possible to track the signal during the pulse. The red curve is also equal to 1 for small interference power

- Perfect pulse blanking (no power regulation and total blanking during the pulses only): when the pulse is perfectly blanked, the initial SNIR (i.e. the SNIR without interference) is weighted by $(1 - \mathrm{DC}_2)$, that is why the dotted line is a plateau. In case of small interferences, a portion of the signal to track is blanked anyway, thus the two previous configurations are more performing. But in case of strong interferences, the blanking allows a good performance.

Remark: The break in the blue and red curves takes place when the interference contribution becomes small in comparison with the noise contribution.

Therefore, for any chosen pulse duty cycle, a receiver with slow AGC will not be able to track a satellite signal when the receiver is located too close to an interfering pseudolite. On the contrary, a range of pulse duty cycles allows a receiver with fast AGC to track a satellite signal (as long as no other interferences occur) for any received power in theory. For $\mathcal{P}^l \ll \sigma^2$:

$$\mathrm{SNIR} = \frac{\frac{\mathcal{P}^l}{\sigma^2} \cdot (1 - \mathrm{DC}_2)^2}{\frac{N_0}{T\sigma^2} \cdot (1 - \mathrm{DC}_2) + \frac{T_c}{T} \cdot \mathrm{DC}_2}$$

As expected, this expression does not depend on the interfering signal power. Therefore, the maximal value for DC_2 such that it is always possible (in theory) to track a satellite signal will be approximately the same for any GNSS receiver with a fast AGC. In our case, this limit value is 0.25. In consequence, let us consider this value as a maximal duty cycle which can be allocated to a single interfering pulse. This value corresponds to an ideal case. Indeed, the SNIR may be even more impacted if other external interferences take place outside the initial pulse. Thus, a margin for the value of pulse duty cycle should be taken in account, with consideration of the possibilities for unexpected interferences.

6.2.3 Emission Power

As already discussed, the pseudolite emission power has no real impact in a receiver with fast AGC as long as the pulse duty cycle is below the limit estab-

lished before.
The impact of the parameter will be studied for the case of slow AGC. The associated SNIR for satellite tracking is (with WCC = 1):

$$\mathrm{SNIR} = \frac{\mathcal{P}^l}{\frac{N_0}{T} + \mathrm{DC}_2 \mathcal{P}^k \frac{T_c}{T}}$$

When writing $\mathrm{SNIR}_{\mathrm{lim}}$ the limit of SNIR for satellite tracking, it can be deduced:

$$\mathrm{DC}_2 \mathcal{P}^k = \frac{T}{T_c}\left(\frac{\mathcal{P}^l}{\mathrm{SNIR}_{\mathrm{lim}}} - \frac{\sigma^2}{\beta T}\right)$$

Let us consider now the distance to the interfering source. It is assumed that the interfering source, situated at a distance d^k to the receiver, emits with a carrier angular frequency ω_c and a power $\mathcal{P}_0^k$. For a free-space isotropic transmission, the received power signal is expressed as:

$$\mathcal{P}^k = \mathcal{P}_0^k \left(\frac{c}{2\omega_c d^k}\right)^2$$

Consequently:

$$d^k = \sqrt{\frac{\mathrm{DC}_2 \cdot \mathcal{P}_0^k \cdot T_c \left(\frac{c}{2\omega_c}\right)^2}{T\left(\frac{\mathcal{P}^l}{\mathrm{SNIR}_{\mathrm{lim}}} - \frac{\sigma^2}{\beta T}\right)}}$$

This result allows to plot in figure 6.2 the radius of the area around the emitter where the SNIR is below $\mathrm{SNIR}_{\mathrm{lim}}$ (according to a minimal required SNIR of 6 dB) and in consequent, where it is not possible to track a satellite signal.

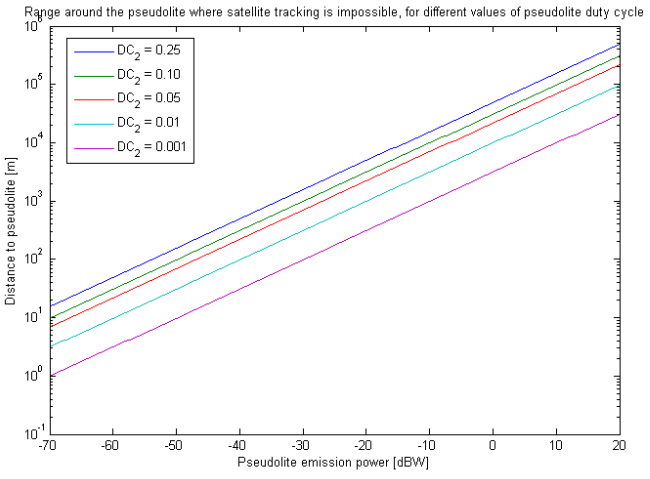

Figure 6.2: Radius of the zone around a pseudolite where satellite signal tracking is impossible, with respect to the emission power and different values of duty cycle

Chapter 7

Conclusions and Future Work

7.1 Conclusions

The signal-to-noise ratio of the correlator output provides information about the ability of a GNSS receiver to acquire, track and demodulate the navigation signal for later processing. The evaluation of this figure of merit is therefore essential to estimate the impact of interfering sources on the signal tracking leading to SNIR degradation. The implementation of pseudolites in an area, used usually for the augmentation of the existing GNSS constellation, induces typically strong degradations and may prevent the tracking of the satellite signals in this area. It is therefore essential to be able to estimate the SNIR for different situations. Nevertheless, existing models are not totally satisfying because they do not fully take the AGC dynamics into consideration, a possible blanker in the front-end is not considered and the contribution of the interfering signals is not completely correct. Concerning this last point, the model of Cobb, which has been one of the most encountered models, considers the maximal correlation value taken over the complete code sequence and supposes moving sources like satellites. However, for pseudolite applications, it has been noted that codes participating to the SNIR are limited to the pulse duration, and furthermore, these ground emitters are *de facto* static.

The main part of this work has concentrated on the derivation of new and more representative analytical models for the SNIR. In section 3, after the introduction of approximations, a baseline model has been derived without considering any AGC dynamics or blanker, especially to give a new way to calculate the interference contribution to the SNIR with consideration of the characteristics of pulsed signals and static emitters. Then, in section 4, the AGC dynamics and blanker are considered but the complexity of the system has led to determine three standard situations where the derivations were possible: 1) the situation of "low-power navigation signals" where the noise is predominant, 2) the situation of "predominant navigation signal" and 3) the situation of "similar-high-power navigation signals" where multiple navigation signals are predominant and with approximately the same received power. These analytical models have been tested with Monte Carlo simulations in section 5. The results show that the

models are valid for the proposed parameters. Nevertheless, some small discrepancies could still be observed and their origins are not yet isolated. Finally, in section 6, some concepts of improvement have been proposed for the pulsing scheme.

7.2 Future Work

7.2.1 Improvements in Front-end and Signal Modelling

Doppler Effect

The Doppler effect has not been taken into consideration in the derivations. It is actually important to consider this effect because when tracking a satellite for example, the demodulation frequency is known (regulation by FLL) but is not necessarily the same as the carrier frequency of the pseudolite signals. Hence, a further work will consist in considering the Doppler effect in the equations.

Power Saturation

The analytical expressions have been established with consideration of a blanker, and the cases without blanker have been established for an infinite blanking threshold. The signal amplitude is actually limited by the ADC which clips all signals which are over the clipping voltage. Even with a blanker, strong signals may saturate in the front-end chain because of limited working range of the components. All these effects of power saturation could also be taken into consideration in the derivations.

Filter Considerations

In the main developments, the filter $h(t)$ has not been considered, e.g. no distortions of the signal waveforms due to filtering was applied. However, when the filter bandwidth approaches the Gabor bandwidth of the navigation signal, the previous approximation is not valid anymore. It seems nevertheless that the analytical derivations would be extremely more difficult to proceed when considering the filter function $h(t)$, especially to determine the effects of the blanking on a signal having ripples due to filtering.

A proposition would consist in neglecting the effects of the ripples due to filtering (i.e. assumed that the waveforms still have constant plateaus) as done in this work but in addition, taking into account the power loss due to filtering with an adapted signal power $\int_{-\frac{\beta}{2}}^{\frac{\beta}{2}} S_{c^l}(f)df$ instead of $\mathcal{P}^l = \int_{-\infty}^{\infty} S_{c^l}(f)df$.

Quantization

It has been considered in this study that the quantization losses induced by the ADC can be neglected, according toApprox. 9, because the ADC works on a large number of bits (8 bits in our simulations). In reality, the number of bits in the quantization can be smaller for some GNSS receivers. Therefore, a further work will consist in considering the effects of the quantization on the signals.

7.2.2 Improvements for the Validations

Monte Carlo Simulations

Some discrepancies have been encountered for the Monte Carlo simulations for the model of "predominant pulse". It is not yet known where it comes from: either from model limitations or from the software used for the Monte Carlo evaluations. This point should be therefore studied further in details in order to determine the origin of these discrepancies.

Moreover, the Monte Carlo simulations have been proceeded only for the SNIR for satellite tracking in situations of "low-power signals" and "one predominant signal". It could be also interesting to extend the simulations to satellite tracking in situation of "similar-high-power signals" and to pseudolite tracking in all situations.

Tests in Real Conditions

The software tool which simulates the receiver front-end aims at reflecting a real front-end but the components are nevertheless idealized. Thus, an idea is to make a campaign of signal acquisition in a real context of pseudolite interference with a real receiver front-end, in order to evaluate the validity of the software tool and the models.

7.2.3 Proposal for a Pulsing Scheme

The established models could be used to determine the parameters and estimate the performance of a new pulsing scheme. The idea is to take advantage of the knowledge of the time of start and end of the pulses in a dedicated front-end in order to augment the perfomance for pseudolite tracking. For example, if the receiver uses the same synchronised shift register as the pseudolites, it will be able to determine the position of the next pulses. It seems appropriate then to implement two acquisition channels in the dedicated receiver:

- Function "pseudolite tracking": signal acquisition only during *a priori* time of pulse presence.
- Function "satellite tracking": signal acquisition only during *a priori* time of pulse absence.

In addition, each channel could have a specific AGC regulation in order to avoid possibly long transitions which may lead to SNIR degradation and also to adapt to the characteristic of each part of the signal.

Moreover, signal overlapping allows the implementation of processing methods in the dedicated received for the mitigation of the inter-interferences, possibly by knowing the spreading codes of other pseudolites (methods of interference cancellation).

Finally, the performance of the new pulsing scheme could be compared with others like RTCA and RTCM. For an on-site integration, e.g. on an airport, one should determine the parameters such that the exclusion zones are limited. The application of the analytical models allows to determine the size of the areas where satellite or pseudolite signal tracking is not possible due to too low SNIR, as qualitatively represented in figure 7.1.

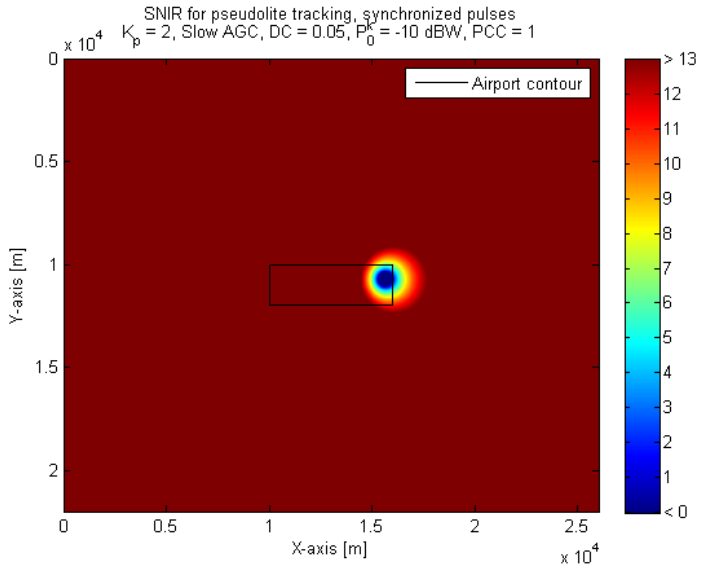

(a) SNIR for the tracking of the signal emitted by the pseudolite on the left

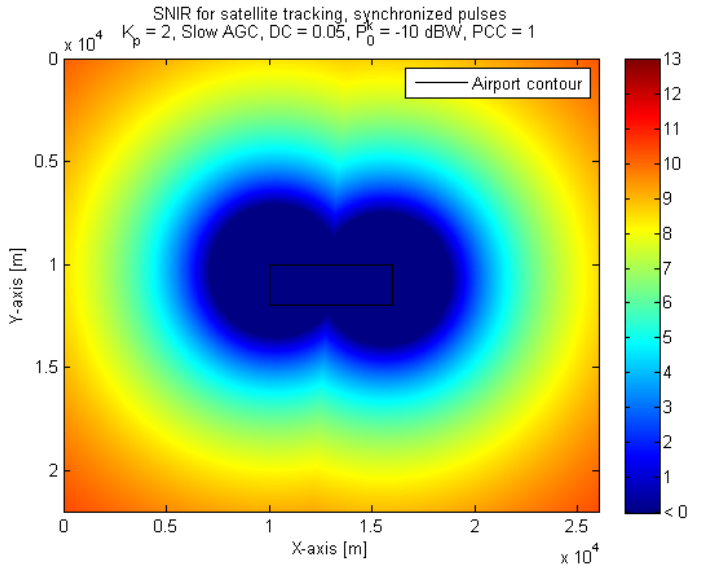

(b) SNIR for satellite tracking,

Figure 7.1: SNIR representation in the case of two pseudolites emitting simultaneously (same configuration as for figures 4.10)

Appendix A

Developments With Taylor Series

A.1 Expression for the Mean of C for Low-Power Signals

The aim is to derive a second order of approximation from the expression for the mean of the correlator output. Following is the expression of $\mathcal{E}[C]$ derived in case of only one navigation signal received:

$$\int_{-\frac{\mathrm{BTH}}{G_0}-\sqrt{\mathcal{P}^l}}^{\frac{\mathrm{BTH}}{G_0}-\sqrt{\mathcal{P}^l}} \left(\sqrt{\mathcal{P}^l}+n\right)\frac{1}{\sqrt{2\pi}\sigma}e^{-\frac{n^2}{2\sigma^2}}dn$$

$$= \underbrace{\sqrt{\mathcal{P}^l}\int_{-\frac{\mathrm{BTH}}{G_0}-\sqrt{\mathcal{P}^l}}^{\frac{\mathrm{BTH}}{G_0}-\sqrt{\mathcal{P}^l}} \frac{1}{\sqrt{2\pi}\sigma}e^{-\frac{n^2}{2\sigma^2}}dn}_{\mathcal{E}_1} + \underbrace{\int_{-\frac{\mathrm{BTH}}{G_0}-\sqrt{\mathcal{P}^l}}^{\frac{\mathrm{BTH}}{G_0}-\sqrt{\mathcal{P}^l}} \frac{n}{\sqrt{2\pi}\sigma}e^{-\frac{n^2}{2\sigma^2}}dn}_{\mathcal{E}_2}$$

1) Approximation of the term $\mathcal{E}_1$

$$\mathcal{E}_1 = \sqrt{\mathcal{P}^l}\int_{-\frac{\mathrm{BTH}}{G_0}-\sqrt{\mathcal{P}^l}}^{\frac{\mathrm{BTH}}{G_0}-\sqrt{\mathcal{P}^l}} \frac{1}{\sqrt{2\pi}\sigma}e^{-\frac{n^2}{2\sigma^2}}dn$$

$$= \sqrt{\mathcal{P}^l}\int_{\frac{-\mathrm{BTH}-G_0\sqrt{\mathcal{P}^l}}{G_0\sigma}}^{\frac{\mathrm{BTH}-G_0\sqrt{\mathcal{P}^l}}{G_0\sigma}} \frac{1}{\sqrt{2\pi}}e^{-\frac{n'^2}{2}}dn'$$

$$= \sqrt{\mathcal{P}^l}\left[Q_0\left(\frac{-\mathrm{BTH}-G_0\sqrt{\mathcal{P}^l}}{G_0\cdot\sigma}\right) - Q_0\left(\frac{\mathrm{BTH}-G_0\sqrt{\mathcal{P}^l}}{G_0\cdot\sigma}\right)\right]$$

Reminder: $Q_0(x) = \int_x^{+\infty} \frac{1}{\sqrt{2\pi}} e^{-\frac{u^2}{2}} du$

Remark: $\mathcal{E}_1$ could also be expressed with the complementary error function: $\mathcal{E}_1 = \sqrt{\mathcal{P}^l} \cdot \frac{1}{2} \left[\text{erfc}\left(\frac{-\text{BTH} - G_0\sqrt{\mathcal{P}^l}}{\sqrt{2} G_0 \sigma} \right) - \text{erfc}\left(\frac{\text{BTH} - G_0\sqrt{\mathcal{P}^l}}{\sqrt{2} G_0 \cdot \sigma} \right) \right]$.

Since $\sqrt{\mathcal{P}^l}$ is factored out, to obtain the second order we just have to formulate the first order of $Q_0\left(\frac{\text{BTH} - G_0\sqrt{\mathcal{P}^l}}{G_0\sigma} \right)$. It is considered that $G_0\sqrt{\mathcal{P}^l} \ll$ BTH.

$$\begin{aligned} Q_0\left(\frac{\text{BTH} - G_0\sqrt{\mathcal{P}^l}}{G_0\sigma} \right) &= Q_0\left(\frac{\text{BTH}}{G_0\sigma} \cdot \left(1 - \frac{G_0\sqrt{\mathcal{P}^l}}{\text{BTH}} \right) \right) \\ &= F_1\left(\frac{G_0\sqrt{\mathcal{P}^l}}{\text{BTH}} \right) \end{aligned}$$

F_1 is the function defined as $F_1(\epsilon) = Q_0\left(\frac{\text{BTH}}{G_0 \cdot \sigma} \cdot (1 - \epsilon) \right)$. Here, $\epsilon = \frac{G_0\sqrt{\mathcal{P}^l}}{\text{BTH}}$ with $\epsilon \ll 1$.

Taylor series at first order: $F_1(\epsilon) = F_1(0) + \epsilon \cdot \frac{\partial F_1}{\partial \epsilon}(0) + o(\epsilon)$

- Calculation of $F_1(0)$

$$F_1(0) = Q_0\left(\frac{\text{BTH}}{G_0\sigma} \right)$$

- Calculation of $\frac{\partial F_1}{\partial \epsilon}(0)$

$$\begin{aligned} \frac{\partial F_1}{\partial \epsilon}(0) &= \left(\left(-\frac{\text{BTH}}{G_0\sigma} \right) \cdot \left[\frac{1}{\sqrt{2\pi}} e^{-\frac{u^2}{2}} \right]_{\frac{\text{BTH}}{G_0\sigma} \cdot (1-\epsilon)}^{+\infty} \right) \Bigg|_{\epsilon=0} \\ &= \frac{\text{BTH}}{G_0\sigma} \cdot \frac{1}{\sqrt{2\pi}} e^{-\frac{\text{BTH}^2}{2(G_0\sigma)^2}} \end{aligned}$$

Thus, at first order:

$$Q_0\left(\frac{\text{BTH} - G_0\sqrt{\mathcal{P}^l}}{G_0\sigma} \right) \approx Q_0\left(\frac{\text{BTH}}{G_0\sigma} \right) + \frac{\sqrt{\mathcal{P}^l}}{\sqrt{2\pi}\sigma} e^{-\frac{\text{BTH}^2}{2(G_0\sigma)^2}} \tag{A.1}$$

Similarly:

$$Q_0\left(\frac{-\text{BTH} - G_0\sqrt{\mathcal{P}^l}}{G_0\sigma} \right) \approx Q_0\left(-\frac{\text{BTH}}{G_0\sigma} \right) + \frac{\sqrt{\mathcal{P}^l}}{\sqrt{2\pi}\sigma} e^{-\frac{\text{BTH}^2}{2(G_0\sigma)^2}}$$

And consequently:

$$\begin{aligned} \mathcal{E}_1 &\approx \sqrt{\mathcal{P}^l} \left[Q_0\left(-\frac{\text{BTH}}{G_0\sigma} \right) - Q_0\left(\frac{\text{BTH}}{G_0\sigma} \right) \right] \\ &= \sqrt{\mathcal{P}^l} \left[1 - 2Q_0\left(\frac{\text{BTH}}{G_0\sigma} \right) \right] \end{aligned} \tag{A.2}$$

2) Derivation of the term $\mathcal{E}_2$

$$\begin{aligned}\mathcal{E}_2 &= \sigma \int_{\frac{\mathrm{BTH}}{G_0\sigma}\left(-1-\frac{G_0\sqrt{\mathcal{P}^l}}{\mathrm{BTH}}\right)}^{\frac{\mathrm{BTH}}{G_0\sigma}\left(1-\frac{G_0\sqrt{\mathcal{P}^l}}{\mathrm{BTH}}\right)} \frac{n}{\sqrt{2\pi}} e^{-\frac{n^2}{2}} dn \\ &= \sigma F_2\left(\frac{G_0\sqrt{\mathcal{P}^l}}{\mathrm{BTH}}\right)\end{aligned}$$

F_2 is the function defined as $F_2(\epsilon) = \int_{\frac{\mathrm{BTH}}{G_0\sigma}(-1-\epsilon)}^{\frac{\mathrm{BTH}}{G_0\sigma}(1-\epsilon)} \frac{n}{\sqrt{2\pi}} e^{-\frac{n^2}{2}} dn$. Here, $\epsilon = \frac{G_0\sqrt{\mathcal{P}^l}}{\mathrm{BTH}}$ with $\epsilon \ll 1$.

Taylor serie at second order: $F_2(\epsilon) = F_2(0) + \epsilon\frac{\partial F_2}{\partial x}(0) + \frac{\epsilon^2}{2}\frac{\partial^2 F_2}{\partial x^2}(0) + o\left(\epsilon^2\right)$

- Calculation of $F_2(0)$

$$\begin{aligned}F_2(0) &= \int_{-\frac{\mathrm{BTH}}{G_0\sigma}}^{\frac{\mathrm{BTH}}{G_0\sigma}} \frac{n}{\sqrt{2\pi}} e^{-\frac{n^2}{2}} dn \\ &= 0\end{aligned}$$

- Calculation of $\frac{\partial F_2}{\partial x}(0)$

$$\begin{aligned}\frac{\partial F_2}{\partial \epsilon}(\epsilon) &= \left(\left(-\frac{\mathrm{BTH}}{G_0\sigma}\right)\cdot\left[\frac{n}{\sqrt{2\pi}}e^{-\frac{n^2}{2}}\right]_{\frac{\mathrm{BTH}}{G_0\sigma}\cdot(-1-\epsilon)}^{\frac{\mathrm{BTH}}{G_0\sigma}\cdot(1-\epsilon)}\right) \\ &= -\left(\frac{\mathrm{BTH}}{G_0\sigma}\right)^2 \frac{1}{\sqrt{2\pi}}\left((1-\epsilon)\, e^{-\frac{\mathrm{BTH}^2(1-\epsilon)^2}{2(G_0\sigma)^2}} + (1+\epsilon)\, e^{-\frac{\mathrm{BTH}^2(1+\epsilon)^2}{2(G_0\sigma)^2}}\right) \\ \frac{\partial F_2}{\partial \epsilon}(0) &= -\left(\frac{\mathrm{BTH}}{G_0\sigma}\right)^2 \frac{1}{\sqrt{2\pi}} 2e^{-\frac{\mathrm{BTH}^2}{2(G_0\sigma)^2}}\end{aligned}$$

- Calculation of $\frac{\partial^2 F_2}{\partial \epsilon^2}(0)$

$$\begin{aligned}\frac{\partial^2 F_2}{\partial \epsilon^2}(\epsilon) &= -\left(\frac{\mathrm{BTH}}{G_0\sigma}\right)^2 \frac{1}{\sqrt{2\pi}}\left[\left((1-\epsilon)\left(\frac{\mathrm{BTH}^2(1-\epsilon)}{(G_0\sigma)^2}\right)-1\right)e^{-\frac{\mathrm{BTH}^2(1-\epsilon)^2}{2(G_0\sigma)^2}}\right. \\ &\quad \left. + \left((1+\epsilon)\left(-\frac{\mathrm{BTH}^2(1+\epsilon)}{(G_0\sigma)^2}\right)+1\right)e^{-\frac{\mathrm{BTH}^2(1+\epsilon)^2}{2(G_0\sigma)^2}}\right] \\ \frac{\partial^2 F_2}{\partial \epsilon^2}(0) &= \left(\frac{\mathrm{BTH}}{G_0\sigma}\right)^2 \frac{1}{\sqrt{2\pi}}\left[\left(\frac{\mathrm{BTH}^2}{(G_0\sigma)^2}-1\right)+\left(-\frac{\mathrm{BTH}^2}{(G_0\sigma)^2}+1\right)\right]e^{-\frac{\mathrm{BTH}^2}{2(G_0\sigma)^2}} \\ &= 0\end{aligned}$$

Thus, at second order:

$$\begin{aligned}\mathcal{E}_2 &\approx -\sigma\cdot\frac{G_0\sqrt{\mathcal{P}^l}}{\mathrm{BTH}}\left(\frac{\mathrm{BTH}}{G_0\sigma}\right)^2\frac{1}{\sqrt{2\pi}}\cdot 2e^{-\frac{\mathrm{BTH}^2}{2(G_0\sigma)^2}} \\ &= -\frac{\mathrm{BTH}\sqrt{\mathcal{P}^l}}{G_0\sigma}\cdot\sqrt{\frac{2}{\pi}}e^{-\frac{\mathrm{BTH}^2}{2(G_0\sigma)^2}}\end{aligned} \tag{A.3}$$

3) Summation of $\mathcal{E}_1$ and $\mathcal{E}_2$

$$\mathcal{E}[x(t)c^l(t)] \approx G_0\sqrt{\mathcal{P}^l}\left[1 - 2Q_0\left(\frac{\mathrm{BTH}}{G_0\sigma}\right) - \frac{\mathrm{BTH}}{G_0\sigma}\sqrt{\frac{2}{\pi}}e^{-\frac{\mathrm{BTH}^2}{2(G_0\sigma)^2}}\right]$$

A.2 Expression for the variance of C for Low-Power Signals

The aim is to determine an expression of $\mathcal{E}\left[{f_{\mathrm{B}}}^2\left(G_0\left(\sqrt{\mathcal{P}^l}+n(t)\right)\right)\right]$ with Taylor series.

$$
\begin{aligned}
&\mathcal{E}\left[{f_{\mathrm{B}}}^2\left(G_0\left(\sqrt{\mathcal{P}^l}+n(t)\right)\right)\right] \\
&\quad=\int_{-\infty}^{+\infty}\left[f_{\mathrm{B}}\left(G_0\left(\sqrt{\mathcal{P}^l}+n\right)\right)\right]^2\cdot p\left(n\right)dn \\
&\quad=\int_{G_0\left(\sqrt{\mathcal{P}^l}+n\right)\in[-\mathrm{BTH},\mathrm{BTH}]} G_0^2\left(\sqrt{\mathcal{P}^l}+n\right)^2\frac{1}{\sqrt{2\pi}\sigma}e^{-\frac{n^2}{2\sigma^2}}dn \\
&\quad=G_0^2\left[\underbrace{\mathcal{P}^l\int_{-\frac{\mathrm{BTH}}{G_0}-\sqrt{\mathcal{P}^l}}^{\frac{\mathrm{BTH}}{G_0}-\sqrt{\mathcal{P}^l}}\frac{1}{\sqrt{2\pi}\sigma}e^{-\frac{n^2}{2\sigma^2}}dn}_{\mathcal{E}_1}+\underbrace{2\sqrt{\mathcal{P}^l}\int_{-\frac{\mathrm{BTH}}{G_0}-\sqrt{\mathcal{P}^l}}^{\frac{\mathrm{BTH}}{G_0}-\sqrt{\mathcal{P}^l}}\frac{n}{\sqrt{2\pi}\sigma}e^{-\frac{n^2}{2\sigma^2}}dn}_{\mathcal{E}_2}\right. \\
&\qquad\left.+\underbrace{\int_{-\frac{\mathrm{BTH}}{G_0}-\sqrt{\mathcal{P}^l}}^{\frac{\mathrm{BTH}}{G_0}-\sqrt{\mathcal{P}^l}}\frac{n^2}{\sqrt{2\pi}\sigma}e^{-\frac{n^2}{2\sigma^2}}dn}_{\mathcal{E}_3}\right]
\end{aligned}
$$

1) Derivation of the term $\mathcal{E}_1$

From equation A.2, it can be deduced (at second order):

$$\mathcal{E}_1=\mathcal{P}^l\int_{-\frac{\mathrm{BTH}}{G_0}-\sqrt{\mathcal{P}^l}}^{\frac{\mathrm{BTH}}{G_0}-\sqrt{\mathcal{P}^l}}\frac{1}{\sqrt{2\pi}\sigma}e^{-\frac{n^2}{2\sigma^2}}dn=\mathcal{P}^l\left[1-2Q_0\left(\frac{\mathrm{BTH}}{G_0\sigma}\right)\right]$$

2) Derivation of the term $\mathcal{E}_2$

From equation A.3, it can be deduced (at second order):

$$\mathcal{E}_2=2\sqrt{\mathcal{P}^l}\int_{-\frac{\mathrm{BTH}}{G_0}-\sqrt{\mathcal{P}^l}}^{\frac{\mathrm{BTH}}{G_0}-\sqrt{\mathcal{P}^l}}\frac{n}{\sqrt{2\pi}\sigma}e^{-\frac{n^2}{2\sigma^2}}dn=-2\mathcal{P}^l\frac{\mathrm{BTH}}{G_0\sigma}\sqrt{\frac{2}{\pi}}e^{-\frac{\mathrm{BTH}^2}{2(G_0\sigma)^2}}$$

3) Derivation of the term $\mathcal{E}_3$

$$
\begin{aligned}
\mathcal{E}_3&=\int_{-\frac{\mathrm{BTH}}{G_0}-\sqrt{\mathcal{P}^l}}^{\frac{\mathrm{BTH}}{G_0}-\sqrt{\mathcal{P}^l}}\frac{n^2}{\sqrt{2\pi}\sigma}e^{-\frac{n^2}{2\sigma^2}}dn \\
&=\sigma^2\int_{-\frac{\mathrm{BTH}}{G_0\sigma}-\frac{\sqrt{\mathcal{P}^l}}{\sigma}}^{\frac{\mathrm{BTH}}{G_0\sigma}-\frac{\sqrt{\mathcal{P}^l}}{\sigma}}\frac{n^2}{\sqrt{2\pi}}e^{-\frac{n^2}{2}}dn \\
&=\sigma^2\left[Q_2\left(\frac{-\mathrm{BTH}-G_0\sqrt{\mathcal{P}^l}}{G_0\sigma}\right)-Q_2\left(\frac{\mathrm{BTH}-G_0\sqrt{\mathcal{P}^l}}{G_0\sigma}\right)\right]
\end{aligned}
$$

Reminder: $Q_2(x) = \int_x^{+\infty} \frac{x^2}{\sqrt{2\pi}} e^{-\frac{x^2}{2}} dx$

Again, it is considered that $G_0\sqrt{\mathcal{P}^l} \ll \text{BTH}$.

$$Q_2\left(\frac{\text{BTH} - G_0\sqrt{\mathcal{P}^l}}{G_0\sigma}\right) = Q_2\left(\frac{\text{BTH}}{G_0\sigma}\left(1 - \frac{G_0\sqrt{\mathcal{P}^l}}{\text{BTH}}\right)\right)$$
$$= F_3\left(\frac{G_0\sqrt{\mathcal{P}^l}}{\text{BTH}}\right)$$

F_3 is the function defined as $F_3(\epsilon) = Q_2\left(\frac{\text{BTH}}{G_0\sigma}(1-\epsilon)\right)$. Here, $\epsilon = \frac{G_0\sqrt{\mathcal{P}^l}}{\text{BTH}}$ with $\epsilon \ll 1$.

Taylor series at second order: $F_3(\epsilon) = F_3(0) + \epsilon \cdot \frac{\partial F_3}{\partial \epsilon}(0) + \frac{\varepsilon^2}{2} \cdot \frac{\partial^2 F_3}{\partial \epsilon^2}(0) + o\left(\varepsilon^2\right)$

- Calculation of $F_3(0)$

$$F_3(0) = Q_2\left(\frac{\text{BTH}}{G_0\sigma}\right)$$

- Calculation of $\frac{\partial F_3}{\partial \epsilon}(0)$

$$\frac{\partial F_3}{\partial \epsilon}(\epsilon) = -\frac{\text{BTH}}{G_0\sigma} \cdot \left[\frac{u^2}{\sqrt{2\pi}} e^{-\frac{u^2}{2}}\right]_{\frac{\text{BTH}}{G_0\sigma}(1-\epsilon)}^{+\infty}$$
$$\frac{\partial F_3}{\partial \epsilon}(0) = \frac{\text{BTH}^3}{\sqrt{2\pi}\left(G_0\sigma\right)^3} e^{-\frac{\text{BTH}^2}{2(G_0\sigma)^2}}$$

- Calculation of $\frac{\partial^2 F_3}{\partial \epsilon^2}(0)$

$$\frac{\partial^2 F_3}{\partial \epsilon^2}(\epsilon) = \frac{\text{BTH}^3}{\sqrt{2\pi}\left(G_0\sigma\right)^3}\left(-2(1-\epsilon) + (1-\epsilon)^2\left(-\frac{\text{BTH}^2}{2\left(G_0\sigma\right)^2}\right)(-2(1-\epsilon))\right)$$
$$\cdot\, e^{-\frac{\text{BTH}^2(1-\epsilon)^2}{2(G_0\sigma)^2}}$$
$$\frac{\partial^2 F_3}{\partial \epsilon^2}(0) = \frac{\text{BTH}^3}{\sqrt{2\pi}\left(G_0\sigma\right)^3}\left(\frac{\text{BTH}^2}{\left(G_0\sigma\right)^2} - 2\right) e^{-\frac{\text{BTH}^2}{2(G_0\sigma)^2}}$$

Thus, at second order:

$$Q_2\left(\frac{\text{BTH} - G_0\sqrt{\mathcal{P}^l}}{G_0\sigma}\right) \approx$$
$$Q_2\left(\frac{\text{BTH}}{G_0\sigma}\right) + \left(\frac{\sqrt{\mathcal{P}^l}\text{BTH}^2}{\sqrt{2\pi}{G_0}^2\sigma^3} + \frac{1}{2}\frac{\mathcal{P}^l\text{BTH}}{\sqrt{2\pi}G_0\sigma^3}\left(\frac{\text{BTH}^2}{\left(G_0\sigma\right)^2} - 2\right)\right) e^{-\frac{\text{BTH}^2}{2(G_0\sigma)^2}} \tag{A.4}$$

With same reasoning:

$$Q_2\left(\frac{-\mathrm{BTH}-G_0\sqrt{\mathcal{P}^l}}{G_0\sigma}\right)\approx$$
$$Q_2\left(-\frac{\mathrm{BTH}}{G_0\sigma}\right)+\left(\frac{\sqrt{\mathcal{P}^l}\mathrm{BTH}^2}{\sqrt{2\pi}{G_0}^2\sigma^3}-\frac{1}{2}\frac{\mathcal{P}^l\mathrm{BTH}}{\sqrt{2\pi}G_0\sigma^3}\left(\frac{\mathrm{BTH}^2}{\left(G_0\sigma\right)^2}-2\right)\right)e^{-\frac{\mathrm{BTH}^2}{2(G_0\sigma)^2}}$$

Therefore:

$$\mathcal{E}_3\approx\sigma^2\left[1-2Q_2\left(\frac{\mathrm{BTH}}{G_0\sigma}\right)-\mathcal{P}^l\frac{\mathrm{BTH}}{\sqrt{2\pi}G_0\sigma^3}\left(\frac{\mathrm{BTH}^2}{\left(G_0\sigma\right)^2}-2\right)e^{-\frac{\mathrm{BTH}^2}{2(G_0\sigma)^2}}\right]$$

4) Summation of $\mathcal{E}_1$, $\mathcal{E}_2$ and $\mathcal{E}_3$

$$\mathcal{E}\left[{f_\mathrm{B}}^2\left(G_0\left(\sqrt{\mathcal{P}^l}+n(t)\right)\right)\right]$$
$$\approx G_0^2\sigma^2\left(1-2Q_2\left(\frac{\mathrm{BTH}}{G_0\sigma}\right)\right)+G_0^2\mathcal{P}^l\left(1-2Q_0\left(\frac{\mathrm{BTH}}{G_0\sigma}\right)-\left(\frac{\mathrm{BTH}^2}{\left(G_0\sigma\right)^2}+2\right)\right.$$
$$\left.\frac{\mathrm{BTH}}{\sqrt{2\pi}G_0\sigma}e^{-\frac{\mathrm{BTH}^2}{2(G_0\sigma)^2}}\right)$$

Appendix B

Development for Spectral Separation Coefficient

The SSC (*Spectral Separation Coefficient*) is defined as:

$$\text{SSC} = \int_{-\infty}^{\infty} H_\beta^2(f) \cdot G_{s^k}(f) G_{c^l}(f) df = \int_{-\frac{\beta}{2}}^{\frac{\beta}{2}} G_{s^k}(f) \cdot G_{c^l}(f) df$$

It is considered that a signal $s^k(t)$ has a power spectral density (PSD) S_{s^k} and a normalized power spectral density G_{s^k} which is defined this way:

$$G_{s^k}(f) = \frac{S_{s^k}(f)}{\int_{-\infty}^{\infty} S_{s^k}(f) df} = \frac{S_{s^k}(f)}{\mathcal{P}^k}$$

Remark: $G_{s^k}(f) = S_{c^k}(f) = G_{c^k}(f)$, since $c^k(t)$ is normalized.

In this section, the relation between var $\left[\frac{1}{T}\int_0^T \left(h_\beta * s^k\right)(t)\, c^l(t)\, dt\right]$ and the SSC will be established. Contrary to previous developments, the filter $h(t)$ will be considered in the equations.

$$c^l(t) = \sum_{m=-\infty}^{\infty} c_m^l p^l(t - mT_c)$$

$$s^k(t) = \sqrt{\mathcal{P}^k} \sum_{n=-\infty}^{\infty} c_n^k p^k(t - nT_c - \tau^k)$$

Since code chips are considered random and uniform on $\{-1, 1\}$:

$$\mathcal{E}\left[c_m^k\right] = \mathcal{E}\left[c_m^l\right] = 0$$
$$\mathcal{E}\left[c_m^k c_{m'}^k\right] = \mathcal{E}\left[c_m^l c_{m'}^l\right] = \delta_{m,m'}$$

$$
\begin{aligned}
&\mathcal{E}\left[\left(\frac{1}{T}\int_0^T \left(h_\beta * s^k\right)(t)\, c^l(t)\, dt\right)^2\right] \\
&\quad = \frac{1}{T^2}\int_0^T\int_0^T \mathcal{E}\left[c^l(t)c^l(t')\left(h * s^k\right)(t)\big(h * s^k\big)(t')\right] dtdt' \\
&\quad = \frac{\mathcal{P}^k}{T^2}\int_0^T\int_0^T \sum_{m=-\infty}^{\infty}\sum_{m'=-\infty}^{\infty}\sum_{n=-\infty}^{\infty}\sum_{n'=-\infty}^{\infty} \mathcal{E}\left[c_m^l c_{m'}^l c_n^k c_{n'}^k\right] \\
&\qquad \cdot p^l(t-mT_c)\cdot p^l(t'-m'T_c) \\
&\qquad \cdot \big(h(t) * p^k(t-nT_c-\tau^k)\big)\cdot\big(h(t') * p^k(t'-n'T_c-\tau^k)\big)\ dtdt'
\end{aligned}
$$

And since $\mathcal{E}\left[c_m^l c_{m'}^l c_n^k c_{n'}^k\right] = \mathcal{E}\left[c_m^l c_{m'}^l\right]\cdot\mathcal{E}\left[c_n^k c_{n'}^k\right] = \delta_{m,m'}\cdot\delta_{n,n'}$, it can be written:

$$
\begin{aligned}
&\mathcal{E}\left[\left(\frac{1}{T}\int_0^T \left(h_\beta * s^k\right)(t)\, c^l(t)\, dt\right)^2\right] \\
&\quad = \frac{\mathcal{P}^k}{T^2}\int_0^T\int_0^T \sum_{m=-\infty}^{\infty}\sum_{n=-\infty}^{\infty} p^l(t-mT_c)p^l(t'-mT_c) \\
&\qquad \cdot \big(h(t) * p^k(t-nT_c-\tau^k)\big)\cdot\big(h(t') * p^k(t'-nT_c-\tau^k)\big)\, dtdt' \qquad \text{(B.1)} \\
&\quad = \frac{\mathcal{P}^k}{T^2}\sum_{m=-\infty}^{\infty}\sum_{n=-\infty}^{\infty}\int_0^T\int_0^T\int_{-\infty}^{\infty} P^l(f_1)\ e^{-j2\pi f_1 mT_c}e^{j2\pi f_1 t}df_1 \\
&\qquad \cdot\int_{-\infty}^{\infty} P^{l^*}(f_2)\ e^{j2\pi f_2 mT_c}e^{-j2\pi f_2 t'}df_2 \\
&\qquad \cdot\int_{-\infty}^{\infty} H_\beta(f_3)P^k(f_3)\ e^{-j2\pi f_3 nT_c}e^{-j2\pi f_3\tau^k}e^{j2\pi f_3 t}df_3 \\
&\qquad \cdot\int_{-\infty}^{\infty} H_\beta^*(f_4)P^{k^*}(f_4)\ e^{j2\pi f_4 nT_c}e^{j2\pi f_4\tau^k}e^{-j2\pi f_4 t'}df_4\ dtdt' \\
&\quad = \frac{\mathcal{P}^k}{T^2}\int_{-\infty}^{\infty}\int_{-\infty}^{\infty}\int_{-\infty}^{\infty}\int_{-\infty}^{\infty} P^l(f_1)P^{l^*}(f_2)P^k(f_3)P^{k^*}(f_4)H_\beta(f_3)H_\beta^*(f_4) \\
&\qquad \cdot\int_0^T e^{j2\pi(f_1+f_3)t}dt\cdot\int_0^T e^{-j2\pi(f_2+f_4)t'}dt'\cdot\sum_{m=-\infty}^{\infty} e^{-j2\pi(f_1-f_2)mT_c} \\
&\qquad \cdot\sum_{n=-\infty}^{\infty} e^{-j2\pi(f_3-f_4)nT_c}\cdot e^{-j2\pi(f_3-f_4)\tau^k}df_1df_2df_3df_4
\end{aligned}
$$

One deduces: $\begin{cases}\displaystyle\int_0^T e^{j2\pi(f_1+f_3)t}dt = Te^{j\pi(f_1+f_3)T}\mathrm{sinc}\left(\pi\left(f_1+f_3\right)T\right)\\ \displaystyle\int_0^T e^{-j2\pi(f_2+f_4)t'}dt' = Te^{-j\pi(f_2+f_4)T}\mathrm{sinc}\left(\pi\left(f_2+f_4\right)T\right)\end{cases}$

Since $\displaystyle\sum_{n=-\infty}^{\infty}\delta(t-n) = \sum_{n=-\infty}^{\infty} e^{-j2\pi nt}$, it comes:

$$\begin{cases} \sum_{m=-\infty}^{\infty} e^{-j2\pi(f_1-f_2)mT_c} = \sum_{m=-\infty}^{\infty} \delta\left((f_1-f_2)T_c - m\right) \\ \sum_{n=-\infty}^{\infty} e^{-j2\pi(f_3-f_4)nT_c} = \sum_{n=-\infty}^{\infty} \delta\left((f_3-f_4)T_c - n\right) \end{cases}$$

Consequently:

$$\begin{aligned} &\mathcal{E}\left[\left(\frac{1}{T}\int_0^T \left(h_\beta * s^k\right)(t)\, c^l(t)\, dt\right)^2\right] \\ &\quad = \mathcal{P}^k \int_{-\infty}^{\infty}\int_{-\infty}^{\infty}\int_{-\infty}^{\infty}\int_{-\infty}^{\infty} P^l(f_1) P^{l^*}(f_2) P^k(f_3) P^{k^*}(f_4) H_\beta(f_3) H_\beta^*(f_4) \\ &\qquad \cdot e^{j\pi(f_1+f_3)T} \mathrm{sinc}\left(\pi\left(f_1+f_3\right)T\right) e^{-j\pi(f_2+f_4)T} \mathrm{sinc}\left(\pi\left(f_2+f_4\right)T\right) \\ &\qquad \cdot \sum_{m=-\infty}^{\infty} \delta\left((f_1-f_2)T_c - m\right) \sum_{n=-\infty}^{\infty} \delta\left((f_3-f_4)T_c - n\right) \\ &\qquad \cdot e^{-j2\pi(f_3-f_4)\tau^k} df_1 df_2 df_3 df_4 \end{aligned}$$

This leads to:

$$\begin{aligned} &\mathcal{E}\left[\left(\frac{1}{T}\int_0^T \left(h_\beta * s^k\right)(t)\, c^l(t)\, dt\right)^2\right] \\ &\quad = \frac{\mathcal{P}^k}{{T_c}^2} \sum_{m=-\infty}^{\infty}\sum_{n=-\infty}^{\infty} \int_{-\infty}^{\infty}\int_{-\infty}^{\infty} P^l(f_1) P^{l^*}\left(f_1 - \frac{m}{T_c}\right) P^k(f_3) \\ &\qquad \cdot P^{k^*}\left(f_3 - \frac{n}{T_c}\right) H_\beta(f_3) H_\beta^*\left(f_3 - \frac{n}{T_c}\right) e^{j\pi(f_1+f_3)T} \mathrm{sinc}\left(\pi\left(f_1+f_3\right)T\right) \\ &\qquad \cdot e^{-j\pi\left(f_1+f_3-\frac{m}{T_c}-\frac{n}{T_c}\right)T} \mathrm{sinc}\left(\pi\left(f_1+f_3-\frac{m}{T_c}-\frac{n}{T_c}\right)T\right) e^{-j2\pi\frac{n\tau^k}{T_c}} df_1 df_3 \\ &\quad = \frac{\mathcal{P}^k}{{T_c}^2} \sum_{m=-\infty}^{\infty}\sum_{n=-\infty}^{\infty} \int_{-\infty}^{\infty}\int_{-\infty}^{\infty} P^l(f_1) P^{l^*}\left(f_1 - \frac{m}{T_c}\right) \\ &\qquad \cdot P^k(f_3) P^{k^*}\left(f_3 - \frac{n}{T_c}\right) H_\beta(f_3) H_\beta^*\left(f_3 - \frac{n}{T_c}\right) \mathrm{sinc}\left(\pi\left(f_1+f_3\right)T\right) \\ &\qquad \cdot \mathrm{sinc}\left(\pi\left(f_1+f_3\right)T - \pi\left(\frac{mT}{T_c}+\frac{nT}{T_c}\right)\right) df_1 df_3 e^{-j2\pi\frac{n\tau^k}{T_c}} e^{j\pi\left(\frac{mT}{T_c}+\frac{nT}{T_c}\right)} \end{aligned}$$

The variations of the function

$$(f_1, f_3) \mapsto \mathrm{sinc}\left(\pi\left(f_1+f_3\right)T\right) \mathrm{sinc}\left(\pi\left(f_1+f_3\right)T - \pi\left(\frac{mT}{T_c}+\frac{nT}{T_c}\right)\right)$$

take place on an interval of order of length equal to $1/T$ whereas the variations of the function

$$(f_1, f_3) \mapsto P^l(f_1) P^{l^*}\left(f_1 - \frac{m1}{T_c}\right) P^k(f_3) P^{k^*}\left(f_3 - \frac{n}{T_c}\right)$$

take place on a interval of order of length equal to $1/T_c$. Thus, with the assumption $T \gg T_c$, it can be considered that on the interval of variation of the sinc, P^l is constant. In other words, the following statements can be introduced in the present situation:

$$\begin{aligned} \operatorname{sinc}\left(\pi\left(f_1+f_3\right)T\right) &\approx \tfrac{1}{T}\delta\left(\pi\left(f_1+f_3\right)T\right) &\Rightarrow f_3=-f_1 \\ \operatorname{sinc}\left(\pi\left(\frac{mT}{T_c}+\frac{nT}{T_c}\right)\right) &\approx \delta\left(\pi\left(\tfrac{mT}{T_c}+\tfrac{nT}{T_c}\right)\right) &\Rightarrow n=-m \end{aligned}$$

The assumption $T \gg T_c$ is valid most of the time. As an illustration:

- GPS C/A: $T = 1023\ T_c$
- Galileo E6: $T = 5115\ T_c$

Consequently:

$$\begin{aligned} &\mathcal{E}\left[\left(\frac{1}{T}\int_0^T \left(h_\beta * s^k\right)(t)\, c^l(t)\, dt\right)^2\right] \\ &\quad = \frac{\mathcal{P}^k}{{T_c}^2 T}\sum_{m=-\infty}^{\infty} e^{j2\pi m\frac{\tau^k}{T_c}}\int_{-\infty}^{\infty} P^l(f_1)\, P^{l*}\left(f_1-\frac{m}{T_c}\right) P^k(-f_1) \\ &\qquad \cdot P^{k*}\left(-f_1+\frac{m}{T_c}\right) H_\beta(-f_1) H_\beta^*\left(-f_1+\frac{m}{T_c}\right) df_1 \end{aligned}$$

It is reminded that $P^k(f)$ and $H_\beta(f)$ are symmetric. When making the separation "$m = 0$" and "$m \in \mathbb{Z}^*$", we write:

$$\begin{aligned} &\mathcal{E}\left[\left(\frac{1}{T}\int_0^T \left(h_\beta * s^k\right)(t)\, c^l(t)\, dt\right)^2\right] \\ &\quad = \frac{\mathcal{P}^k}{T}\int_{-\infty}^{\infty} \frac{\left|P^l(f)\right|^2}{T_c}\cdot\frac{\left|P^k(f)\right|^2}{T_c}\cdot\left|H_\beta(f)\right|^2 df + f_0(\tau^k) \end{aligned}$$

With:

$$\begin{aligned} f_0(\tau^k) = \frac{2\mathcal{P}^k}{{T_c}^2 T}\sum_{m=1}^{\infty}\cos\left(2\pi m\frac{\tau^k}{T_c}\right)\cdot\int_{-\infty}^{\infty} P^l(f)\, P^{l*}\left(f-\frac{m}{T_c}\right) \\ \cdot P^k(f)\, P^{k*}\left(f-\frac{m}{T_c}\right) H_\beta(f) H_\beta^*\left(f-\frac{m}{T_c}\right) df \end{aligned}$$

For $h(t)$ a unitary filter in frequency domain ($H_\beta(f) = 1$ on $[-\frac{\beta}{2}, \frac{\beta}{2}]$ and 0 elsewhere):

$$\mathcal{E}\left[\left(\frac{1}{T}\int_0^T \left(h_\beta * s^k\right)(t)\, c^l(t)\, dt\right)^2\right] = \frac{\mathcal{P}^k}{T}\int_{-\frac{\beta}{2}}^{\frac{\beta}{2}} \frac{\left|P^l(f)\right|^2}{T_c}\cdot\frac{\left|P^k(f)\right|^2}{T_c} df + f_0(\tau^k)$$

$$
\begin{aligned}
G_{s^k}(f) = S_{c^k}(f) &= \lim_{T\to\infty} \frac{1}{2T} \left| \mathcal{F}\left\{ c^k_{[-T,T]}(t) \right\} \right|^2 \\
&\approx \frac{1}{T_c} \left| \mathcal{F}\left\{ c^k_{[0,T_c]}(t) \right\} \right|^2 \\
&\approx \frac{1}{T_c} \left| \mathcal{F}\left\{ p^k(t) \right\} \right|^2 \\
&= \frac{1}{T_c} \left| P^k(f) \right|^2
\end{aligned}
$$

$$
\mathcal{E}\left[\left(\frac{1}{T} \int_0^T \left(h_\beta * s^k \right)(t)\, c^l(t)\, dt \right)^2 \right] = \frac{\mathcal{P}^k}{T} \int_{-\frac{\beta}{2}}^{\frac{\beta}{2}} G_{c^l}(f) \cdot G_{s^k}(f) df + f_0(\tau^k)
$$

Moreover, $\forall n \in \mathbb{N}, \int_0^{nT_c} \cos\left(2\pi m \frac{\tau^k}{T_c}\right) d\tau^k = 0$ ($|m| \geq 1$), thus $\left\langle f_0(\tau^k) \right\rangle_{\tau^k} = 0$.
It can be finally deduced:

$$
\left\langle \operatorname{var}\left[\frac{1}{T} \int_0^T \left(h_\beta * s^k \right)(t)\, c^l(t)\, dt \right] \right\rangle_{\tau^k} = \frac{\mathcal{P}^k}{T} \int_{-\frac{\beta}{2}}^{\frac{\beta}{2}} G_{c^l}(f) \cdot G_{s^k}(f) df = \frac{\mathcal{P}^k}{T} \mathrm{SSC} \tag{B.2}
$$

Appendix C

Developments for Waveform Convolution Coefficient

We will derive in this section the intermediate expression (equation B.1) of $\mathcal{E}\left[\left(\frac{1}{T}\int_0^T \left(h_\beta * s^k\right)(t)\, c^l(t)\, dt\right)^2\right]$ of the SSC developments. The aim is to find a better expression with consideration of the delay between the two considered spreading code signals.

It is considered that $T_c^k = T_c^l = T_c$. The respective waveform p^k and p^l of navigation signals $s^k(t)$ and $c^l(t)$ respectively are considered restricted to $[0, T_c]$.

For the sake of simplicity in the equations, we introduce $\tilde{p}^k \equiv h * p^k$.

$$
\begin{aligned}
&\mathcal{E}\left[\left(\frac{1}{T}\int_0^T \left(h_\beta * s^k\right)(t)\, c^l(t)\, dt\right)^2\right] \\
&\quad= \frac{\mathcal{P}^k}{T^2}\sum_{m=-\infty}^{\infty}\sum_{n=-\infty}^{\infty}\left(\int_0^T p^l(t-mT_c)\,\tilde{p}^k\left(t-\tau^k-nT_c\right)dt\right)^2 \\
&\quad= \frac{\mathcal{P}^k}{T^2}\sum_{m=-\infty}^{\infty}\sum_{n=-\infty}^{\infty}\left(\int_{-mT_c}^{T-mT_c} p^l(u)\,\tilde{p}^k\left(u-\tau^k+(m-n)T_c\right)du\right)^2 \\
&\quad= \frac{\mathcal{P}^k}{T^2}\sum_{m=-\infty}^{\infty}\sum_{n=-\infty}^{\infty}\left(\int_{-mT_c}^{T-mT_c} p^l(u)\,\tilde{p}^k\left(u-\tau^k\right)*\delta\left(\tau^k-(m-n)T_c\right)\ du\right)^2 \\
&\quad= \frac{\mathcal{P}^k}{T^2}\sum_{m=-\infty}^{\infty}\sum_{n=-\infty}^{\infty}\left(\int_{-mT_c}^{T-mT_c} p^l(u)\,\tilde{p}^k\left(u-\tau^k\right)du*\delta\left(\tau^k-(m-n)T_c\right)\right)^2
\end{aligned}
$$

Since sampling then squaring a continuous signal is the same as squaring then sampling the same continuous signal, the dirac-functions can be extract of the

brackets

$$= \frac{\mathcal{P}^k}{T^2} \sum_{m=-\infty}^{\infty} \sum_{n=-\infty}^{\infty} \left(\int_{-mT_c}^{T-mT_c} p^l(u)\, \tilde{p}^k\left(u-\tau^k\right) du \right)^2 * \delta\left(\tau^k - (m-n)\,T_c\right)$$

$$= \frac{\mathcal{P}^k}{T^2} \sum_{m=-\infty}^{\infty} \left(\int_{-mT_c}^{T-mT_c} p^l(u)\, \tilde{p}^k\left(u-\tau^k\right) du \right)^2 * \sum_{n=-\infty}^{\infty} \delta\left(\tau^k - (m-n)\,T_c\right)$$

$$= \frac{\mathcal{P}^k}{T^2} \sum_{m=-\infty}^{\infty} \left(\int_{-mT_c}^{T-mT_c} p^l(u)\, \tilde{p}^k\left(u-\tau^k\right) du \right)^2 * \sum_{n_2=-\infty}^{\infty} \delta\left(\tau^k - n_2 T_c\right)$$

$$\sum_{m=-\infty}^{\infty} \left(\int_{-mT_c}^{T-mT_c} p^l(u)\, \tilde{p}^k\left(u-\tau^k\right) du \right)^2$$

$$= \sum_{m=-\infty}^{\infty} \left(\sum_{M=1}^{T/T_c} \int_{(M-m-1)T_c}^{(M-m)T_c} p^l(u)\, \tilde{p}^k\left(u-\tau^k\right) du \right)^2$$

By definition, p^l is zero on $\mathbb{R} \setminus [0, T_c]$, thus is possible to restrict the integration to $[0, T_c]$. It is the case for $M - m - 1 = 0$, which is equivalent to $m = M - 1$, with $m = 0 \cdots \frac{T}{T_c} - 1$ (since $M = 1 \cdots \frac{T}{T_c}$)
Consequently:

$$\sum_{m=-\infty}^{\infty} \left(\int_{-mT_c}^{T-mT_c} p^l(u)\, \tilde{p}^k\left(u-\tau^k\right) du \right)^2 = \sum_{m=0}^{T/T_c-1} \left(\int_{0}^{T_c} p^l(u)\, \tilde{p}^k\left(u-\tau^k\right) du \right)^2$$

$$= \frac{T}{T_c} \left(\int_{0}^{T_c} p^l(u)\, \tilde{p}^k\left(u-\tau^k\right) du \right)^2$$

And now:

$$\mathcal{E}\left[\left(\frac{1}{T} \int_0^T \left(h_\beta * s^k\right)(t)\, c^l(t)\, dt \right)^2 \right]$$

$$= \frac{\mathcal{P}^k}{TT_c} \left(\int_{0}^{T_c} p^l(u)\, \tilde{p}^k\left(u-\tau^k\right) du \right)^2 * \sum_{n_2=-\infty}^{\infty} \delta\left(\tau^k - n_2 T_c\right)$$

The aim now is to "transform" $\tilde{p}^k\left(u-\tau^k\right)$ into $\tilde{p}^k\left(\tau^k-u\right)$.

For BPSK and even BOC with waveform $p(t)$ defined on $[0, T_c]$, $p(t) = p(-t + T_c)$.
For odd BOC, $p(t) = -p(-t + T_c)$.
Thus, for any BPSK and BOC, one can introduce $\mu \in \{-1, 1\}$ (i.e. $\mu^2 = 1$) such that: $p(t) = \mu \cdot p(-t + T_c)$.

For any pattern satisfying this property, it can be deduced:

$$\begin{aligned}
&\mathcal{E}\left[\left(\frac{1}{T}\int_0^T \left(h_\beta * s^k\right)(t)\, c^l(t)\, dt\right)^2\right] \\
&\quad = \frac{\mathcal{P}^k}{TT_c}\left(\int_0^{T_c} \mu \cdot p^l(u)\, \tilde{p}^k\left(\left(\tau^k + T_c\right) - u\right) du\right)^2 \\
&\qquad * \sum_{n_2=-\infty}^{\infty} \delta\left(\left(\tau^k + T_c\right) - (n_2+1)T_c\right) \\
&\quad = \mathcal{P}^k \frac{T_c}{T}\left(\frac{1}{T_c}\int_0^{T_c} p^l(u)\, \tilde{p}^k\left(\tau^k - u\right) du\right)^2 * \sum_{n_2=-\infty}^{\infty} \delta\left(\tau^k - n_2 T_c\right) \\
&\quad = \mathcal{P}^k \frac{T_c}{T}\left(\frac{1}{T_c}\left(\tilde{p}^k * p^l\right)\left(\tau^k\right)\right)^2 * \sum_{n_2=-\infty}^{\infty} \delta\left(\tau^k - mT_c\right)
\end{aligned}$$

It can be equivalently written:

$$\operatorname{var}\left[\frac{1}{T}\int_0^T \left(h_\beta * s^k\right)(t)\, c^l(t)\, dt\right] \tag{C.1}$$

$$= \mathcal{P}^k \frac{T_c}{T}\left(\frac{1}{T_c}\left(h * p^k * p^l\right)\left(\tau^k\right)\right)^2 * \sum_{m=-\infty}^{\infty} \delta\left(\tau^k - mT_c\right) \tag{C.2}$$

We introduce the function $\mathrm{WCC}\left(\tau^k\right)$ such that:

$$\mathrm{WCC}\left(\tau^k\right) = \left(\frac{1}{T_c}\left(h * p^k * p^l\right)\left(\tau^k\right)\right)^2 * \sum_{m=-\infty}^{\infty} \delta\left(\tau^k - kT_c\right)$$

Finally:

$$\operatorname{var}\left[\frac{1}{T}\int_0^T \left(h_\beta * s^k\right)(t)\, c^l(t)\, dt\right] = \mathcal{P}^k \frac{T_c}{T}\mathrm{WCC}\left(\tau^k\right)$$

Appendix D

Mathematical Tools

D.1 Q-Functions

The functions Q_n, $n \in \mathbb{N}$ will be useful for the derivations.

$$Q_n(x) = \int_x^{+\infty} \frac{x^n}{\sqrt{2\pi}} e^{-\frac{x^2}{2}} dx$$

These functions are represented in figure D.1.
Remark: Q_0 is related to the error function erf: $Q_0(x) = \frac{1}{2} - \frac{1}{2}\text{erf}\left(\frac{x}{\sqrt{2}}\right)$

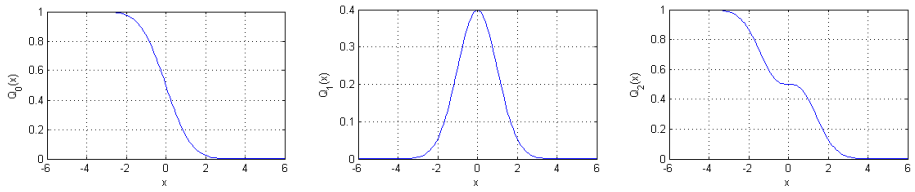

(a) Q_0-function (b) Q_1-function (c) Q_2-function

Figure D.1: Representation of the Q-functions for $n \in \{0, 1, 2\}$

Note: For $n \in \{0, 2\}$: $\lim_{x \to -\infty} Q_n(x) = 1$ and $\lim_{x \to +\infty} Q_n(x) = 0$

The Q-functions have been introduced to simplify the expressions depending on the noise distribution. As an illustration, if the probability that $a + b \cdot n(t) + c \cdot n^2(t)$ belongs to $[-n_1, n_1]$ has to be computed (with $n(t) \sim \mathcal{N}(0, 1)$, and so $p(n) = \frac{1}{\sqrt{2\pi}} e^{-\frac{n^2}{2}}$), then:

$$\begin{aligned}
&\int_{-n_1}^{n_1} \left(a + b \cdot n + c \cdot n^2\right) \cdot p(n) dn \\
&\quad = \int_{-n_1}^{n_1} \frac{a}{\sqrt{2\pi}} e^{-\frac{n^2}{2}} dn + \int_{-n_1}^{n_1} \frac{cn^2}{\sqrt{2\pi}} e^{-\frac{n^2}{2}} dn \\
&\quad = a \cdot [Q_0(-n_1) - Q_0(n_1)] + c \cdot [Q_2(-n_1) - Q_2(n_1)] \\
&\quad = a \cdot [1 - 2Q_0(n_1)] + c \cdot [1 - 2Q_2(n_1)]
\end{aligned}$$

D.2 Relation between Pulsed and Continuous Signals in the Variance Expression

The objective here is to define the relation between the terms $\text{var}\left[\frac{1}{T}\int_0^T \tilde{f}(t)dt\right]$ and $\text{var}\left[\frac{1}{T}\int_0^T f(t)dt\right]$ for a signal $f(t)$ satisfying the two following conditions:

- $f(t)$ has the same properties of randomness on $[0,T]$ as $\tilde{f}(t)$ during the pulse.
- The variance of the (normalized) integration of f is proportional to the time of integration: $\text{var}\left[\frac{1}{T}\int_0^T f(t)dt\right] = K/T$ with K the factor of proportionality.

The interval of activity of $\tilde{f}(t)$ is called I, with L_I the length of the interval $[0,T] \cap I$.

By definition: $\tilde{f}\,(t) = \begin{cases} f\,(t) & t \in I \\ 0 & \text{otherwise} \end{cases}$

Let us now derive the expression:

$$\begin{aligned} \text{var}\left[\frac{1}{T}\int_0^T \tilde{f}(t)dt\right] &= \text{var}\left[\frac{1}{T}\int\limits_{[0,T]\cap I} f(t)dt\right] \\ &= \frac{{L_I}^2}{T^2}\cdot \text{var}\left[\frac{1}{L_I}\int\limits_{[0,T]\cap I} f(t)dt\right] \\ &= \frac{{L_I}^2}{T^2}\cdot\frac{K}{L_I} \end{aligned}$$

And in conclusion:

$$\text{var}\left[\frac{1}{T}\int_0^T \tilde{f}(t)dt\right] = \frac{L_I}{T}\cdot \text{var}\left[\frac{1}{T}\int_0^T f(t)dt\right]$$

Remark: The ratio $\frac{L_I}{T}$ corresponds to the pulse duty cyle of $\tilde{f}\,(t)$.

Bibliography

[1] P. Misra and P. Enge, *Global Positioning System: Signals, Measurements, and Performance*. Ganga-Jamuna Press, second ed., 2006.

[2] H. S. Cobb, *GPS Pseudolites: Theory, Design, and Applications*. PhD thesis, Stanford University, 1997.

[3] K. Borre, "The E1 Galileo Signal," tech. rep., Aalborg University, Denmark, May 2009.

[4] A. J. Van Dierendonck, P. Fen, and C. Hegarty, "Proposed Airport Pseudolite Signal Specification for GPS Precision Approach Local Area Augmentation Systems," *PROCEEDINGS OF ION GPS*, vol. 10, no. 1, pp. 1603–1612, 1997.

[5] E. A. Lemaster, *Self-Calibrating Pseudolite Arrays: Theory and Experiment*. PhD thesis, Stanford University, 2002.

[6] T. A. Stansell, Jr., "RTCM SC-104 Recommended Pseudolite Signal Specification," *NAVIGATION*, vol. 33, no. 1, pp. 42–59, 1986.

[7] RTCA SC-159, *GNSS-Based Precision Approach Local Area Augmentation System (LAAS) Signal-in-Space Interface Control Document (ICD)*, January 2000. RTCA/DO-246A.

[8] T. Pany, *Navigation signal processing for GNSS software receivers*. GNSS technology and applications series, Artech House, 2010.

[9] C. Hegarty, A. J. Van Dierendonck, D. Bobyn, M. Tran, T. Kim, and J. Grabowski, "Suppression of Pulsed Interference Through Blanking," *Proceedings of the IAIN World Congress, San Diego*, p. 399, June 2000.

[10] E. D. Kaplan and C. J. Hegarty, eds., *Understanding GPS – Principles and Applications*, ch. Satellite Signal Acquisition, Tracking, and Data Demodulation. Artech House, second ed., 2006.

[11] C. Hegarty, "Analytical Model for GNSS Receiver Implementation Losses," *NAVIGATION*, vol. 58, no. 1, pp. 29–44, 2011.

[12] C. Zecha and F. Soualle, "Analysis of the Impact of Pulsed Interference on GNSS Receivers," tech. rep., EADS Astrium, November 2010.

[13] CEPT ECC, Dublin, *Compatibility Studies between Pseudolites and Services in the Frequency Band 1164–1215, 1215–1300 and 1559–1610 MHz*, January 2009. ECC REPORT 128.